



CSIRO

Land and Water

Groundwater Discharge from the Burdekin Floodplain Aquifer, North Queensland

P.G. Cook, T. Stieglitz and J. Clark



Queensland Government
Natural Resources, Mines and Energy

CSIRO Land and Water Technical Report No 26/04
August 2004

Copyright and Disclaimer

© 2004 CSIRO To the extent permitted by law, all rights are reserved and no part of this publication covered by copyright may be reproduced or copied in any form or by any means except with the written permission of CSIRO Land and Water.

Important Disclaimer:

CSIRO Land and Water advises that the information contained in this publication comprises general statements based on scientific research. The reader is advised and needs to be aware that such information may be incomplete or unable to be used in any specific situation. No reliance or actions must therefore be made on that information without seeking prior expert professional, scientific and technical advice. To the extent permitted by law, CSIRO Land and Water (including its employees and consultants) excludes all liability to any person for any consequences, including but not limited to all losses, damages, costs, expenses and any other compensation, arising directly or indirectly from using this publication (in part or in whole) and any information or material contained in it.

ISSN 1446-6171

**GROUNDWATER DISCHARGE FROM THE BURDEKIN FLOODPLAIN AQUIFER,
NORTH QUEENSLAND**

P.G. Cook¹, T. Stieglitz² and J. Clark³

¹ CSIRO Land and Water, Adelaide

**² School of Mathematical and Physical Sciences, James Cook University,
Townsville**

³ University California, Santa Barbara

Technical Report No. 26/04

August 2004

EXECUTIVE SUMMARY

Groundwater discharge from the floodplain aquifers of the lower Burdekin has been estimated using radon and radium isotopes in conjunction with numerical modelling. Surface water samples were collected from the Burdekin River, Haughton River, Barratta Creek, Sheepstation Creek, Plantation Creek and Saltwater Creek, as well as from a number of drainage canals and lagoons, and analysed for major ions, nitrate and radon (^{222}Rn) activity. A total of 95 sites were sampled, with the majority of the sampling taking place in December 2003 and April-May 2004. Offshore samples were collected from Bowling Green Bay, using the AIMS RV Titan. In April 2004, eight samples were collected for radium isotope analyses (^{223}Ra , ^{224}Ra , ^{226}Ra and ^{228}Ra), six of which were collected along a north-south transect extending to 30 km offshore. Measurements of radon activity were made on 9 February 2004 and 29 April 2004, along a shore-parallel transects, approximately one nautical mile offshore. Groundwater samples were collected from 40 NRM&E bores: samples from 38 bores were analysed for radon and five were analysed for radium isotopes.

Groundwater inflows to the Burdekin River, Haughton River, Barratta Creek and Plantation Creek have been estimated using a simple one-dimensional model that simulates radon input to the river due to groundwater inflow, and radon loss due to radioactive decay and gas exchange with the atmosphere. The input parameters to which the model results are most sensitive are the radon activity in groundwater inflow, the gas transfer velocity across the water surface and the river width. A constant value for the gas exchange velocity of 1 m/day was used for the Burdekin River, Haughton River and Barratta Creek, and a value of 8 m/day was used for Plantation Creek. The choice of value was based on published studies, but it was also adjusted during the model calibration. More accurate determination of this parameter would improve the accuracy of the estimated groundwater inflows. River width was measured at a few sites along each river and creek, although more accurate determination would also improve the accuracy of the model. The model does not allow for variations in river width or depth in response to variations in flow rate, nor does it account for losses of water due to pumping from the river. These are not considered to be serious omissions.

Because the model assumes steady-state flow, it is difficult to use it to simulate radon activities in tidal parts of the rivers and creeks. We have attempted to correct the measured radon activities within the tidal reaches for dilution with seawater, based on measured electrical conductivities and an assumed radon activity and electrical conductivity of the seawater end-member. This approach has allowed us to obtain estimates of groundwater discharge for tidal reaches, although the confidence of the inferred groundwater inflows is lower in these regions.

Over the 40 km reach immediately downstream of Clare Weir, the groundwater inflow to the Burdekin River is estimated to be 127 ML/day, based on samples collected on 2 May 2004. Sampling over a portion of this river reach on four separate occasions between 9 December 2003 and 27 April 2004, gave groundwater inflows that are between 42 and 72% of the inflow estimated for 4-6 May. Groundwater flow rates at these five sampling times ranged between 9.5 and 202 m³/s, although the flow rate for the 12 month period until 6 May 2004 ranged between 0.09 and 846 m³/s. (The median flow was 16.8 m³/s.) Calculation of mean annual groundwater inflow is therefore difficult. Comparison of surface water and groundwater hydrographs suggests that greatest groundwater inflow may occur in April – May, when groundwater levels remain high from the previous wet season, and surface water

levels have fallen. Mean annual groundwater inflows for the 40 km reach of Burdekin may therefore be around 100 ML/day.

In May 2004, the estimated groundwater inflow for the 26 km reach of the Haughton River between the Haughton Main Channel outlet and Giru Weir was 12.3 – 32.3 ML/day, with the uncertainty being due to the infrequency of sampling in the upper reaches. Immediately below Giru Weir, a groundwater inflow of 5.0 ML/day occurs, and this is attributed to the raised groundwater levels surrounding the Weir. A total of 13.5 ML/day inflow occurs between Giru Weir and the mouth. On Barratta Creek, groundwater inflow between Clare Road and a site just below the tidal limit was 1.5 ML/day in December 2003 and 6.4 ML/day in May 2004. A further inflow of 24 ML/day in May 2004 occurred in the tidal section of the creek.

Sensitivity analysis suggested that estimated $\pm 50\%$ errors in estimated groundwater inflows would arise from approximately 50% errors in river width, gas exchange velocity and radon activity of groundwater inflow. It is difficult to accurately estimate the uncertainty of the estimated groundwater inflows, because the uncertainties of all the model parameters are unknown. Nevertheless, we estimate that the predictions are probably accurate to within a factor of between 2 and 3 in the upstream reaches. Within the tidal reaches, the uncertainty would be somewhat higher.

Groundwater discharge to the ocean has been estimated from radon and radium activities measured within Bowling Green Bay. The data has been interpreted using a one-dimensional model that simulates advection and mixing within the ocean, as well as radioactive decay, gas exchange and production within seafloor sediments. Radon and radium produced within the seafloor sediments is released into the water column by advection caused by wave action and tidal fluctuations. The input parameters for the model include the eddy mixing coefficient, the gas exchange velocity (for radon only), the mean water flux that moves in and out of the sediments each tidal cycle in response to wave and tidal pumping (termed the recycled seawater exchange rate), the equilibrium activity within the seafloor sediments, the submarine groundwater discharge rate, and the mean activities of submarine groundwater discharge and of discharges from Haughton River and Barratta Creek. The eddy mixing coefficient is estimated from the short-lived radium isotopes. The gas exchange velocity has not been directly estimated, and this constitutes a significant source of error for estimation of submarine groundwater discharge from the radon activity of seawater. The radium activities of Haughton River and Barratta Creek have not been well constrained, although the radium flux contributed by surface water appears to be relatively small, and so inaccuracies in these parameters may not be of major concern. Although the activities within seafloor sediments have not been measured, we have assumed that the production rate within seafloor sediments is the same as that within the groundwater, and thus estimated it from the mean activities measured in groundwater samples. Perhaps the largest source of error is the exchange rate of recycled seawater, which has not been directly estimated.

Simulation of all four radium isotopes and ^{222}Rn has allowed some constraints to be placed on the possible values for the groundwater discharge rate (Q_G) and the recycled seawater exchange rate (Q_s/z). In particular, the groundwater discharge rate appears to be bounded between $Q_G = 4.0 \times 10^5$ and 1.0×10^6 m³/day (150 000 – 370 000 ML/yr). The recycled seawater exchange rate is in the order of $Q_s/z = 0.2 - 0.4$ day⁻¹. Larger values of either Q_G or Q_s/z result in radon activities that are much greater than the measured values. Higher values of Q_G and Q_s/z would only be possible if the gas exchange coefficient k/z were greater than 20 day⁻¹, which seem unreasonable based on literature data. Lower values of Q_G would be produced if the

radium activities of groundwater inflow are much greater than the measured radium activities in groundwater, or if the annual radium flux in surface water is significantly greater than that measured at the time of sampling. These uncertainties mean that the actual range in the submarine groundwater discharge rate is probably closer to 50 000 – 400 000 ML/yr.

McMahon et al. (2002) estimated total recharge for the Burdekin River delta (area 850 km²) to be between 430 000 and 850 000 ML/yr. Groundwater pumping is estimated to be between 440 000 and 830 000 ML/yr. Analysis of radon activities in surface waters gives a total estimated groundwater discharge to surface waters for the entire alluvial floodplain of 30 000 – 150 000 ML/yr. (This assumes also that the majority of the discharge to surface waters occurs to the Burdekin River, Haughton River, Barratta Creek and Plantation Creek.) The groundwater discharge directly into Bowling Green Bay is estimated to be 50 000 – 400 000 ML/yr. (Groundwater discharge would also occur to the coast between Peters Island and Cape Bowling Green, although this has not been quantified.) It should be noted that the groundwater discharge estimates apply to a larger region than the estimates of groundwater recharge and pumping. The uncertainties in the estimates could be reduced by additional sampling to better understand seasonal variations, additional measurements of river width, and independent estimates of gas exchange rates and recycled seawater exchange rates. Some of this work is currently being planned.

Table of Contents

EXECUTIVE SUMMARY	3
1. INTRODUCTION	9
2. METHODS	11
2.1. General	11
2.2. River Flows and Aquifer Hydraulics	11
2.3. Surface Water and Groundwater Sampling	13
2.4. Radon Analyses	17
2.5. Radium Analyses	18
3. DISCHARGE TO STREAMS	19
3.1 Introduction	19
3.2. Theory	20
3.3. Radon Activity in Groundwater	21
3.4. Burdekin River and Groper Creek	22
3.5. Haughton River	28
3.6. Barratta Creek	34
3.7. Plantation Creek	39
3.8. Sheepstation Creek	41
3.9. Inkerman Region	42
4. DISCHARGE TO THE OCEAN	44
4.1. Introduction	44
4.2. Theory	45
4.3. Radium	48
4.4. Radon	53
4.5. Modelling	56
5. DISCUSSION AND CONCLUSIONS	60
5.1. Discharge to Surface Waters	60
5.2. Submarine Groundwater Discharge	63
5.3. Conclusions	64
6. REFERENCES	65
7. ACKNOWLEDGEMENTS	67
APPENDIX 1: Field Measurements of River Width	69
APPENDIX 2: Locations of Sampling Sites	70
APPENDIX 3: Results of Chemical Analyses	76
APPENDIX 4: Comparison of surface water gauge heights and groundwater elevations.	87

1. INTRODUCTION

The Burdekin River Delta covers an area of approximately 850 km², and represents one of the largest unconfined coastal aquifer systems in eastern Australia (McMahon et al., 2002). The Burdekin River, Haughton River, Barratta Creek and a number of minor watercourses drain the delta and surrounding floodplain area, which together cover an area of approximately 2760 km². The Burdekin River has a mean annual flow volume of approximately 9.3 million ML, almost 80% of which occurs between January and March. The mean annual flow volume of the Haughton River is 380 000 ML, and for Barratta Creek it is 140 000 ML. Flow of the Burdekin River is regulated at Burdekin Falls Dam, and at Clare Weir. Two weirs have also been constructed on the Haughton River to provide storages for irrigation water, and the river is also supplemented by water pumped from the Burdekin River. There are no weirs on Barratta Creek. Both surface water and groundwater are extensively used for irrigation within the floodplain region. Currently more than 350 km² of land is irrigated, with sugarcane the major crop.

Recharge to the unconfined aquifers of the Burdekin River floodplain is from a combination of natural and artificial processes, including natural infiltration of rainfall, leakage from beds and banks of the Burdekin River and other watercourses, overland floods, inflow from bedrock and adjacent areas, irrigation return flows and artificial recharge pits and channels. McMahon et al. (2002) estimated total recharge from these various sources for the Burdekin River Delta to be between 430 000 and 850 000 ML/year. Groundwater pumping is estimated to be between 440 000 and 830 000 ML/year.

Because the rate of groundwater extraction is close to the aquifer recharge rate, estimation of the volume of groundwater discharge to streams and to the ocean from a water balance is difficult. The direction of groundwater – surface water flow (i.e. distinguishing losing from gaining streams) can usually be obtained from a comparison of surface water levels and hydraulic heads in piezometers adjacent to streams. However, it is often difficult to accurately quantify the flow rate from this data because hydraulic conductivity is difficult to characterise on this scale.

Environmental tracer methods have been used to quantify groundwater discharge to rivers for the past few decades. They offer advantages over physically-based methods in that they can potentially provide more accurate information on the spatial distribution of groundwater inflows with a much lower investment of resources. An environmental tracer will be useful for estimating groundwater inflows to rivers when the concentration of the tracer in groundwater is relatively uniform and significantly different to that in the river. One of the most powerful tracers for this purpose is radon (²²²Rn). With a half-life of 3.8 days, radon is produced in the subsurface by the radioactive decay of uranium-series isotopes. After groundwater containing radon discharges to surface water bodies, radon activities decrease due to gaseous exchange with the atmosphere and radioactive decay (Ellins et al., 1990; Lee and Hollyday, 1993). High radon activities are therefore present in surface waters only in the immediate vicinity of points of groundwater inflow, and for relatively short distances downstream of such locations. In some cases, ion chemistry can also be used to quantify groundwater inflow (Genereux et al., 1993; Cook et al., 2003), although changes in groundwater inflow rates will not always cause changes in ion concentrations.

Quantification of groundwater discharge to the ocean is more difficult. One of the more commonly used methods uses naturally occurring radium isotopes (Moore, 1996). The flux of groundwater is determined by closing the mass balance, which requires knowledge of the groundwater activities, the flushing rate of the coastal water, surface water fluxes, and the removal pathways of the tracer within the marine environment (e.g., radioactive decay, gas exchange with the atmosphere).

The Department of Natural Resources, Mines and Energy (NRM&E) are currently constructing a groundwater model of the Burdekin Delta to assist in water allocation planning. The current project aims to use existing hydraulic data (groundwater heads and surface water levels) together with groundwater and surface water chemistry sampling to quantify locations and magnitudes of groundwater discharge to streams, estuaries and to the marine environment in the lower Burdekin. Groundwater and surface water chemistry will focus on use of the radon and radium isotopes, and major ion chemistry.

2. METHODS

2.1. General

Groundwater discharge to rivers and creeks within the Burdekin River floodplain has been estimated from consideration of aquifer hydraulics (comparison of surface water and groundwater elevations), and from comparison of radon and major ion chemistry in surface water and groundwater samples. Submarine groundwater discharge has been estimated from comparison of radon and radium isotope activities in groundwater and ocean water.

2.2. River Flows and Aquifer Hydraulics

Flow rates for the major rivers at the time of sampling were obtained from gauging stations with automatic stage recorders located on the Burdekin River at Clare (Station 120006B), Barratta Creek at Northcote (Station 119101A) and Haughton River at Powerline (Station 119003A; Figure 2.1). Stage height information was also obtained from 31 surface water monitoring sites on the NRM&E database. For these sites, stage heights are manually recorded at approximately monthly intervals, although only ten of the 31 sites are currently operational. Stage heights for all stations were converted to AHD, and compared with groundwater level observations at nearby monitoring bores. The five closest bores were selected for this comparison, up to a maximum distance of 5 km from the surface water monitoring site. (Bores that were not considered representative of the regional aquifer were excluded from this comparison.) Differences between the water table and surface water elevation were used to determine the direction of surface water – groundwater flow. Locations of the surface water monitoring sites, and the bores used for the comparison are shown in Figure 2.1. River widths were measured at a number of sites using a laser range finder (see Table A1.1 in Appendix 1), or estimated from aerial photography.

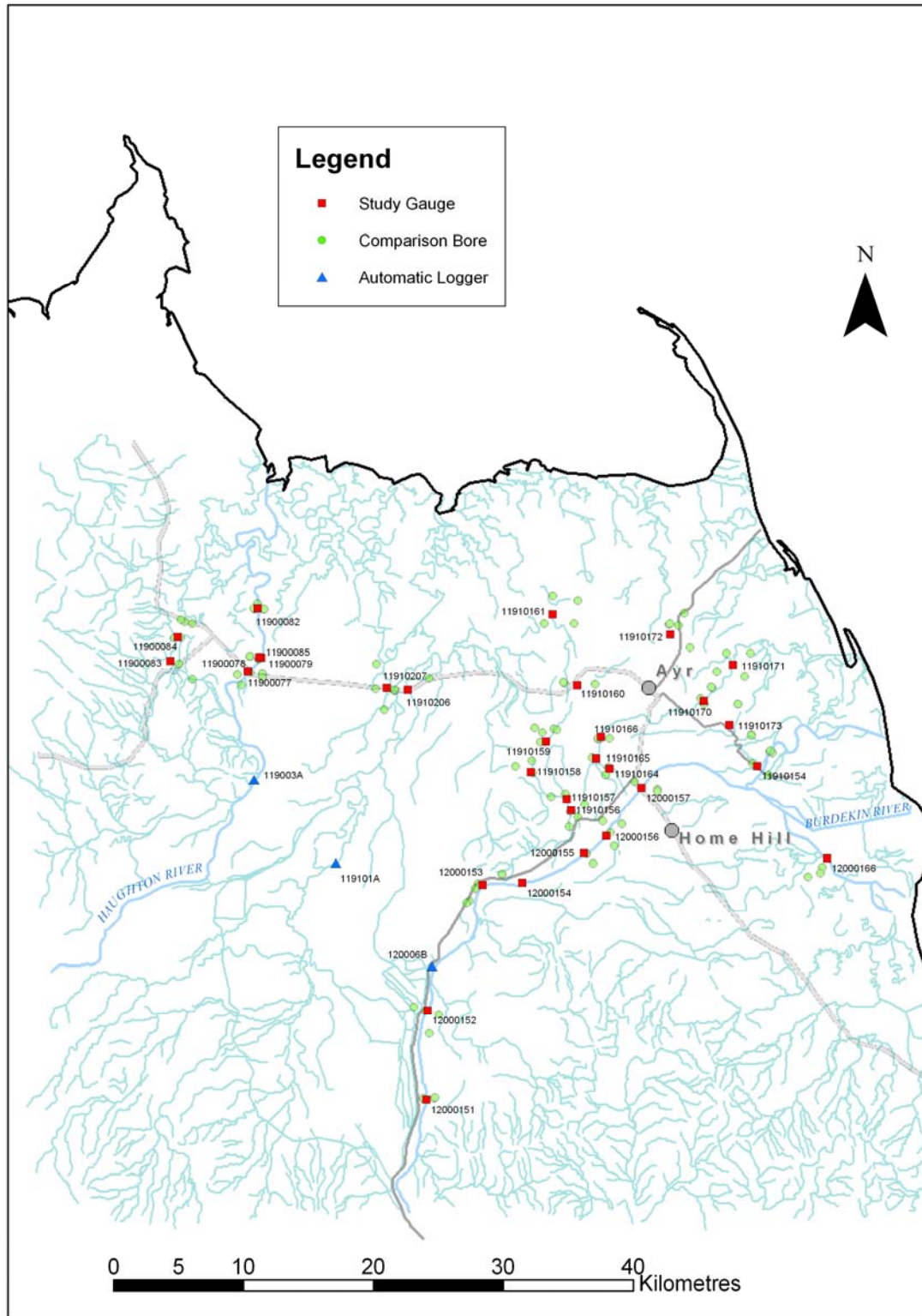


Figure 2.1. Locations of surface water gauging sites and bores used for comparison of hydraulic heads.

2.3. Surface Water and Groundwater Sampling

Groundwater samples were collected from 40 NRM&E monitoring wells. NRM&E monitoring wells have been constructed in 15 cm and 20 cm radius boreholes. They are mostly constructed of 50 mm PVC casing, with slotted intervals between 3 and 12 m in length. Between 19-28 December 2003, samples were collected from 30 wells for analyses of ^{222}Rn . Between 27-28 April 2004, a further eight wells were sampled for ^{222}Rn and five wells were sampled for radium isotopes. Groundwater samples were collected after purging approximately six well volumes from each piezometer. After purging, field measurements were made of dissolved oxygen (DO), electrical conductivity (EC), pH, Eh and temperature. Analytical methods for ^{222}Rn and radium isotope determination are described below. The locations of all bores sampled are listed in Table A2.3 (Appendix 2) and shown in Figure 2.2.

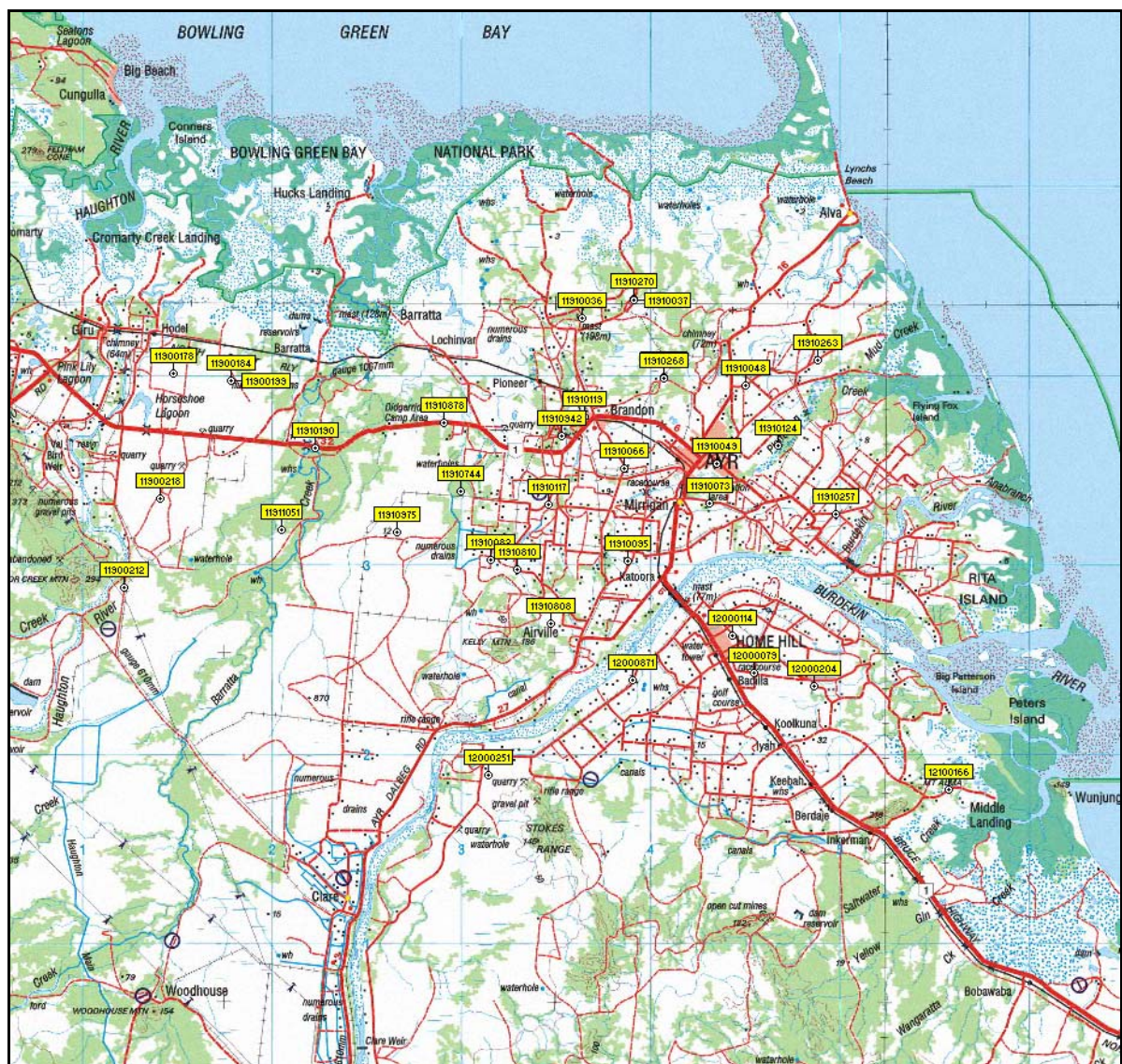


Figure 2.2. Locations of groundwater bores sampled for ^{222}Rn and radium isotopes.

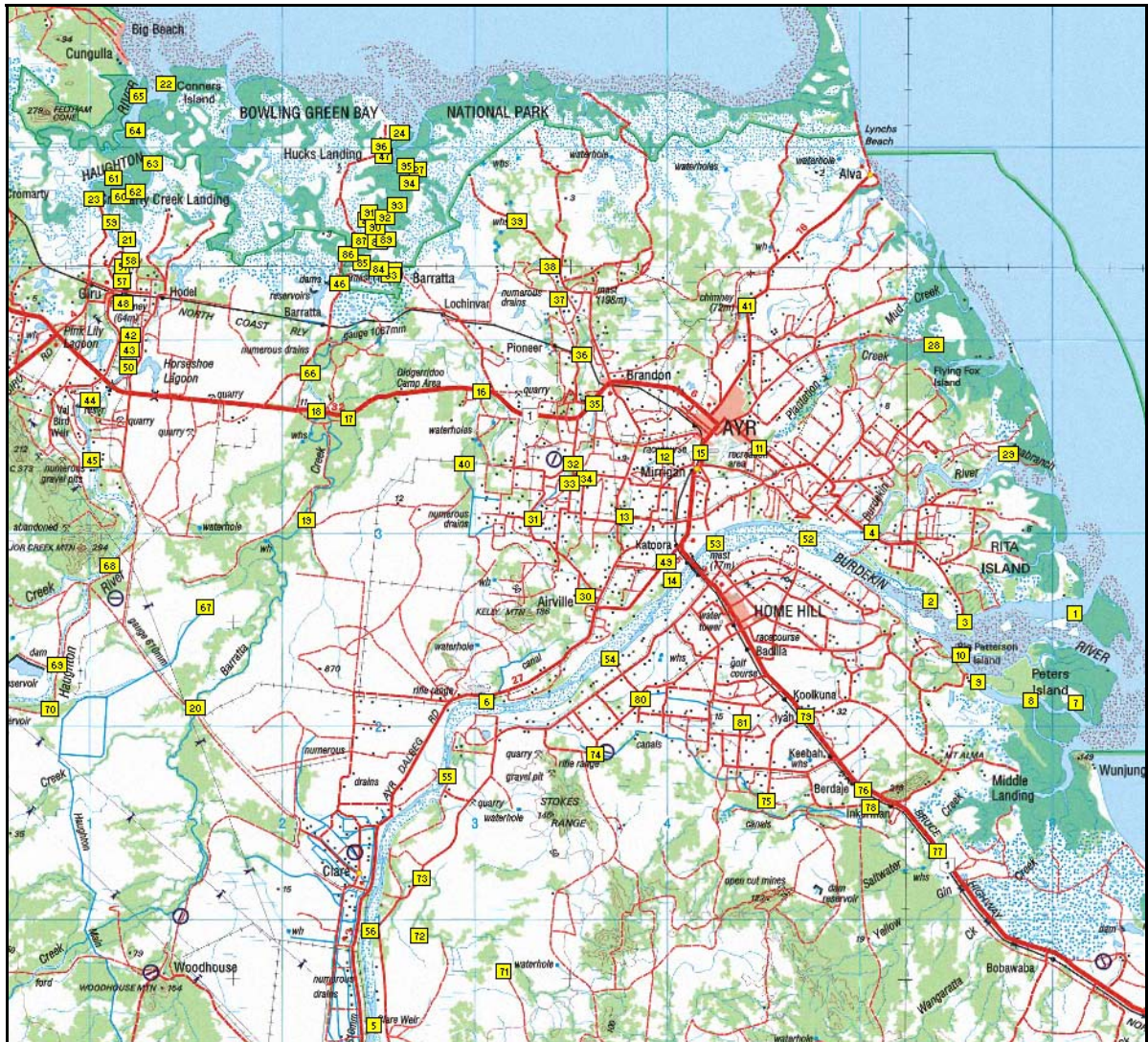


Figure 2.3. Locations of surface water sampling sites. A larger scale map of the lower reaches of the Haughton River and Barratta Creek is provided as Figure 2.4.

Stream samples were collected from the Burdekin River, Haughton River, Barratta Creek, Sheepstation Creek, Plantation Creek and Saltwater Creek, as well as from a number of drainage canals and lagoons. Samples from the lower reaches of the Burdekin River, Haughton River and Barratta Creek were collected using a small boat, whereas samples from the upper reaches were collected where road access permitted. In both cases, a small pump was used to pump water samples from between 0.3 and 0.5 m depth below the water surface. Field measurements were made of DO, EC, pH and temperature. Samples for major ion and nitrate analysis were collected in 1 L plastic bottle. Samples for ²²²Rn analysis were collected either in 1 L or 1250 ml bottles, and radon was extracted as described below. Forty five sites were sampled between 8-16 December 2003, six sites between 3-6 February 2004, and 78 sites between 26 April and 4 May 2004. (Twenty eight sites were sample both in December 2003 and April-May 2004, and five sites were sampled on all three occasions.) Samples for radium isotope analysis were collected from three sites in April-May 2004. Surface water sampling sites are listed in Table A2.2 (Appendix 2), and their locations are shown in Figures 2.3 and 2.4.

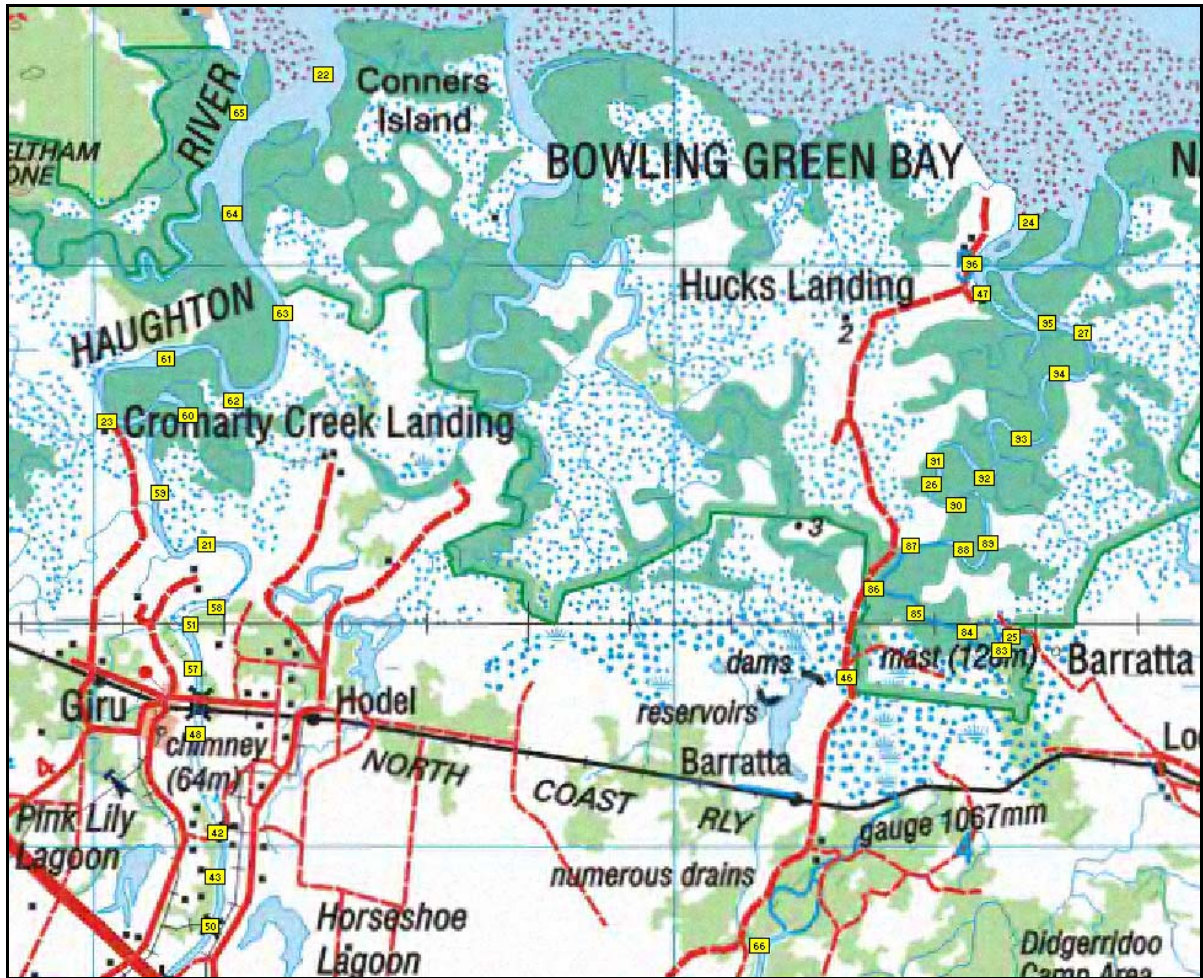


Figure 2.4. Detailed map showing locations of surface water sampling sites on the lower reaches of Haughton River and Barratta Creek.

Offshore samples were collected from Bowling Green Bay, using the AIMS RV Titan. On 28 April 2004, eight samples were collected for radium isotope analyses. Six samples formed a north-south transect as shown in Figure 2.5. The remaining two samples were collected near the mouth of the Haughton River and in the protected, southeast corner of Bowling Green Bay. Their precise locations are given in Table A2.4 in Appendix 2. Measurements of radon activity were made on 9 February 2004 and 29 April 2004, along a shore-parallel east-west transect approximately 1 nautical mile (1850 m) from the coast (Figure 2.6). Radon analyses were performed onboard the vessel, as water was continuously pumped while travelling from east to west at 3 – 5 knots. Salinity and temperature were also logged during this traverse. At eight points along the transect, water samples also collected in 1.25 L plastic bottles and later analysed for ^{222}Rn by liquid scintillation counting.

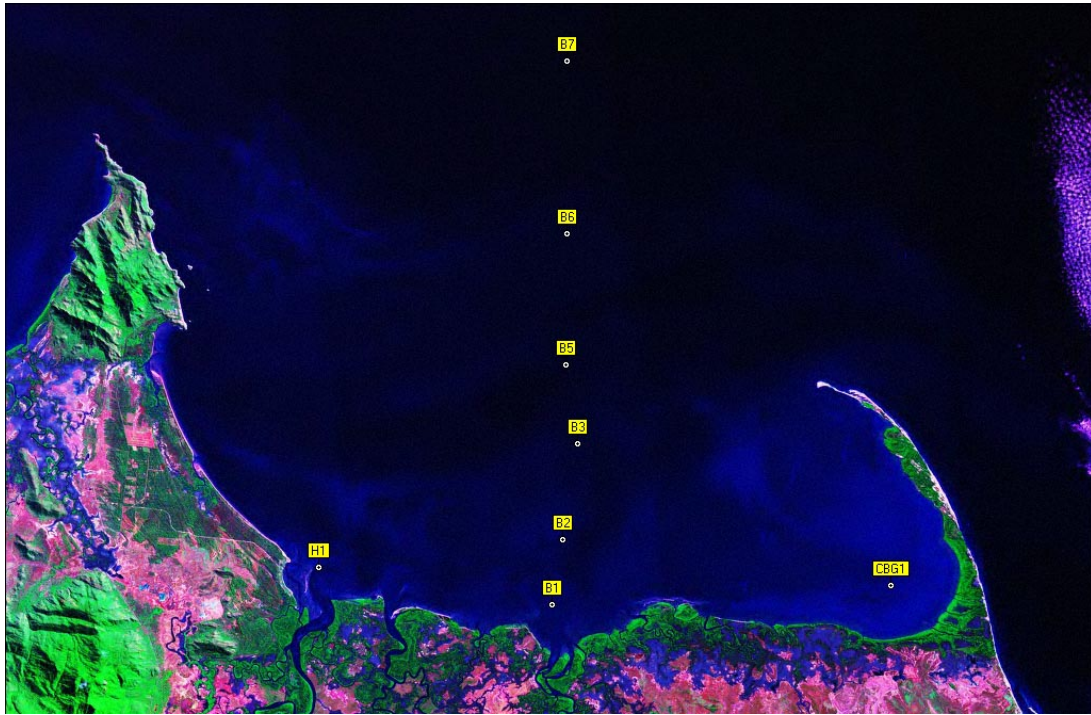


Figure 2.5. Locations of offshore radium samples.

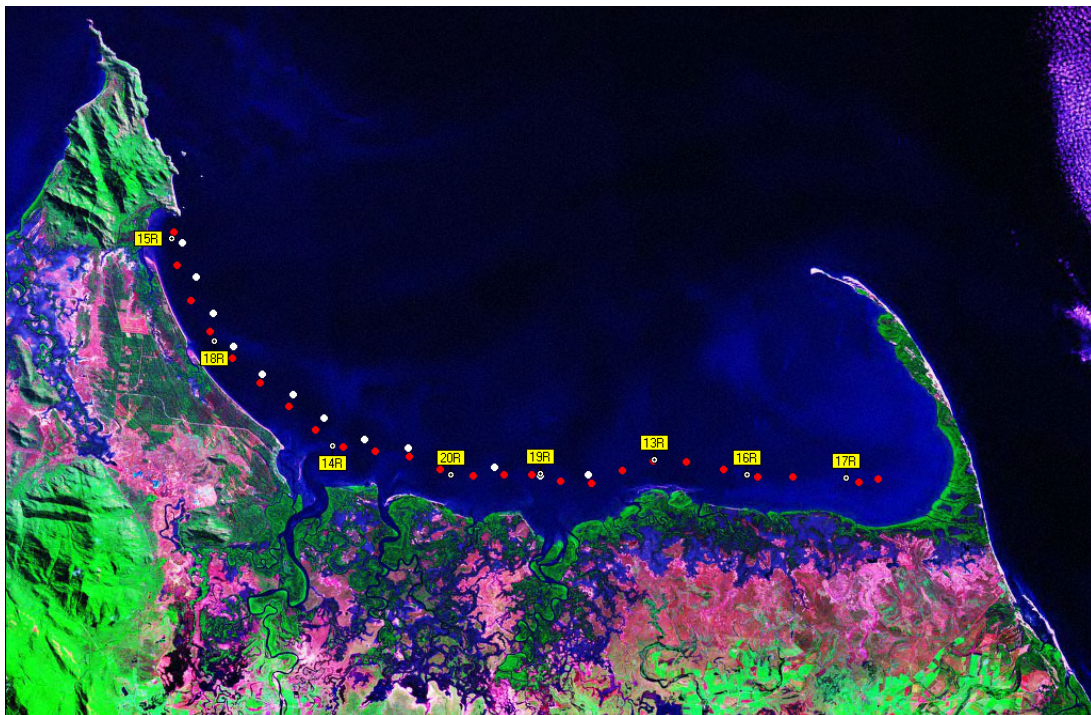


Figure 2.6. Locations of offshore radon samples. Numerals refer to sites where radon samples were obtained for scintillation counting in April 2004. White and red dots denote locations of gas stripping measurements in February and April 2004, respectively.

2.4. Radon Analyses

Measurements of radon activity in groundwater were made on 14 ml samples that were collected directly from the pump outlet using a syringe. The water sample was transferred to a pre-weighed teflon-coated PTFE scintillation vial containing 6 ml Packard NEN mineral oil cocktail. The radon activity was counted in the laboratory by liquid scintillation, on a LKB Wallac Quantulus counter using the pulse shape analysis program to discriminate alpha and beta decay (Herczeg et al., 1994). Corrections were made for radioactive decay that occurs between the time of sampling and time of analysis in the laboratory.

Radon activities in surface waters were measured using both liquid scintillation counting and a radon-in-air monitor. Samples for liquid scintillation counting were collected in 1250 ml plastic bottles, which were filled without headspace. Within 24 hours of sample collection, radon was extracted from these water samples by shaking with mineral oil scintillant. Approximately 1000 ml of water was placed into a 1 litre teflon-coated separatory funnel, to which was added approximately 20 ml of Packard NEN mineral oil cocktail from a 22 ml pre-weighed scintillation vial. The flask was shaken for four minutes to degas the radon and equilibrate it between the water-gas-scintillant phases. After allowing the scintillant to settle to the top of the inverted flask (about 1 minute), the scintillant was returned to the vial, sealed and the time recorded. The vials were returned to Adelaide by courier for counting within 7 days of sample collection, and counted by liquid scintillation. Efficiency of radon extraction and counting was $49 \pm 2\%$. Duplicates were within 5%.

Radon activities were also measured using a commercial radon-in-air monitor (Burnett and Dulaiova, 2003). Seawater was pumped directly through an air-water exchanger, which removes ^{222}Rn from the water by evasion into the chamber. The ^{222}Rn -enriched air was circulated in a closed air-loop connected to the monitor. The monitor counts α -decays of radon daughters, and discriminates different decays in energy-specific windows. With this method, continuous measurements of ^{222}Rn can be made.

Figure 2.7 depicts a comparison of measured radon activities using scintillation counting and gas stripping methods. Comparisons were made on a single bore (Alligator Creek, south of Townsville), seven stream and estuary samples, and on eight offshore seawater samples. For the offshore samples, measurements by gas stripping were made every 15 minutes, while the boat was travelling at a speed of 3 – 5 knots, and so each measurement represents an average over a distance of approximately 1800 m. In contrast, samples for scintillation counting were collected at discrete locations. Differences in measured activities may thus in part be due to this difference in spatial resolution of the methods. The mean difference between measured activities was approximately 60%, with measured activities ranging between 3 and 41 mBq/L. (The highest and lowest values were measured by scintillation counting, which is consistent with less spatial averaging in this method.) Comparison of stream, estuary and bore samples were not made from a mobile platform, and so are more directly comparable. For stream and estuary samples, the mean difference in activity between the two methods is 30%, with activities ranging between 50 and 174 mBq/L. For the single bore sample, an activity of 49 900 mBq/L was measured by scintillation counting, with 25 350 measured by the gas stripping method. The difference is attributed to non-linearity at such high activities of the counter used in the gas stripping method.

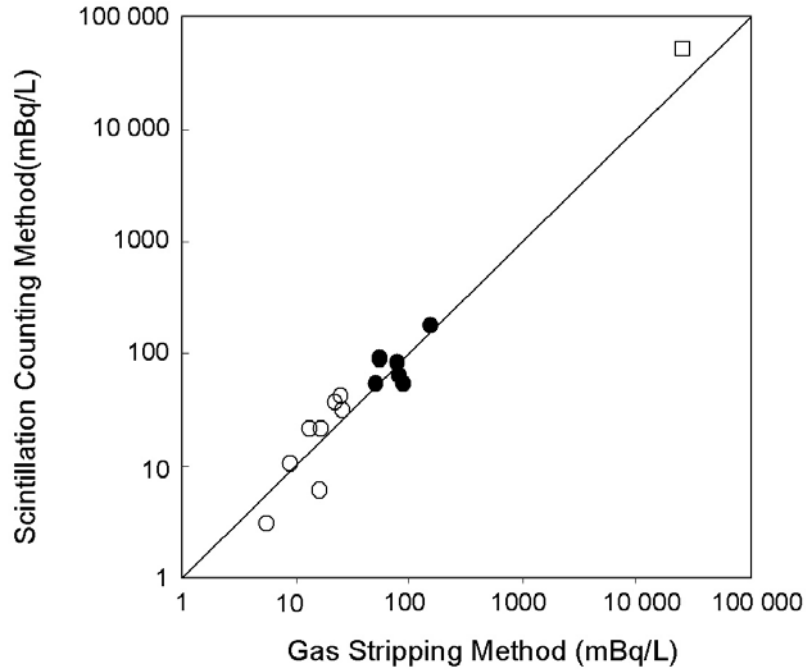


Figure 2.7. Comparison of radon activities measured using scintillation counting and gas stripping methods. Open circles denote seawater samples, closed circles denote river and estuary samples and the square represents a groundwater sample.

2.5. Radium Analyses

Radium isotopes were extracted from large volume water samples by adsorbing the isotopes onto MnO₂-coated acrylic fibers (Moore, 1976). Water was gravity-fed or slowly pumped past the MnO₂-fibers, thereby removing nearly all of the dissolved radium. Between 30 and 50 litres of water was used for groundwater samples, between 60 and 100 litres for surface water samples, and between 135 and 210 litres for seawater samples. Activities of the short-lived isotopes ²²³Ra and ²²⁴Ra are measured in the laboratory shortly after sample collection by the detection of the α -decay of their respective daughter nuclides (²¹⁹Rn and ²²⁰Rn) with photomultiplier tubes, and their identification with a delayed coincidence circuit (Moore and Arnold, 1996). Activities of the long-lived radium isotopes, ²²⁶Ra and ²²⁸Ra, are determined by α -ray spectrometry (Moore, 1984).

3. DISCHARGE TO STREAMS

3.1 Introduction

Although the direction and relative magnitude of groundwater – surface water exchange can be assessed from a comparison of surface water and groundwater heads, the dynamic nature of the aquifer and the uncertainty in hydraulic parameters mean that it is difficult to quantify the flux using hydraulic methods. In this chapter, inflows of groundwater to the Burdekin River, Haughton River, Barratta Creek, and also to other surface water bodies within the Burdekin River floodplain have been estimated based on comparison of radon activities and ion concentrations in surface waters and groundwater. The major surface water sampling took place between 26 April and 4 May 2004, designed to coincide with the time of expected maximum groundwater inflow. Samples were also collected between 8-16 December 2003 when groundwater inflows were expected to be low, and between 3-6 February 2004. Figure 3.1 depicts flow rates of the Burdekin River, Haughton River and Barratta Creek between 1 November 2003 and 31 May 2004, and rainfall at Giru over this same period.

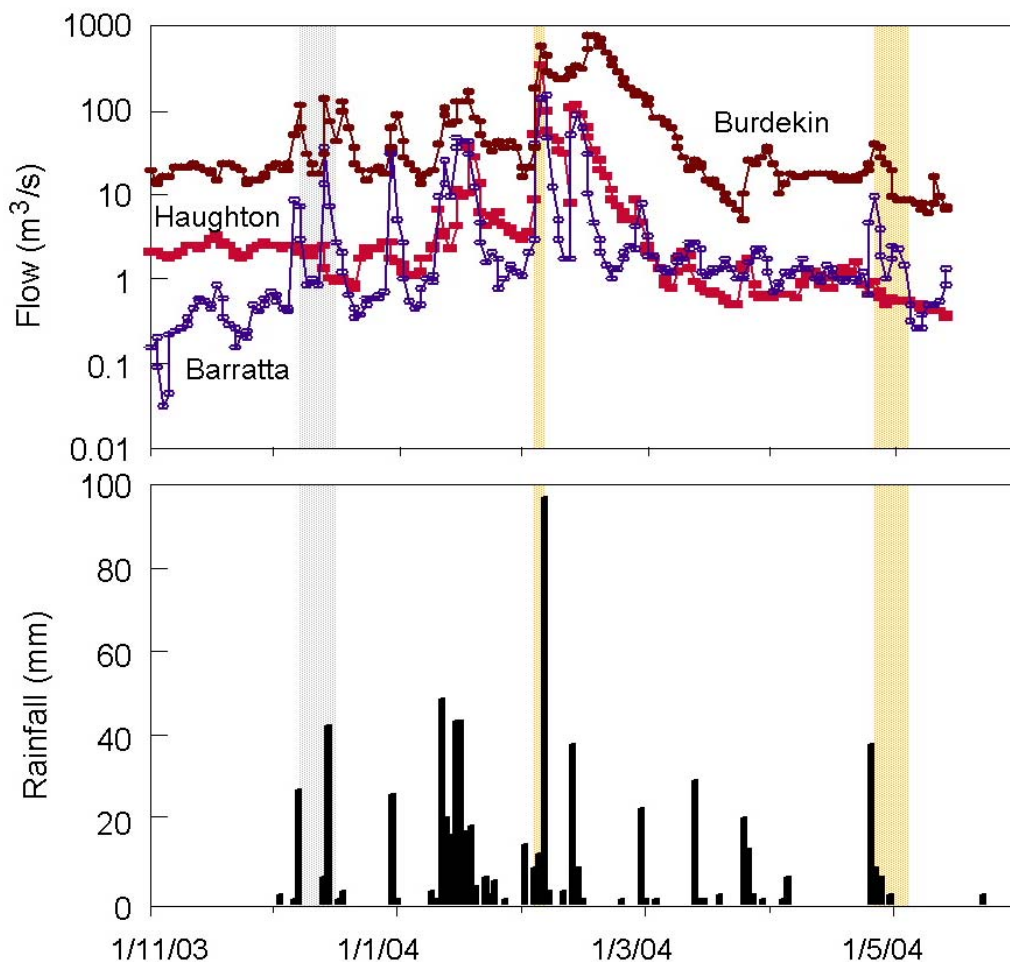


Figure 3.1. Flow rates of Burdekin River at Clare (Station 120006B), Haughton River at Powerline (119003A) and Barratta Creek at Northcote (119101A), and daily rainfall at Giru between 1 November 2003 and 31 May 2004. Surface water sampling times are indicated by shaded regions.

3.2. Theory

The radon content of a stream will be a balance between radon added in groundwater and surface water inflow and radon lost in groundwater outflow, groundwater pumping, gas exchange with the atmosphere and radioactive decay. The radon lost in groundwater outflow and groundwater pumping from the river can usually be neglected, as it will only be significant where this constitutes a significant fraction of the total river flow. Water exchange with the hyporheic zone can also be significant, particularly when other groundwater inflows are low or negligible. It is not considered here. With these simplifications, changes in radon content within a stream receiving only groundwater inflow can be expressed:

$$\frac{\partial Qc}{\partial x} = Ic_i - kwc - \lambda dwc \quad [3.1]$$

where c is the radon activity within the stream, c_i is the activity in groundwater inflow, Q is the stream flow rate (m^3/day), I is the groundwater inflow rate per unit of stream length ($\text{m}^3/\text{m}/\text{day}$), k is the gas transfer velocity across the water surface (m/day), λ is the radioactive decay constant (day^{-1}), w is the width of the river surface (m), d is the mean stream depth (m), and x is distance in the direction of flow.

In the absence of surface water inflow or direct rainfall input, change in flow with distance is simply given by:

$$\frac{\partial Q}{\partial x} = I - Ew \quad [3.2]$$

where E is the evaporation rate (m/day), so that the equation for activity with distance becomes:

$$Q \frac{\partial c}{\partial x} = I(c_i - c) + wEc - kwc - dw\lambda c \quad [3.3]$$

The decay coefficient for radon is $\lambda = 0.18 \text{ day}^{-1}$. The last three terms in Equation 3.3 represent changes in activity due to evaporation (which increases the radon activity in the remaining water), gas exchange (which decreases the radon activity) and radioactive decay (which decreases the activity). The relative magnitudes of these three terms are proportional to E , k and $d\lambda$, respectively. Since E is usually in the range $10^{-3} - 10^{-2} \text{ m}/\text{day}$ (1-10 mm/day), and k is usually in the range $0.5 - 25 \text{ m}/\text{day}$ (Wanninkof et al., 1990), it is clear that the evaporation term will usually be negligible. The relative magnitudes of the gas exchange and radioactive decay terms will depend on the value of k and the river depth. For a gas exchange velocity of $k = 1 \text{ m}/\text{day}$, the radioactive decay term will dominate when the river depth exceeds approximately $d = 5.5 \text{ m}$. For shallow streams, gas exchange is the main process controlling radon loss.

If for a particular reach of the river, parameters I , E and k do not change with distance, then

$$Q(x) = Q_0 + (I - Ew)x \quad [3.4]$$

where Q_0 is the river flow rate at the start of the river reach ($x = 0$). We can then calculate the concentration as a function of distance by solving Equation 3.3 subject to boundary condition

$$c = c_0 \text{ at } x = 0 \quad [3.5]$$

The change in activity with distance over this reach is:

$$c(x) = \left(c_0 - \frac{Ic_i}{I - wE + kw + dw\lambda} \right) \left(\frac{Q_0}{Q_0 + Ix - wEx} \right)^p + \frac{Ic_i}{I - wE + kw + dw\lambda} \quad [3.6]$$

where

$$p = \frac{I - wE + kw + dw\lambda}{I - wE} \quad [3.7]$$

As x increases, the activity will approach

$$c_\infty = \frac{Ic_i}{I - wE + kw + dw\lambda} \quad [3.8]$$

It is easy to show that the scale length for the change in activity (i.e., the distance at which the activity is halfway between the initial value, c_0 , and its equilibrium value, c_∞) will be

$$x = \frac{Q_0}{I - Ew} (2^{1/p} - 1) \quad [3.9]$$

If parameters I , E or k change with distance, then Equation 3.3 needs to be solved numerically.

3.3. Radon Activity in Groundwater

The distribution of radon activities measured in groundwater are shown in Figure 3.2. (Activities measured at each bore are listed in Table A3.1 in Appendix 3.) For the 38 sampled wells, activities ranged between 2735 and 33 750 mBq/L, although 70% of sampled bores had activities between 5000 and 15 000 mBq/L. There is no obvious spatial patterning to these observed variations. The mean activity of all bores is approximately 13 700 mBq/L.

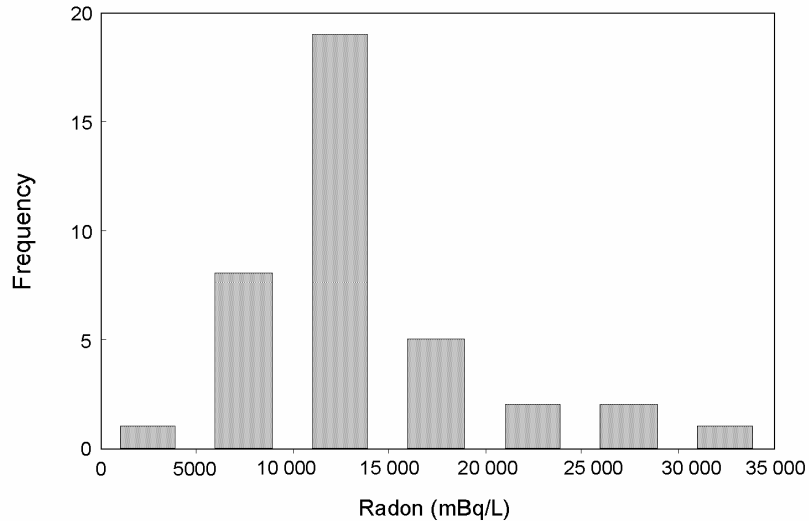


Figure 3.2. Distribution of radon activities in groundwater, grouped into 5000 mBq/L classes. The mean activity is approximately 13 700 mBq/L.

3.4. Burdekin River and Groper Creek

Nine gauging stations are located on the Burdekin River and Groper Creek systems, although only five of these have been operational since the construction of the Burdekin River Dam. At Clare Weir (Station 12000151) the surface water level is more than 10 m above water levels in surrounding monitoring bores (see Appendix 4). At Clare 'A' Pump Station (12000152), located approximately 7 km below the Clare Weir, groundwater levels on both sides of the river are above the surface water level by 2-3 m. Further downstream, river levels are above groundwater levels at The Rocks Pumping Station (12000153) and at SBWB Pumping Station (12000155). At the Annabranche Bridge (11910154), surface water and groundwater levels are similar, and it appears that the river may change from gaining to losing through the year (Figure 3.3).

Radon activities, electrical conductivities, molar chloride to bicarbonate ratios and nitrate concentrations measured in the Burdekin River in December 2003 and April-May 2004 are shown in Figure 3.4. In December 2003, the radon activity of the Burdekin River increases downstream from 25 mBq/L at Clare Weir (Site 5) to 43 mBq/L at The Rocks Pumping Station (Site 6) and 114 mBq/L at Pump Station No. 3 (Site 14). Over this same reach, the electrical conductivity increases from 147 to 165 to 173 $\mu\text{S}/\text{cm}$. Downstream of Pump Station No. 3 the radon activity decreases, and is 60 mBq/L at Site 2. The radon activity also decreases from 61 mBq/L at the confluence of the Groper Creek and MacDonald Creek (Site 10) to 44 mBq/L at Groper Creek boat ramp (Site 9) and at the confluence with Heath Creek (Site 8). At the Groper Creek mouth (Site 7) the radon activity is 21 mBq/L. The decrease in radon activity in the tidal section of the river may be in part due to dilution with seawater.

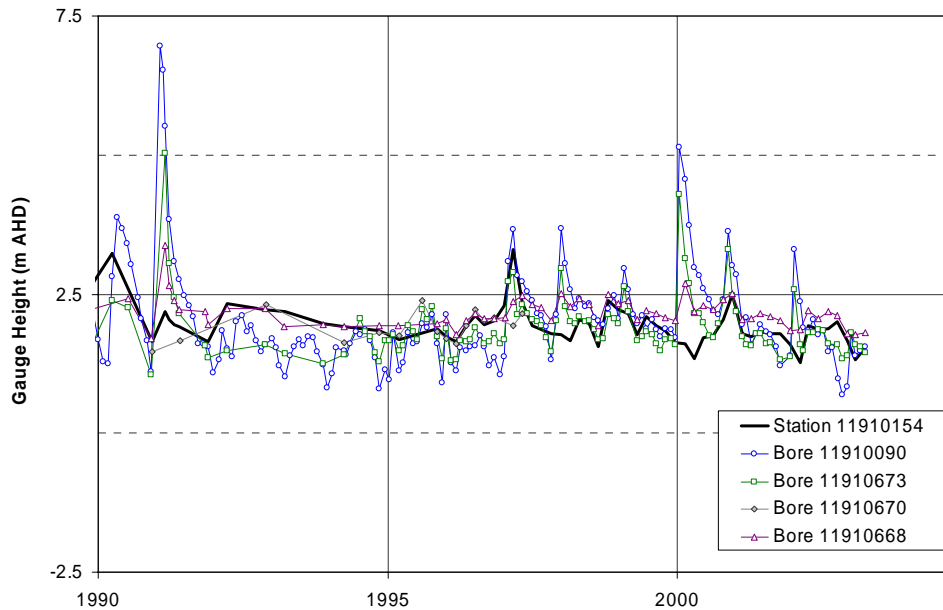


Figure 3.3. Comparison of surface water stage height measured at the Anabranch Bridge on the Burdekin River with water table elevations of nearby bores.

In April-May 2005, samples from the Burdekin River were taken on three separate occasions, spanning a period of six days. On April 26, the radon activity was 79 mBq/L at The Rocks Pumping Station, 174 mBq/L at Pumping Station No. 3, and 77 mBq/L at Rita Island boat ramp. On April 27, the radon activity was 51 mBq/L at Clare Weir, 66 mBq/L at The Rocks Pumping Station and 119 mBq/L at Pump Station No. 3. On May 2, radon activities were 263 mBq/L 5 km downstream of Clare Weir (Site 56), 298 mBq/L at Site 55, 452 mBq/L at Site 54, 495 mBq/L at Site 53, 206 mBq/L at Site 52 and 130 mBq/L at Rita Island Boat Ramp (Site 3). Flow rates at Clare Weir were 42 m³/s on April 26, 39 m³/s on April 27 and 9.5 m³/s on May 2. The much higher radon activities measured on May 2, compared with April 26-27 are consistent with the decrease in river flow, and hence a greater proportion of flow the being derived from groundwater input.

In February 2004, radon samples were collected only at Sites 6 and 14, where activities were 27 and 46 mBq/L, respectively.

Figure 3.5 depicts the relationship between flow rate of the Burdekin River at Clare and radon activity at Pump Station No. 3 (Site 14). It shows a general trend of decreasing radon activity at higher flow rates. Also shown is the relationship between flow rate at Clare, and the total radon flux at Pump Station No. 3 (calculated as the radon activity multiplied by the river flow rate). Although river flow rate varies by more than a factor of 20, the radon flux varies only by a factor of two, which is consistent with a radon input upstream of this location that is relatively stable over time.

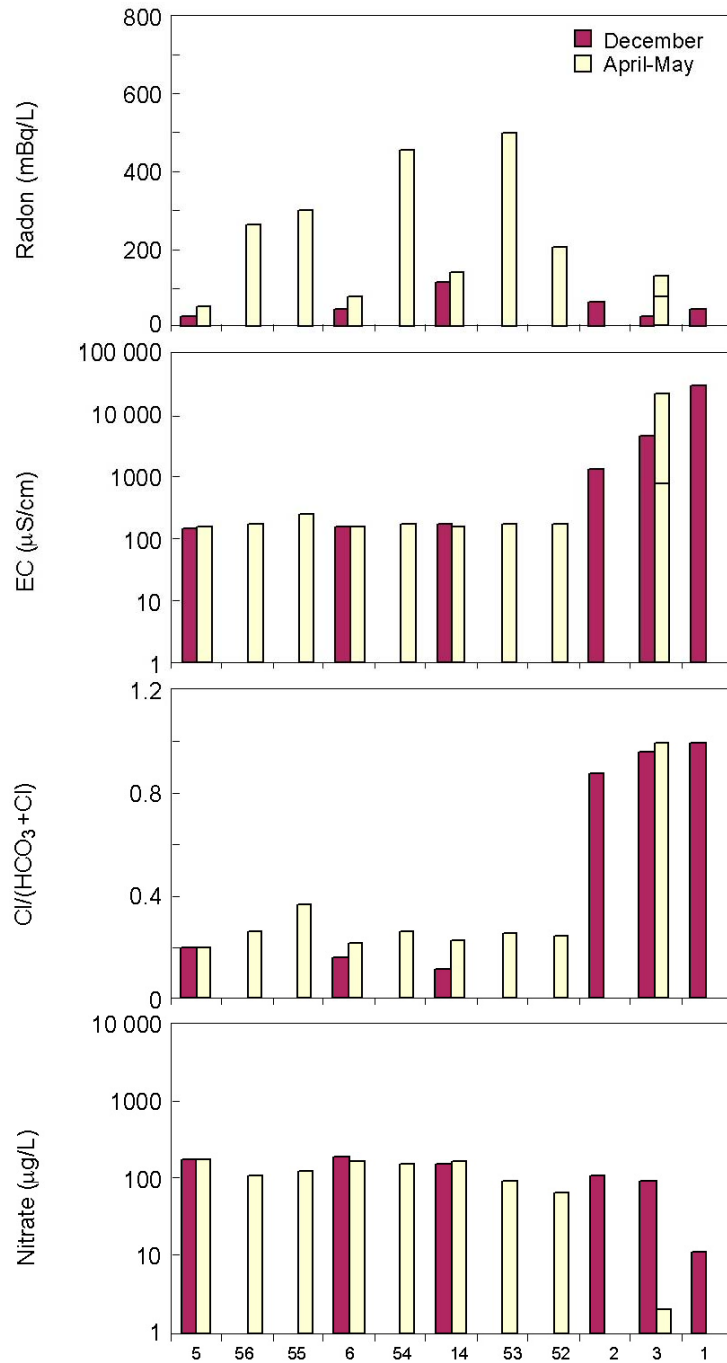


Figure 3.4. Water chemistry of the Burdekin River. Numerals on the x-axis refer to site numbers, as shown on Figure 2.3. (Flow direction is from left to right.) (a) Radon activity; (b) electrical conductivity; (c) molar chloride to bicarbonate ratio; (d) nitrate concentration ($\mu\text{g N}$ per litre). The stacked bar for radon and electrical conductivity at Site 3 represents samples collected at different times in April-May 2004.

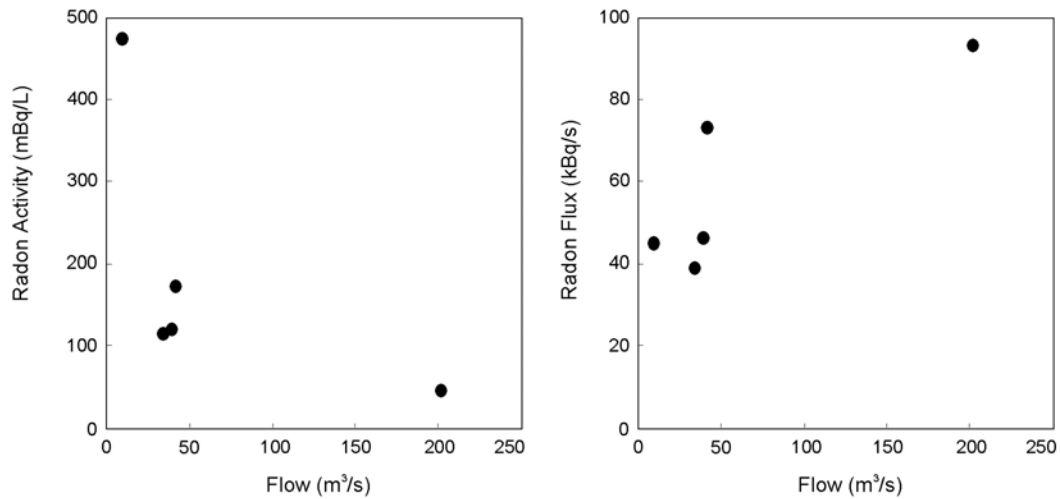


Figure 3.5. Relationship between flow rate of the Burdekin River at Clare and radon activity and radon flux at Pump Station No. 3 (Site 14). (On May 2, the radon activity for Pump Station No. 3 has been interpolated from measured activities at Sites 53 and 54.)

Figure 3.6 compares radon activities measured on 2 May 2004 with results of a numerical model describing the change in radon activity with distance downstream of Clare Weir (Equation 3.3). Parameters required by the model are the initial flow rate (Q_0) and radon activity (c_0) at the start of the river reach being modelled, the radon activity in groundwater inflow (c_i), the groundwater inflow rate per unit of stream length (I), the evaporation rate (E), the gas transfer velocity across the water surface (k), the river width (w) and mean depth (d). Studies on low gradient rivers suggest values for the gas exchange velocity of $0.5 < k < 2$ m/day (Hibbs et al., 1998; Chapra and Wilcock, 2000; Raymond and Cole, 2001). The simulation shown in Figure 3.6 uses parameters $Q_0 = 9.5$ m³/s, $c_0 = 240$ mBq/L, $c_i = 13$ 000 mBq/L, $k = 1$ m/day, $d = 1$ m, $w = 100$ m between 0 and 31 km and $w = 135$ m downstream of 31 km (Table 3.1). The evaporation rate has been modelled as $E = 7$ mm/day, although the simulations are insensitive to this parameter. The estimated groundwater inflow between Site 56 and Site 55 is 2.8 m³/day/m, increasing to 4.7 m³/day/m for the river reach between Site 55 and 31 km (near Site 14). A further increase in groundwater discharge to 6.3 m³/day/m is required between 31 km and Site 53 to compensate for the increase in river width. The observed decrease in radon activity downstream of Site 53 is consistent with negligible groundwater inflow, and radon loss through exchange with the atmosphere (Figure 3.6b). The total estimated groundwater inflow over the 29.7 km distance between Site 56 and Site 53 is 127 300 m³/day.

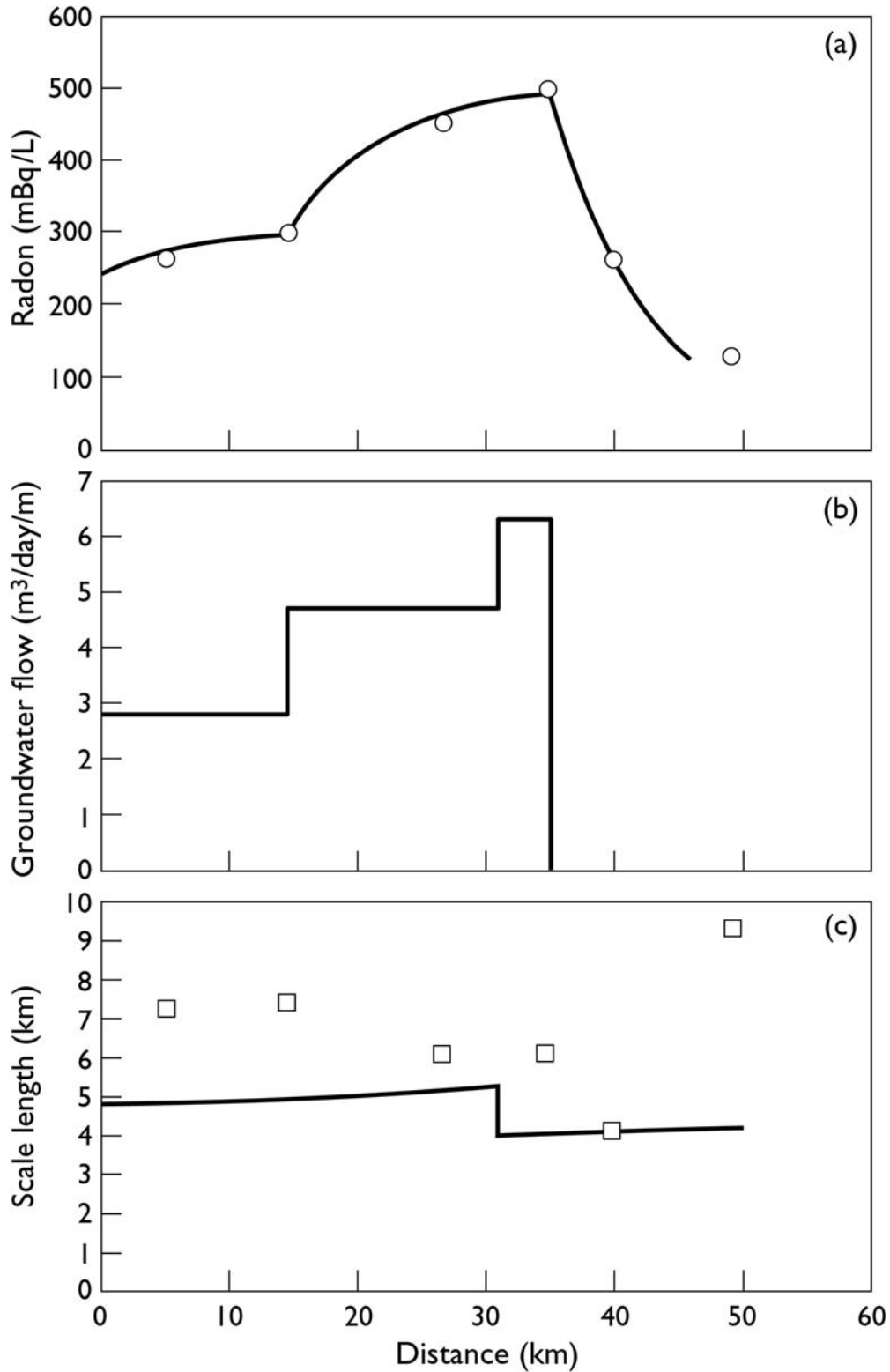


Figure 3.6. Numerical simulation of radon activity in the Burdekin River. (a) Comparison of radon activity measured in the Burdekin River on 2 May 2004 with results of numerical model. (b) Estimated groundwater inflows. (c) Comparison of scale length for changes in radon activity and sampling frequency. The solid line depicts the scale length, as given by Equation 3.9. Symbols denote the distance between sampling sites for 2 May 2004. The comparison of the scale length with the sampling intensity provides an indication of the reliability of the inferred groundwater inflows.

Figure 3.6c depicts the scale length for changes in radon activity within the river, calculated using Equation 3.9. The scale length reflects the ability of the model to resolve small-scale changes in any of the input parameters (particularly I , k and w), and is related to the mean values of these parameters. For the Burdekin River, variations in any of these parameters on a scale much less than 5 km could not be resolved with radon sampling. Rather, the method is sensitive to mean values of these parameters over this scale. Figure 3.6c also shows the distance between sampling sites for 2 May 2004. The comparison of the scale length with the sampling intensity provides an indication of the reliability of the inferred groundwater inflows. Where the distance between sampling points is much greater than the scale length, groundwater inflow rates will not be well-constrained, irrespectively of the accuracy of the other model parameters. In this case, the distance between sampling sites is generally within 50% of the scale length, and so inflow rates are regarded as well-constrained over the entire river length.

Table 3.1. Input parameters used for modelling of radon activities in rivers.

Parameter	Burdekin River	Haughton River	Barratta Creek		Plantation Creek	
	2 May 2004	May 2004	Dec 2003	May 2004	Dec 2003	Feb 2004
Q_0 (m ³ /s)	9.5	0.5	1	0.5	6.0	6.0
c_0 (mBq/L)	240	140	16	75	114	46
c_i (mBq/L)	13 000	13 000	13 000	13 000	13 000	13 000
k (m/day)	1	1	1	1	8	8
w (m)	100/135	variable	variable	variable	6	6
d (m)	1	1	1	1	1	1

Even in regions where the sampling frequency is sufficiently close, modelled groundwater inflows rates will still be dependent on values of the other model parameters (e.g., k , d , w , c_i), none of which are known with a high degree of certainty. We have performed a simple sensitivity analysis on this modelling, by varying some of these input parameters over the river reach between Sites 55 and 54. As mentioned above, changing the evaporation rate within an acceptable range has negligible effect on the modelled radon activities. An increase in river width of 50% (to 150 m) results in a decrease in river velocity and also causes an increase in the gas loss to the atmosphere. Simulation of the observed data with this increased river width therefore requires an increase in groundwater inflow of 50% to compensate for the increased radon loss through gas exchange. Similarly, a 50% decrease in river width (to 50 m) can be compensated for by a 45% decrease in groundwater inflow. Figure 3.7 shows the sensitivity of estimated groundwater inflow to changes in river depth, gas exchange velocity and radon activity in groundwater, as well as river width. As can be seen, the estimated groundwater inflows are most sensitive to changes in radon activity of groundwater inflow and least sensitive to the river depth.

Over the 5.2 km reach between Sites 53 and 52, however, groundwater inflows are modelled to be zero, and so reduction in either the river width or the gas exchange rate cannot be compensated for by decreasing groundwater inflows. In this reach of the river, the rate of decrease in radon activity constrains the value of the parameter $kw > 100$ m²/day. Increasing the gas exchange rate or river width by 50% can be compensated for by increasing the groundwater inflow to 1.5 – 1.8 m³/day/m. Because zero groundwater inflow is modelled, the sensitivity to radon activity of

groundwater inflow is nil. As for the upstream reach, the sensitivity to river depth is very small.

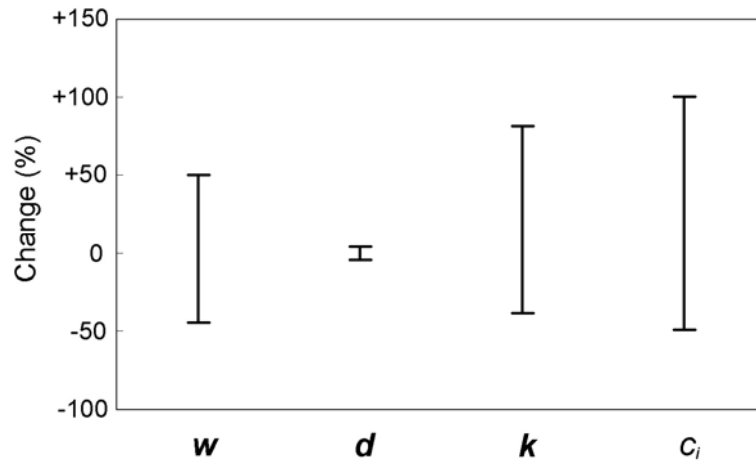


Figure 3.7. Sensitivity of estimated groundwater inflows between Sites 55 and 54 to changes in river width (w), river depth (d), gas exchange velocity (k) and radon activity of groundwater inflow (c_i). The y-axis shows percentage changes in estimated groundwater inflow for $\pm 50\%$ changes in the other parameters. An increase in river width, river depth and gas exchange velocity results in an increase in estimated groundwater inflow. For radon activity in groundwater inflow, the sensitivity is reversed.

Groundwater inflow at other times of year can be estimated for part of this river reach from measurements of radon activity made at different times through the year at Sites 6 and 14. On December 9 (river flow of $34 \text{ m}^3/\text{s}$ at Clare), the groundwater inflow between Site 6 and Site 14 is estimated to be $2.1 \text{ m}^3/\text{day}/\text{m}$. On February 3, the groundwater inflow between these same two sites is estimated to be $2.4 \text{ m}^3/\text{day}/\text{m}$ (river flow $202 \text{ m}^3/\text{s}$). On April 26 and 27 the groundwater inflow is estimated to be $3.4 \text{ m}^3/\text{day}/\text{m}$ (river flow $42 \text{ m}^3/\text{s}$) and $2.0 \text{ m}^3/\text{day}/\text{m}$ (river flow $39 \text{ m}^3/\text{s}$), respectively. The relatively constant input of groundwater throughout the year suggested by the model is consistent with the inverse relationship between radon activity and river flow rate apparent in Figure 3.5.

3.5. Haughton River

Haughton River levels have been measured at the Highway Bridge (11900077) since 1972 (Figure 3.8). Comparison of surface water levels with groundwater heads in nearby bores indicates that the river is losing at this location. Gauging stations 11900079 and 11900085 show similar patterns, with surface water levels consistently above groundwater levels since the late 1980s.

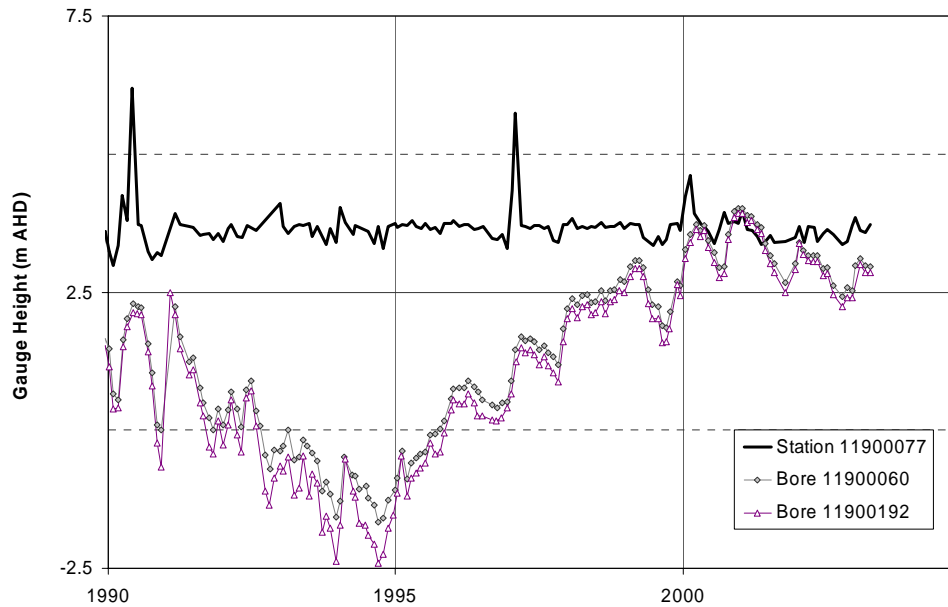


Figure 3.8. Comparison of surface water stage height measured at the highway bridge on the Haughton River with water table elevations of nearby bores.

Figure 3.9 shows the width of the Haughton River in June 2004, based on measurements of river width at 14 points, given in Table A1.1 (Appendix 1). At Site 70, where the DPI channel discharges into the Haughton River, the river width was measured to be 5 m. Further downstream, the river width increases to 10 m at Site 69 and 8 m at the road crossing 1.5 km upstream of Site 68. Further downstream the river width increases rapidly, and near Site 45, the river width was measured to be 85 m. The abrupt decreases in river width at 19 km and 26 km reflect the locations of Val Bird Weir and Giru Weir, respectively. Immediately below Giru Weir, the river width was only 2 m in June 2004, although flow had almost ceased at this time. At Site 51, the river width was 10 m. The river width increases in the tidal section of the river, to be more than 100 m downstream of Site 23.

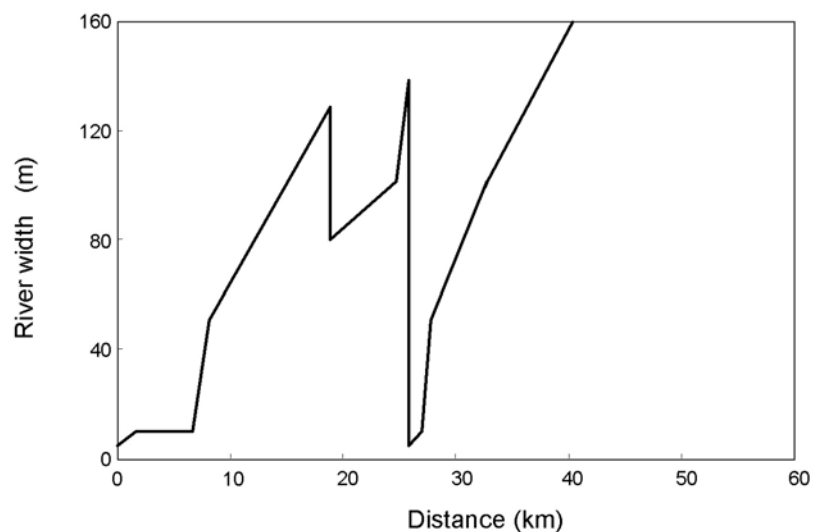


Figure 3.9. Simplified diagram showing approximate width of the Haughton River as a function of distance below Site 70. The abrupt decreases in river width at 19 km and 26 km reflect the locations of Val Bird Weir and Giru Weir.

The highest radon activity measured in December 2003 was 263 mBq/L, 5 km upstream of the boat ramp on the Houghton River (Site 21; Figure 3.10). The radon activity then decreases downstream to 29 mBq/L at the boat ramp (Site 23) and to 13 mBq/L at the mouth (Site 22). In February 2004, activities of 294 mBq/L and 97 mBq/L were measured at Sites 42 and 23 respectively.

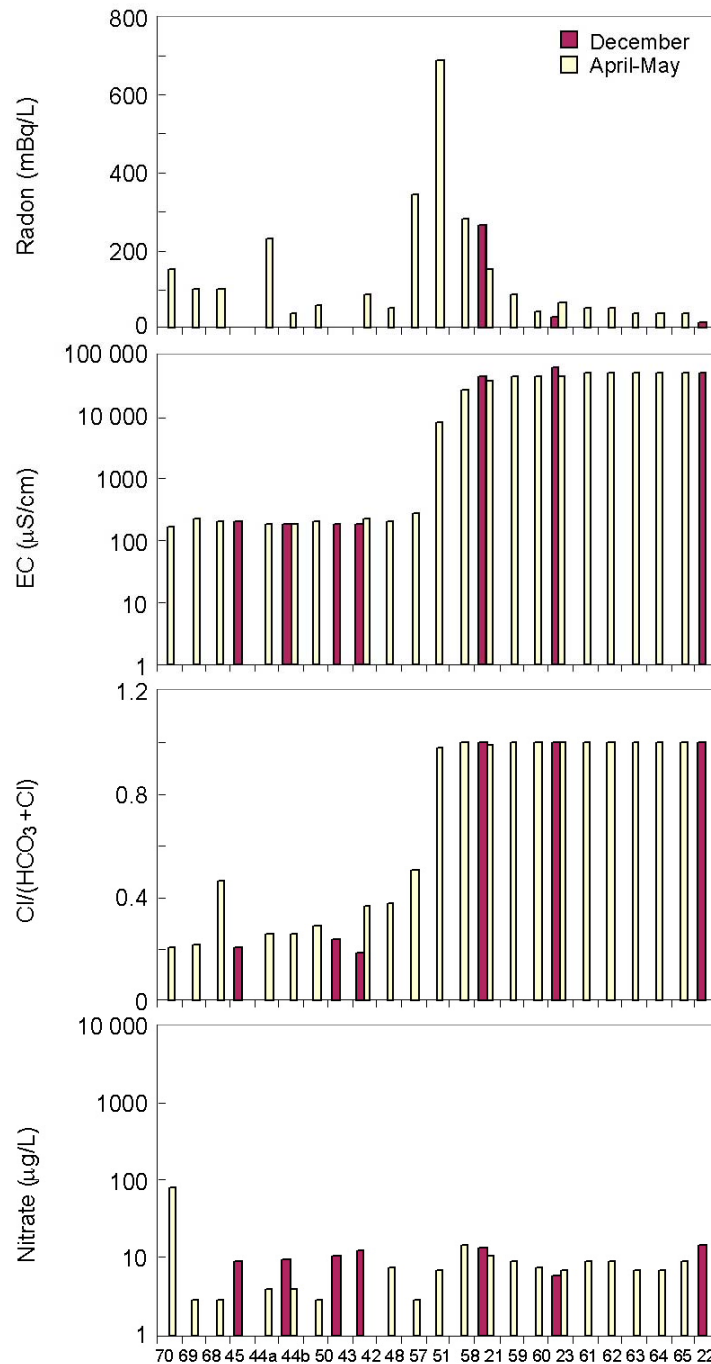


Figure 3.10. Water chemistry of the Houghton River. Numerals on the x-axis refer to site numbers, as shown on Figure 2.3. Sites 44a and 44b refer to samples collected immediately above and below Val Bird Weir, respectively. (Flow direction is from left to right.) (a) Radon activity; (b) electrical conductivity; (c) molar chloride to bicarbonate ratio; (d) nitrate concentration ($\mu\text{g N per litre}$).

The most detailed radon sampling occurred between 4-6 May 2004, when the flow rate of the Houghton River at Powerline (Station 119003A) was approximately 0.5 m³/s. The radon activity decreased from 153 mBq/L at Site 70, to 98 and 99 mBq/L at Sites 69 and 68, and 226 mBq/L above Val Bird Weir (Site 44). A significant decrease in radon activity occurred as the water flowed over Val Bird Weir, and the radon activity immediately below the weir was only 38 mBq/L. The activity then increased downstream to 57 mBq/L at Site 50 and 79 mBq/L at Site 42, before decreasing to 53 mBq/L at Site 48, immediately above Giru Weir. Electrical conductivity follows the same trend as the radon, increasing from 190 μ S/cm at Val Bird Weir to 210 μ S/cm at Site 50, then 236 μ S/cm at Site 42, and decreasing to 213 μ S/cm at Site 48. The decrease in both radon activity and electrical conductivity between Sites 42 and 48 coincides with an increase in nitrate concentration, and may indicate inflow of a small volume of irrigation tailwater. The molar chloride to bicarbonate ratio increases from 0.26 at Val Bird Weir to 0.36 at Site 42, which is also consistent with inflow of groundwater of high chloride concentration.

Immediately below Giru Weir, there is a large increase in radon activity, with the highest activity being 686 mBq/L measured at Site 51. Further downstream, radon activities decrease and electrical conductivities increase. The river is tidal downstream of the weir, and radon activities appear to be diluted with seawater. Figure 3.11 shows the relationship between electrical conductivity and radon activity for samples collected downstream of the Giru Weir. With one exception, these samples fall on a straight line, indicating mixing of fresh water and seawater. The linear relationship suggests that gas exchange along this reach of the river is approximately balanced by groundwater inflow. However, the volume of groundwater inflow must also be small compared to the volume of tidal water, or the salinity would be affected. The sample that does not fit on this linear trend is for the furthest upstream of these samples (Site 57), and indicates that significant groundwater inflow occurs between Sites 57 and 58.

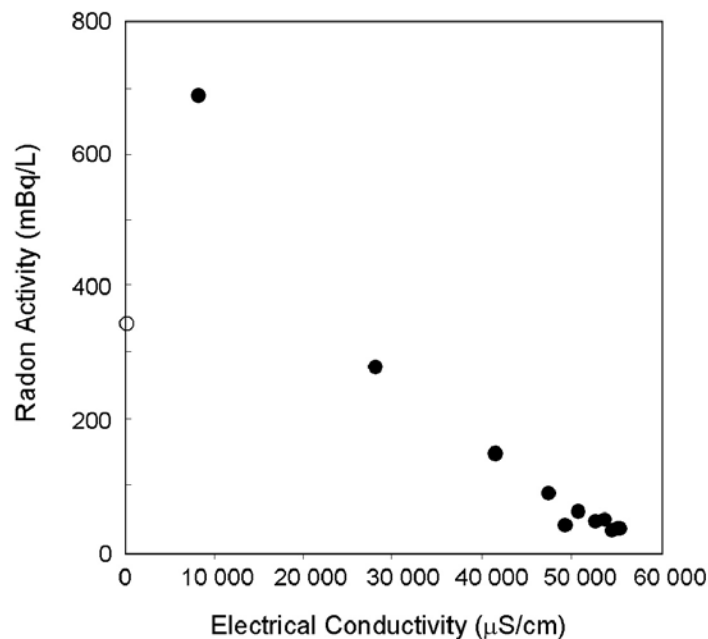


Figure 3.11. Relationship between radon activity and electrical conductivity for samples collected below Giru Weir in May 2004.

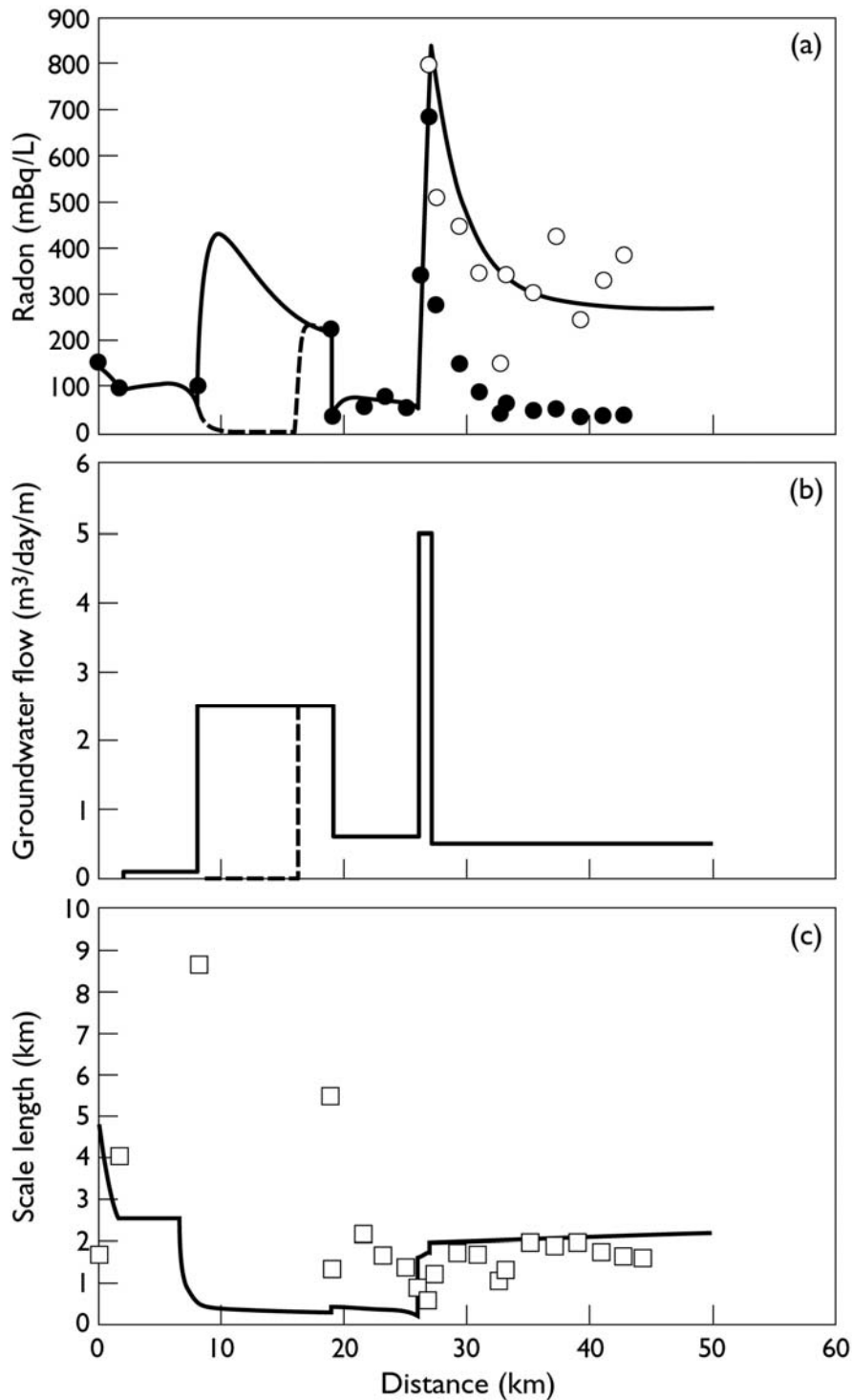


Figure 3.12. Numerical simulation of radon activity in the Houghton River. (a) Comparison of radon activity measured in the Burdekin River in May 2004 with results of numerical model. Closed circles denote measured radon activities, and open circles denote activities that have been corrected for seawater dilution (see text). The decrease in activity at 19 km is due to degassing during flow across Val Bird Weir. Solid and broken lines represent alternative simulations that both fit observed data. (b) Estimated groundwater inflows. (c) Comparison of scale length for changes in radon activity and sampling frequency. The solid line depicts the scale length, as given by Equation 3.9. Symbols denote the distance between sampling sites. The comparison of the scale length with the sampling intensity provides an indication of the reliability of the inferred groundwater inflows.

Figure 3.12a compares radon activities with results of the numerical model. The river width used in the modelling is shown in Figure 3.9, except that we have used a constant river width of 20 m downstream of Giru Weir. Other model parameters are given in Table 3.1. The estimated groundwater inflows along the length of the river are shown in Figure 3.12b. The total groundwater inflow for the 26 km reach between Site 70 and Giru Weir is estimated to be 32 300 m³/day, although most of this is attributed to the 8 – 16 km reach, where there is an absence of radon measurements. If there was no groundwater inflow along this reach, then the fit to the observed radon data is still satisfactory, and the groundwater inflow between Site 70 and Giru Weir becomes 12 300 m³/day. The unreliability of the groundwater inflows predicted between 8 and 16 km is apparent from Figure 3.12c, which shows that the spacing between sampling sites in this area is much greater than the scale length for changes in radon activity. An additional groundwater inflow of 5000 m³/day is required immediately below Giru Weir (at 27 km), to produce the observed sharp increase in radon activity. Because groundwater inflow in this short reach of river dominates the radon budget, the model shows little sensitivity to other parameters. For example $\pm 50\%$ uncertainty in gas exchange velocity produces less than $\pm 15\%$ uncertainty in inflow rate.

Downstream of Site 51, groundwater inflow rates can be determined from radon activities only after first correcting for the dilution of radon by mixing with seawater. Since the volume of groundwater input relative to the river flow rate is relatively small, we can estimate the proportion of seawater in the mixture using a simple mass balance:

$$p = \frac{EC_{mix} - EC_B}{EC_A - EC_B} \quad [3.10]$$

where EC_{mix} , EC_A and EC_B are the electrical conductivities of the mixture and of end-members A and B , and p is the proportion of end-member A in the mixture. If the radon activity is known in one end-member and in the mixture, we can then determine the activity in the unknown second end-member using

$$C_A = \frac{C_{mix} - (1 - p)C_B}{p} \quad [3.11]$$

Using $EC_B = 55\,000\ \mu\text{S}/\text{cm}$ as the electrical conductivity of seawater, $EC_A = 200\ \mu\text{S}/\text{cm}$ as the electrical conductivity of river water, and $C_B = 20\ \text{mBq}/\text{L}$ as the radon activity of seawater, we can estimate the radon activities that would have occurred in the river if they were not diluted by seawater. These corrected radon activities are indicated on Figure 3.12a. There is some scatter in this data, largely due to uncertainties in this correction process. The corrected activities are simulated using a groundwater inflow rate of approximately $0.5\ \text{m}^3/\text{day}/\text{m}$ between 27 km and 44 km river distance. This represents an additional groundwater input of $8\,500\ \text{m}^3/\text{day}$, giving a total inflow of between $25\,800$ and $45\,800\ \text{m}^3/\text{day}$ for the 44 km reach of river between Site 70 and the mouth (Site 22) for May 2004.

It is difficult to directly compare the estimates of groundwater inflow derived from radon activities with the limited hydraulic information derived from comparison of surface water heights and groundwater levels. Hydraulic information (Figure 3.8) suggests that the river is losing at the Highway bridge (at $\sim 21\ \text{km}$), whereas we have modelled low rates of groundwater inflows along the entire reach between Val Bird

Weir and Giru Weir. While the increase in radon activity between Val Bird Weir and Site 50 suggests some groundwater inflow in this reach, this is not inconsistent with a losing river over some part of the reach. As groundwater levels will vary depending on locations of pumping bores and rates of groundwater extraction, small-scale variation in groundwater inflows, and variations between losing and gaining are entirely possible.

3.6. Barratta Creek

There are two surface water gauging stations on Barratta Creek (11910206 and 11910207), although only one (11910207) is currently operational. Comparison of gauge heights on West Barratta Creek (11910207) with nearby bores indicates that the river is gaining for most of the time (Figure 3.13). The gradient only reverses during the wet season, when the water level in the river may rise by up to 5 m in response to rainfall within the catchment. An exception to this occurred between 1995 and 1997 when groundwater levels were relatively low, and were below the level of the river.

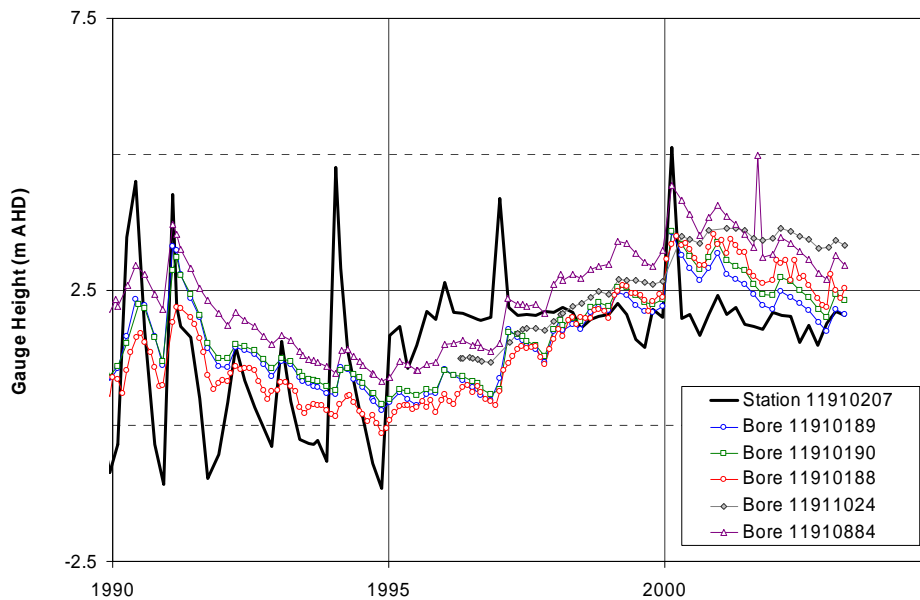


Figure 3.13. Comparison of surface water stage height measured near the highway bridge over West Barratta Creek with water table elevations of nearby bores.

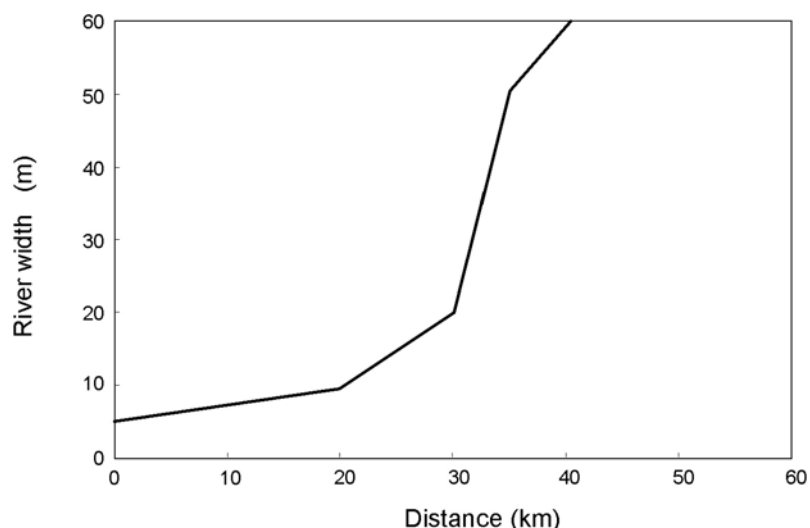


Figure 3.14. Approximate river width for East Barratta Creek.

Barratta Creek was sampled between Clare Road (Site 20) and the mouth (Site 24). At the Clare Road crossing, the river width in June 2004 was approximately 5 m. Approximately 17.5 km downstream of the crossing the river bifurcates. Sites 18, 66 and 46 sample the West Barratta Creek, which drains into Bowling Green Bay east of Conners Island. The remainder of the samples occur on East Barratta Creek, which enters Bowling Green Bay downstream of Hucks Landing. The width of East Barratta Creek was measured to be approximately 30 m above the Highway bridge, but decreased to only 5 m immediately downstream. Field measurements of river width were not made further downstream, but have been estimated from aerial photography (Figure 3.14). In the wet season, the river spreads across the floodplain north of the railway line.

Radon activities, electrical conductivities, molar chloride to bicarbonate ratios and nitrate concentrations measured in Barratta Creek in December 2003 and April-May 2004 are shown in Figure 3.15. In December 2003, the radon activity increased from 17 mBq/L at Clare Road (Site 20) to 32 mBq/L at Allen Road (Site 19), 53 mBq/L in East Barrattas Creek at the highway (Site 17) and 87 mBq/L at Site 26, before decreasing to 33 mBq/L at Site 27 and 12 mBq/L at the mouth (Site 24). Electrical conductivity increases from 249 $\mu\text{S}/\text{cm}$ at Clare Road to 426 $\mu\text{S}/\text{cm}$ at Allen Road and 471 $\mu\text{S}/\text{cm}$ at the highway, and the chloride to bicarbonate ratio increases from 0.23 at Clare Road to 0.43 at Allen Road and 0.49 at the highway. These increases are consistent with inflow of groundwater with a high chloride concentration in the upper reaches of the river.

In May 2004, the radon activity was 74 mBq/L at Site 20, 113 mBq/L at Site 19, 85 mBq/L at Site 18 and 55 mBq/L at Site 66. The radon activity then increased sharply to be 337 mBq/L at Site 46 and 406 mBq/L at Site 83. A gradual decrease in activity was observed between Site 83 and the mouth (64 Bq/L at Site 24).

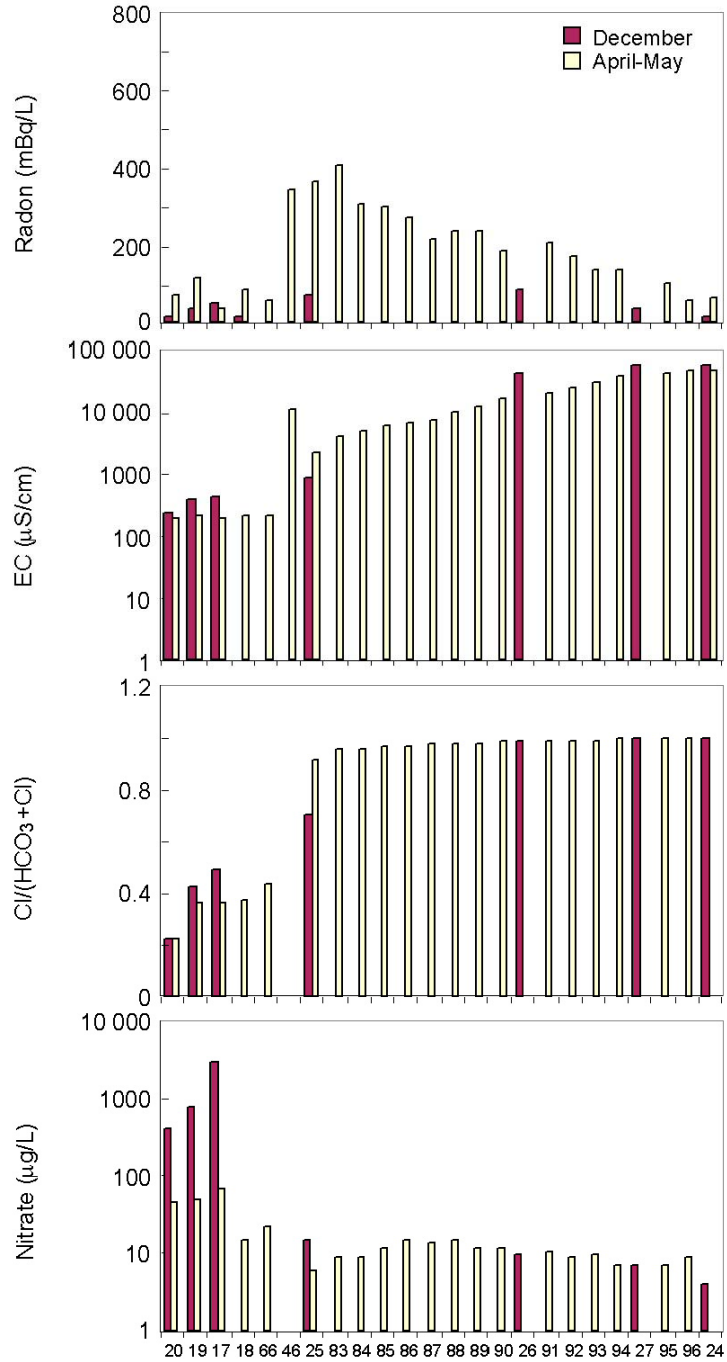


Figure 3.15. Water chemistry of the Barratta Creek. Numerals on the x-axis refer to site numbers, as shown on Figure 2.3. (Flow direction is from left to right.) (a) Radon activity; (b) electrical conductivity; (c) molar chloride to bicarbonate ratio; (d) nitrate concentration ($\mu\text{g N}$ per litre). Sites 20 and 19 occur upstream of where the Barratta Creek bifurcates to form East Barratta Creek and West Barratta Creek. Sites 18, 66 and 46 occur on West Barratta Creek, with the remainder on East Barratta Creek.

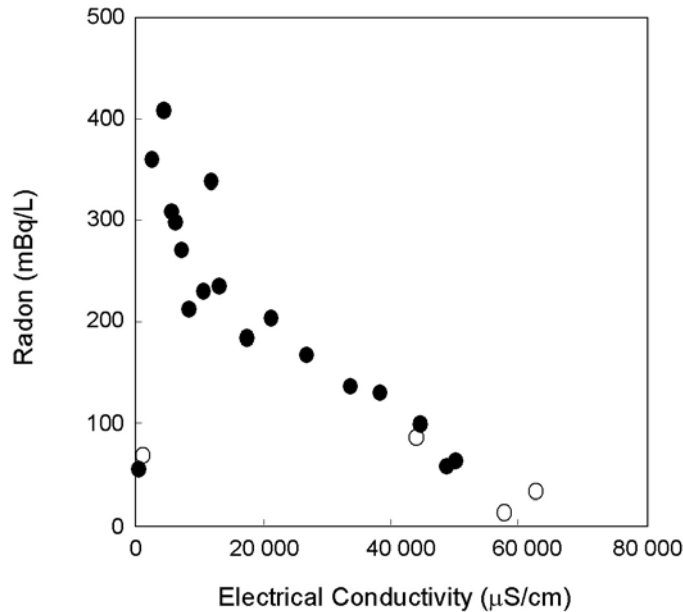


Figure 3.16. Relationship between radon activity and salinity for Barratta Creek samples collected north of the highway in December 2003 (open circles) and May 2004 (closed circles).

Figure 3.16 depicts the relationship between radon activity and electrical conductivity for Barratta Creek samples collected north of the highway. Sites 17, 18 and 66 have radon activities between 13 and 85 mBq/L, and electrical conductivities between 190 and 480 $\mu\text{S}/\text{cm}$. By Site 25, the radon activity has increased to 359 mBq/L in April-May 2004, and the electrical conductivity is 2320 $\mu\text{S}/\text{cm}$. Samples further downstream appear to fall on a mixing line with seawater.

In December 2003, nitrate concentrations in Barratta Creek increased from 400 $\mu\text{g N}/\text{L}$ at Clare Road (Site 20) to 803 $\mu\text{g N}/\text{L}$ at Allen Road (Site 19) and 3060 $\mu\text{g N}/\text{L}$ at the highway (Site 17). The latter was the highest concentration measured at any site. The April-May 2004 data also shows an increase in nitrate concentration along this reach of the river, although the concentrations are lower. The increase probably suggests inflows of irrigation tailwater. (The volume of groundwater inflow along this reach appears insufficient to cause the increase in nitrate concentration.)

Figure 3.17 compares radon activities downstream of Site 20 measured in December and May with results of the numerical model. The river width used in the model is depicted in Figure 3.14, except that a constant value of 50 m has been used in the tidal section of the river, downstream of Site 85. The initial flow rate was approximately 1.0 m^3/s at the time of sampling in December 2003, and 0.5 m^3/s at the time of the May 2004 sampling. The observed radon activities between Site 20 (at zero kilometres) and Site 83 for May 2004 are reproduced using a gas transfer velocity of $k = 1 \text{ m}/\text{day}$ and mean river depth of $d = 1 \text{ m}$. The groundwater inflow rate is thus estimated to be approximately 0.15 $\text{m}^3/\text{day}/\text{m}$ for 12 km downstream of Site 20, decreasing to 0.02 $\text{m}^3/\text{day}/\text{m}$ further downstream. There is a small escarpment immediately north of the railway line (at approximately 30 km river distance), and a groundwater inflow of 1.4 $\text{m}^3/\text{day}/\text{m}$ immediately downstream of this escarpment (between 30 and 33 km) is required to produce the observed increase in radon activity in this region. The total inflow over the 33 km reach between Site 20 and Site 25 is thus estimated to be 6360 m^3/day . In December 2003, the observed radon

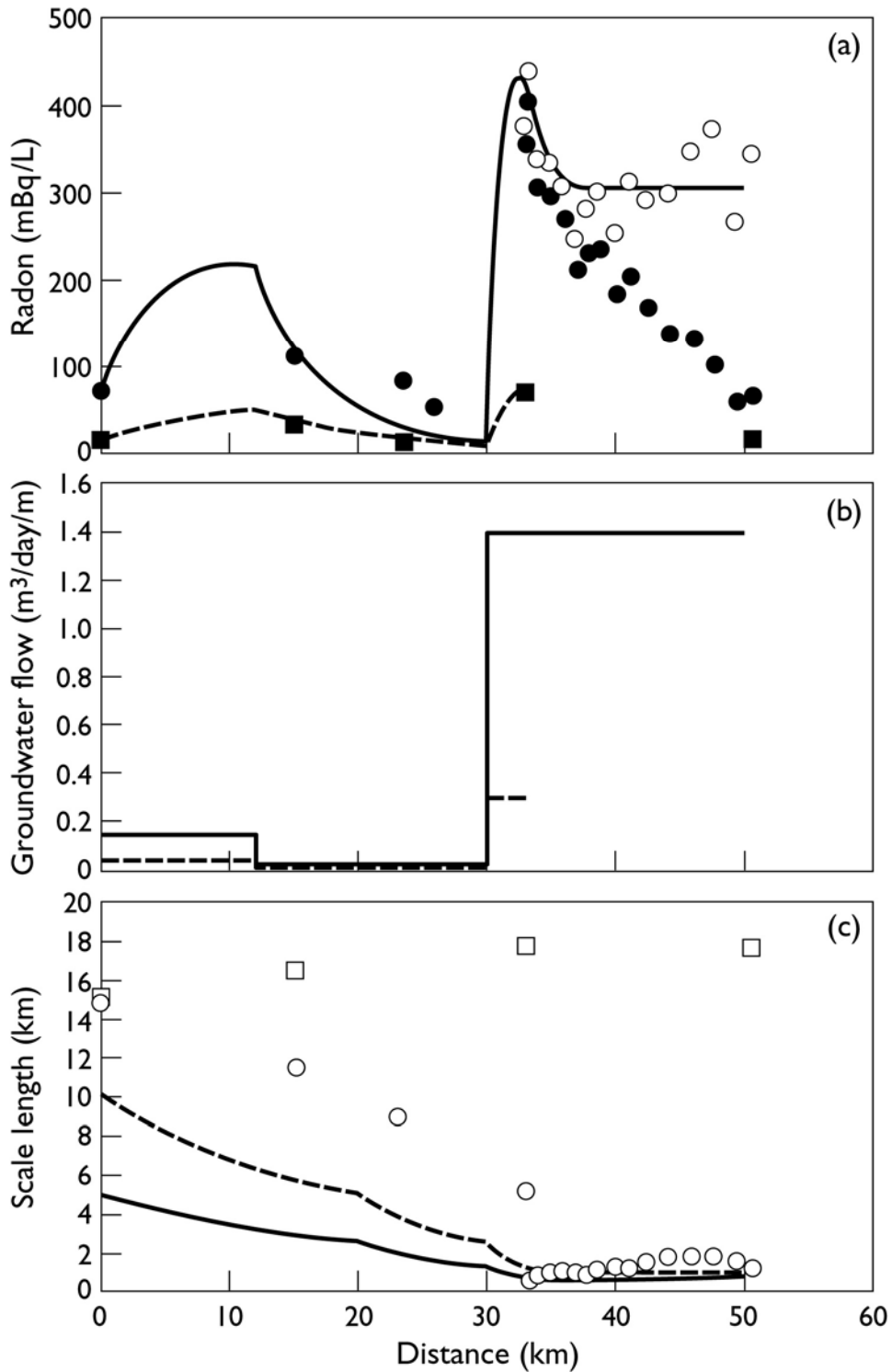


Figure 3.17. Numerical simulation of radon activity in Barratta Creek. (a) Numerical model of radon activity measured in Barratta Creek between 10-11 December 2003 (broken line and squares) and 1-6 May 2004 (solid line and closed circles), and results of numerical model. Open circles denote activities for May 2004 that have been corrected for seawater dilution (see text). (b) Estimated groundwater inflows. (c) Comparison of scale length for changes in radon activity and sampling frequency. The solid line depicts the scale length, as given by Equation 3.9. Symbols denote the distance between sampling sites. The comparison of the scale length with the sampling intensity provides an indication of the reliability of the inferred groundwater inflows.

activities are reproduced with the same model parameters, and groundwater inflow rates approximately 30% of those used for May 2004.

In May 2004, the radon activity between Sites 19 (15.1 km) and 17 (23 km) on East Barratta Creek decreases from 113 to 37 mBq/L. If there was no groundwater inflow along this reach, then the mean value of kw along this reach that would be required to reproduce this observed decrease is 5 m²/day. If groundwater inflow is occurring, then higher values of kw are required. Thus, this observed decrease in activity imposes a minimum value on kw . Similarly, the decrease in activity between Sites 19 and 18 observed in December 2003 constrains $kw > 7$ m²/day for this reach.

Radon activities downstream of Site 25 have been corrected for dilution with seawater, as discussed above. The corrected radon activities are simulated using a groundwater inflow rate of approximately 1.4 m³/day/m between 33 km and 50 km river distance. This represents as additional groundwater input of 23 800 m³/day, giving a total inflow of 30 160 m³/day/m for the 50 km reach of river between Site 20 and the mouth for May 2004.

3.7. Plantation Creek

Five gauging stations are located on Plantation Creek (11910164, 11910165, 11910166, 11910170, 11910171). In the upstream reaches (11910164, 11910165, 11910166), surface water heads are significantly above groundwater levels since the early 1980s. However, groundwater levels show large variation, and during continued periods of high rainfall groundwater levels may rise above the surface water level of the creek (Figure 3.18). In the lower reaches (11910171), surface water levels and groundwater levels are similar, suggesting that the river may switch from losing to gaining through the year (Figure 3.19).

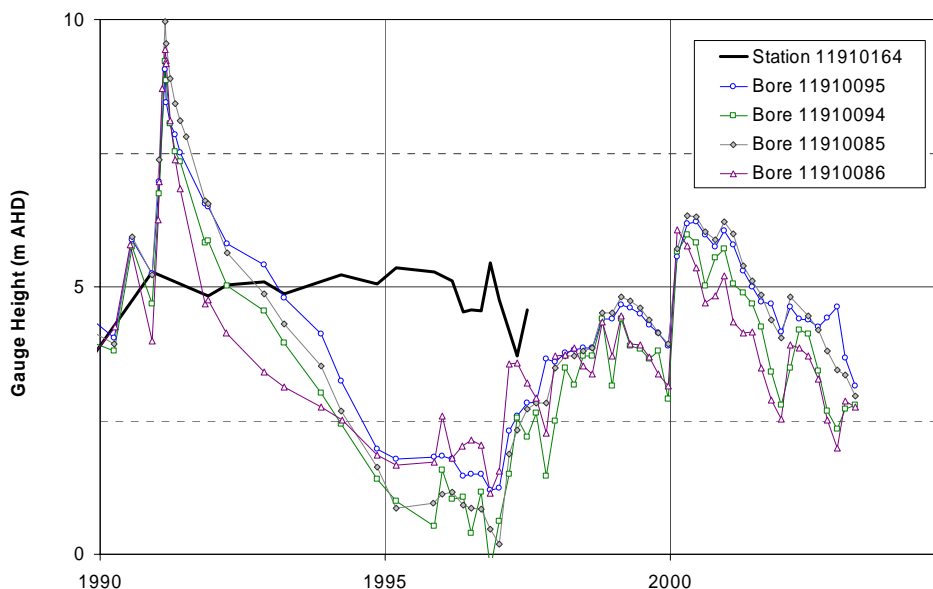


Figure 3.18. Comparison of surface water stage height measured on Plantation Creek at Old Clare Road with water table elevations of nearby bores.

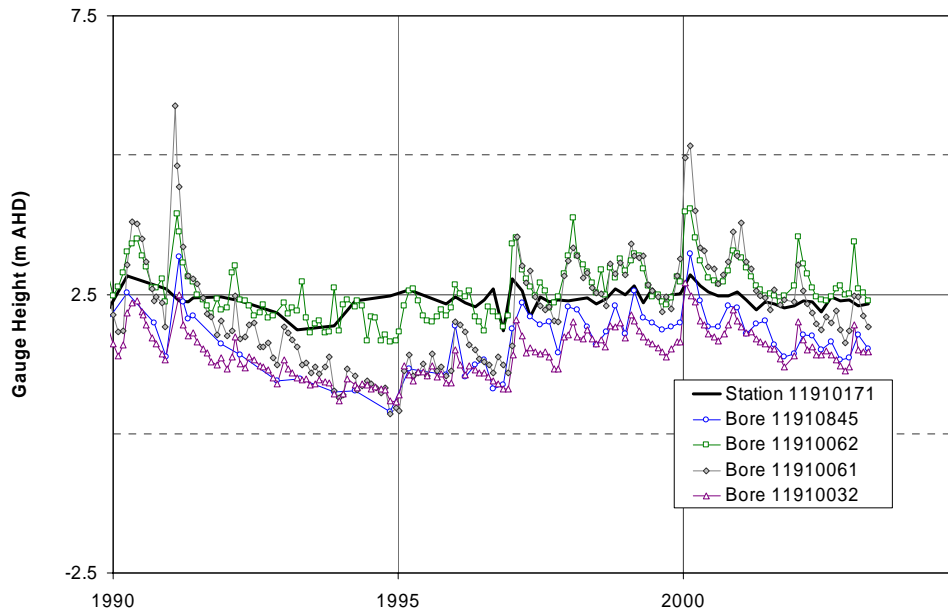


Figure 3.19. Comparison of surface water stage height measured on Plantation Creek at the Kalamia tramline with water table elevations of nearby bores.

In December 2003, the radon activity at Pump Station No. 3 (Site 14), where water from the Burdekin River is pumped into Plantation Creek was measured to be 114 mBq/L. The radon activity then decreased downstream, and was 83 mBq/L at Site 13, 33 mBq/L at Site 12, 42 mBq/L at Site 15, and 38 mBq/L at Site 11. There was no significant change in electrical conductivity along this reach of the creek. Near the mouth the radon activity rose to be 96 mBq/L at Site 28 (electrical conductivity 57 800 $\mu\text{S}/\text{cm}$). Figure 3.20 shows results of modelling of radon activities in Plantation Creek. Parameters used in the model are listed in Table 3.1. The decrease in radon activity observed between Sites 14 and 11 is consistent with radon loss through radioactive decay and gas exchange with the atmosphere, using a gas exchange rate of $k = 8.0 \text{ m}/\text{day}$. The high value of k is consistent with more turbulent flow in Plantation Creek than in the major rivers. The increase in activity between Site 11 and Site 28 is consistent with a mean groundwater inflow along this reach of the river of $0.5 \text{ m}^3/\text{day}/\text{m}$. This is equivalent to a total groundwater inflow of $6500 \text{ m}^3/\text{day}$.

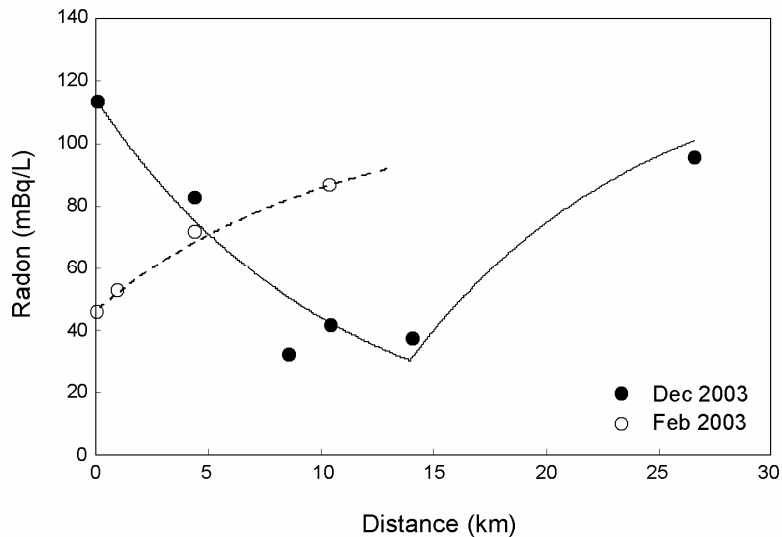


Figure 3.20. Comparison of radon activity measured in Plantation Creek between 9-12 December 2003 and 3 February 2004, and results of numerical model.

In February 2003, radon activities increased from 46 mBq/L at the pumping station (Site 14), to 53 mBq/L at Site 49, 63 mBq/L at Site 13 and 87 mBq/L at Site 15. Using the same gas transfer velocity of $k = 8$ m/day gives a groundwater inflow in the upper section of Plantation Creek of 0.42 m³/day/m. This represents an inflow of 4200 m³/day for the 10 km reach of river above Site 15.

On 4 May 2004, Plantation Creek was dry above the reservoir at Site 12. A high activity of 812 mBq/L was measured in the reservoir on May 4. At the time of sampling on May 2 the radon activity of the Burdekin River at Pump Station No. 3 was between 452 and 495 mBq/L. (These activities were measured in the Burdekin River upstream at Site 54 and downstream at Site 53, respectively.) Higher activities may have occurred at other times. Thus the high activities measured at Site 12 are attributed to activities at Pump Station No. 3 in the recent past. The radon activity decreased to 66 mBq/L between Site 12 and Site 15, and then increased to 256 mBq/L at Site 11 and 275 mBq/L by Site 28, indicating significant groundwater inflow in the lower reaches of Plantation Creek.

3.8. Sheepstation Creek

Six gauging stations are located on Sheepstation Creek (11910156, 11910157, 11910158, 11910159, 11910160, 11910161), although only one of these is currently operational. All show surface water levels significantly above groundwater levels (Figure 3.21).

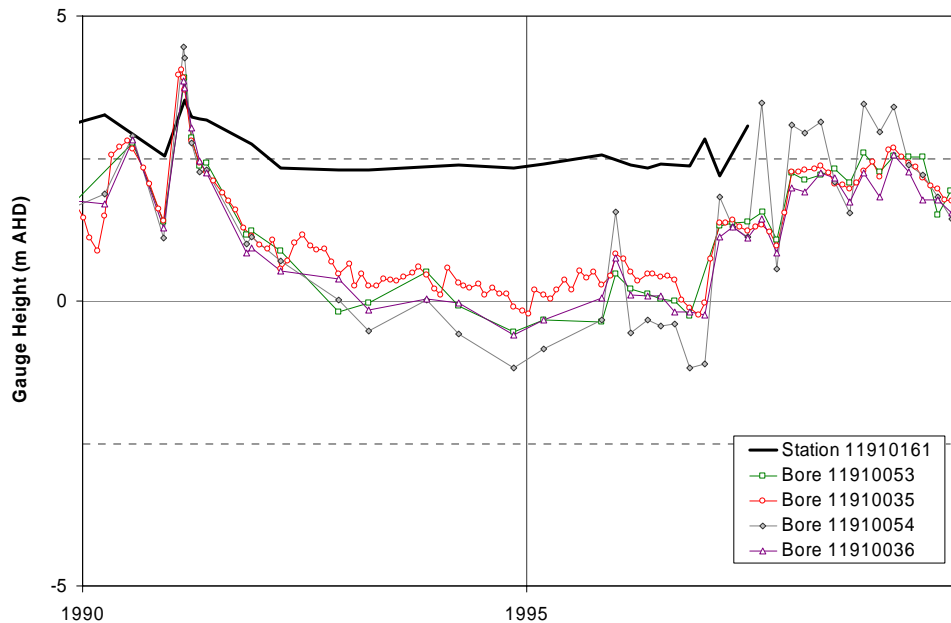


Figure 3.21. Comparison of surface water stage height on Sheepstation Creek with water table elevations of nearby bores.

In December 2003, radon activities on Sheepstation creek and associated drains ranged between 9 and 23 mBq/L (Sites 30, 35, 36, 38, 39). These values are generally low, and show little evidence of groundwater discharge. A small, but significant increase in electrical conductivity occurs along the creek, with values increasing from 166 $\mu\text{S}/\text{cm}$ at Site 30 to 204 $\mu\text{S}/\text{cm}$ at Site 38, and 343 $\mu\text{S}/\text{cm}$ at Site 39.

In April-May 2004, radon activities are much higher. The radon activity of Sheepstation Creek at Ahern Bridge (Site 30) is 123 mBq/L, which is significantly greater than that of the water pumped into the creek from the Burdekin River at The Rocks Pumping Station. This may indicate some groundwater inflow from Mount Kelly into the upper reaches of Sheepstation Creek. The activity increases to 166 mBq/L at Pyards Culvert (Site 31), before decreasing to 56 mBq/L at Site 32 and 26 mBq/L at Site 35. The radon activity then increases to 47 mBq/L at Site 36 and 247 mBq/L at Site 37, indicating additional groundwater inflow in the lower reaches. However, electrical conductivity and molar chloride to bicarbonate ratio show little change, suggesting that the inflowing groundwater must be of relatively low salinity.

3.9. Inkerman Region

Drainage channels and creeks south of the Burdekin River were only sampled in April 2004. Radon activities in many of the surface waters were high, indicating significant groundwater inflow. Radon activities were 27 mBq/L at Fowlers Lagoon culvert (Site 74), 97 mBq/L at Papale's Farm drainage channel (Site 80), 43 mBq/L at Sibon Road channel crossing (Site 81), 63 mBq/L at Iyah Creek (Site 79), 46 mBq/L at Harper Road / Oats Road channel crossing (Site 75), 26 mBq/L at Inkerman Lagoon waterboard channel (Site 78), 92 mBq/L at Saltwater Creek at the highway crossing (Site 77), 155 mBq/L at Alma Creek channel (Site 76), 24 mBq/L at the Sunwater gauging station at Site 71, 122 mBq/L at Site 72, and 385 mBq/L at the gauging station at Site 73.

Samples with highest radon activity (Sites 73 and 76) also have highest electrical conductivities and chloride to bicarbonate ratios, which is consistent with groundwater inflows. Figure 3.22 shows radon activity versus chloride to bicarbonate ratio for all samples south of the Burdekin River, which illustrates this correlation.

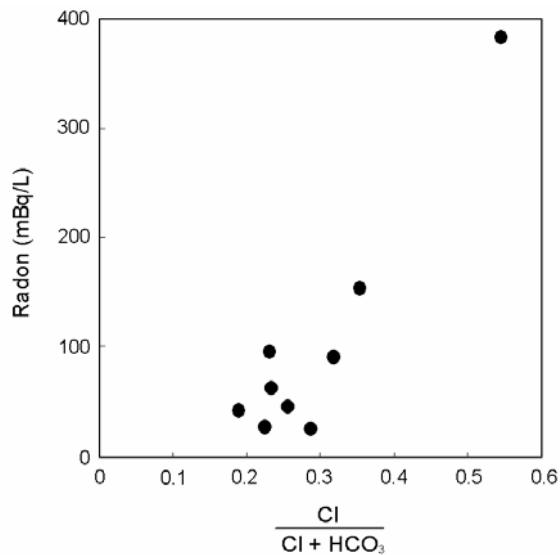


Figure 3.22. Relationship between molar chloride to bicarbonate ratio and radon activity for surface water samples collected for the region south of the Burdekin River.

4. DISCHARGE TO THE OCEAN

4.1. Introduction

Submarine groundwater discharge (SGD) may occur either as diffuse seepage or as focused flow at vents or seeps, depending on the hydrogeological setting. Due to its greater density, a wedge of saline water usually occurs towards the base of unconfined aquifers in coastal regions. The traditional model for diffuse groundwater discharge to the ocean involves fresh groundwater flowing over the top of the saline wedge, to discharge within the inter-tidal zone. Density differences between freshwater and seawater usually prevent discharge further offshore, unless the aquifer is confined, and driven by much greater hydraulic heads. Within the Great Barrier Reef region, Stieglitz and Ridd (2000) have described apparent point discharge of groundwater occurring several kilometres offshore (termed 'wonky holes'). The origin of these features is uncertain, and their volumetric discharge has yet to be quantified. They have not been recorded within Bowling Green Bay, and are unlikely to be a significant discharge mechanism for the Lower Burdekin aquifer. For this reason, this report focusses on estimation of diffuse groundwater discharge occurring within the intertidal zone.

A common approach for quantifying submarine groundwater discharge rates is to use geochemical tracers. Tracers that are naturally enriched in groundwater relative to seawater and have well understood chemistries within the marine environment are well suited for this problem, and radium and radon isotopes are most commonly used (Moore, 2003). Uranium and thorium series radionuclides occur naturally in earth material, and their decay chains include isotopes of uranium (^{238}U , ^{235}U , ^{234}U), thorium (^{232}Th , ^{234}Th , ^{230}Th), radium (^{228}Ra , ^{226}Ra , ^{224}Ra , ^{223}Ra), and radon (^{222}Rn , ^{220}Rn , ^{219}Rn). While uranium, radium, and radon are relatively mobile in aqueous systems, thorium adsorbs strongly to sediment particles. Activities of thorium within the ocean water column are therefore very low, and so is the *in situ* (water column) production of its daughters: the radium isotopes. The principle sources of radium to the ocean are external and include river discharge, submarine groundwater discharge, and production within the seafloor sediments (which is subsequently transported by either diffusion or advection into the water column). The principal loss mechanisms are radioactive decay, advection by coastal currents, horizontal dispersion, and for the noble gas radon, air-sea gas exchange.

The half-life of the longest lived radium isotope, ^{226}Ra ($t_{1/2} = 1602$ yr), is comparable to the mixing time of the ocean, while the other isotopes (^{223}Ra , ^{224}Ra and ^{228}Ra) have much shorter half-lives. Their half-lives are on the order of the mixing time of coastal embayments and the continental shelf. Away from the external sources, the activities of the short-lived radium isotopes are very low due to dilution and radioactive decay. Small groundwater fluxes to the ocean can be distinguished with radium isotopes because of a large contrast in activity between seawater and groundwater. Although ^{222}Rn is lost from seawater by gas exchange at the water-air interface as well as by radioactive decay, the activity contrast between groundwater and seawater is usually even greater than for the radium isotopes, which makes this also a useful indicator of submarine groundwater discharge.

4.2. Theory

The usual approach for estimating submarine groundwater discharge using radium isotopes applies a one-dimensional analysis. The short-lived radium isotopes ^{223}Ra and ^{224}Ra constrain the mixing time of near-shore waters. The mixing times determined from these isotopes are used to interpret the offshore gradients of the long-lived radium isotopes ^{226}Ra and ^{228}Ra .

The change in activity (c) with time (t) as a function of distance offshore (x) is given by:

$$\frac{dc}{dt} = K_h \frac{\partial^2 c}{\partial x^2} - v \frac{\partial c}{\partial x} - \lambda c - \frac{k}{z} c + \frac{F}{z} \quad [4.1]$$

where c is the activity of radon or radium isotopes, K_h is the eddy mixing coefficient, v is the advective water velocity, λ is the radioactive decay constant, k is the gas exchange velocity ($k = 0$ for radium isotopes), z is the water depth, F is the flux due to production in seafloor sediments and x is the distance offshore. (In the case of radon, c is actually the unsupported radon activity, which is the radon activity less the activity of its parent, ^{226}Ra .)

The flux due to diffusion from seafloor sediments can be expressed

$$F = \sqrt{\lambda D} \left(\frac{\gamma}{\lambda} - c \right) \quad [4.2]$$

where γ is the production rate within aquifer sediments (Bq/L/day), D is the diffusion coefficient in the sediments, γ/λ is the activity in equilibrium with the seafloor sediments, and c is the activity in the overlying seawater (Martens et al., 1980). However, where water moves in and out of the sediments in response to tidal fluctuations and wave action, then the radium and radon contributed from the sediments will be much greater than from diffusion alone (Li et al., 1999). After water moves into the sediments, its activity will increase according to

$$c_s(t) = \frac{\gamma}{\lambda} + \left(c - \frac{\gamma}{\lambda} \right) e^{-\lambda t} \quad [4.3]$$

where $c_s(t)$ is the activity of water within the sediments, c is the initial activity of the overlying water that moves into the sediments, and t is the residence time of water in the subsurface. Since tidal movements are likely to be the main driving force for this water exchange in Bowling Green Bay, $t_R = 0.5$ days is used to represent this mean residence time. The flux into the overlying water column can then be expressed

$$F = Q_s (c_s(t_R) - c) \quad [4.4]$$

where Q_s is the mean advective water flux into and out of the sediments ($\text{m}^3/\text{m}^2/\text{day}$) and t_R is the mean residence time of water in the sediments. The flux Q_s is referred to

as the recycled seawater exchange rate, to distinguish it from the flux of *terrestrial* groundwater. Substituting into Equation 4.1 gives

$$\frac{dc}{dt} = K_h \frac{\partial^2 c}{\partial x^2} - v \frac{\partial c}{\partial x} - \alpha c + \beta \quad [4.5]$$

where

$$\alpha = \lambda + \frac{k}{z} + \frac{Q_s}{z} (1 - e^{-t_R \lambda}) \quad [4.6]$$

$$\beta = \frac{Q_s}{z} (1 - e^{-t_R \lambda}) \frac{\gamma}{\lambda} \quad [4.7]$$

The solution to Equation 4.5 under steady state conditions ($\partial c / \partial t = 0$) and boundary conditions:

$$-K_h \frac{\partial c}{\partial x} + vc \Big|_{x=0} = vc_0 \quad [4.8]$$

and

$$\frac{\partial c}{\partial x} \Big|_{x=\infty} = 0 \quad [4.9]$$

is

$$c(x) = \frac{\beta}{\alpha} + \left(c_0 - \frac{\beta}{\alpha} \right) \frac{2v}{u+v} \exp \left[-x \frac{(u-v)}{2K_h} \right] \quad [4.10]$$

where

$$u = v \left(1 + \frac{4\alpha K_h}{v^2} \right)^{1/2} \quad [4.11]$$

Radioactive decay coefficients are $\lambda = 0.061 \text{ day}^{-1}$ (half-life: 11.4 days) for ^{223}Ra , $\lambda = 0.19 \text{ day}^{-1}$ (half-life: 3.65 days) for ^{224}Ra , $\lambda = 1.19 \times 10^{-6} \text{ day}^{-1}$ (half-life: 1600 years) for ^{226}Ra , and $\lambda = 3.33 \times 10^{-4} \text{ day}^{-1}$ (half-life: 5.7 years) for ^{228}Ra .

Within Bowling Green Bay, the advective water velocity, v , can be related to the groundwater discharge rate, Q_G , by

$$v = \frac{Q_H + Q_B + Q_G}{wd} \quad [4.12]$$

where Q_H and Q_B are the discharge rates of Haughton River and Barratta Creek, respectively, w is the width of the coastal zone, and d is the water depth. c_0 is related to the mean activity of groundwater discharge by

$$c_0 = \frac{Q_H c_H + Q_B c_B + Q_G c_G}{vwd} \quad [4.13]$$

where c_H and c_B are the activities of discharge from Haughton River and Barratta Creek, respectively, and c_G is the activity of groundwater discharging directly to the coast.

If the flux from sediments is negligible ($Q_s = 0$), and the exchange is dominated by eddy diffusion rather than advection, then a plot of $\ln^{223}\text{Ra}$ or $\ln^{224}\text{Ra}$ as a function of distance from the coast may be used to estimate K_h :

$$\frac{\ln[c(x_1)] - \ln[c(x_2)]}{x_2 - x_1} = \sqrt{\frac{\lambda}{K_h}} \quad [4.14]$$

If groundwater discharge to the coast is negligible, then radon and radium will be contributed only through exchange with submarine sediments. Ignoring changes in water depth resulting from tidal fluctuations, the steady-state radon or radium activity in seawater will be given by

$$c = \frac{Q_s \frac{\gamma}{\lambda} (1 - e^{-\lambda R})}{Q_s (1 - e^{-\lambda R}) + \lambda z + k} \quad [4.15]$$

The solution to Equation 4.5 under steady state conditions ($\partial c / \partial t = 0$) and boundary conditions:

$$-K_h \frac{\partial c}{\partial x} + vc \Big|_{x=0} = vc_0 \quad [4.16]$$

and

$$c = c_L \text{ at } x = L \quad [4.17]$$

is:

$$c(x) = \left(c_L - \frac{\beta}{\alpha} \right) \exp[k_1(x - L)] + k_3 \left(\exp[k_2 x] - \exp[k_1(x - L) + k_2 L] \right) + \frac{\beta}{\alpha} \quad [4.18]$$

where:

$$k_1 = \frac{v + \sqrt{v^2 + 4K_h\alpha}}{2K_h} \quad [4.19]$$

$$k_2 = \frac{v - \sqrt{v^2 + 4K_h\alpha}}{2K_h} \quad [4.20]$$

$$k_3 = \frac{v\left(c_0 - \frac{\beta}{\alpha}\right) + \left(c_L - \frac{\beta}{\alpha}\right)(K_h k_1 - v)\exp[-k_1 L]}{v - K_h k_2 + (K_h k_1 - v)\exp[k_2 L - k_1 L]} \quad [4.21]$$

4.3. Radium

Activities of radium isotopes measured in offshore samples, surface water samples and groundwater samples are given in Table A3.4 (Appendix 3). Figure 4.1 depicts radium isotope activities of offshore samples as a function of distance offshore. A general trend of decreasing activities with increasing distance offshore is apparent for all isotopes. Highest activities of all isotopes were measured in the sample taken offshore from the Haughton river mouth (sample H1).

Because of their shorter half-life ^{223}Ra and ^{224}Ra activities should decrease with distance offshore much more rapidly than the longer-lived isotopes ^{226}Ra and ^{228}Ra . According to Equation 4.14, the rate of decrease of the natural logarithm of the isotope activities should be directly proportional to the square root of the radioactive decay coefficient. Within the 0 – 5 km nearshore zone, rates of activity decrease for ^{223}Ra , ^{224}Ra , ^{226}Ra and ^{228}Ra are $m = 0.3, 0.4, 0.2$ and 0.4 log cycles per km, respectively (Figure 4.2). This is inconsistent with Equation 4.14, which suggests that the slope for ^{223}Ra and ^{224}Ra should be more than $200 \times$ greater than that of ^{226}Ra . The apparent discrepancy can be explained by the geometry of the coastline and the resulting ocean currents. Samples between 0 and 15 km distance are within the relatively sheltered waters of Bowling Green Bay, whereas samples from further offshore are in regions that are exposed to much greater mixing. Samples from beyond 15 km would have had their radium activities diluted by mixing with regional ocean water. (Chung et al. (1974) report a mean ^{226}Ra activity for the Pacific Ocean of 1.03 mBq/L.) The relatively rapid rate of decrease in ^{226}Ra and ^{228}Ra activities in the nearshore zone thus reflects mixing between the nearshore zone and the offshore zone. Notwithstanding this, the rate of decrease of the shorter-lived isotopes can be used to estimate the mixing rate of the nearshore zone. Based on the rate of decrease of ^{223}Ra and ^{224}Ra within the 0 – 5 km zone, and the decay coefficients of these isotopes, the estimated mixing rates are $K_h = 6.8 \times 10^5$ and $K_h = 1.2 \times 10^6$ m^2/day , respectively (Equation 4.14).

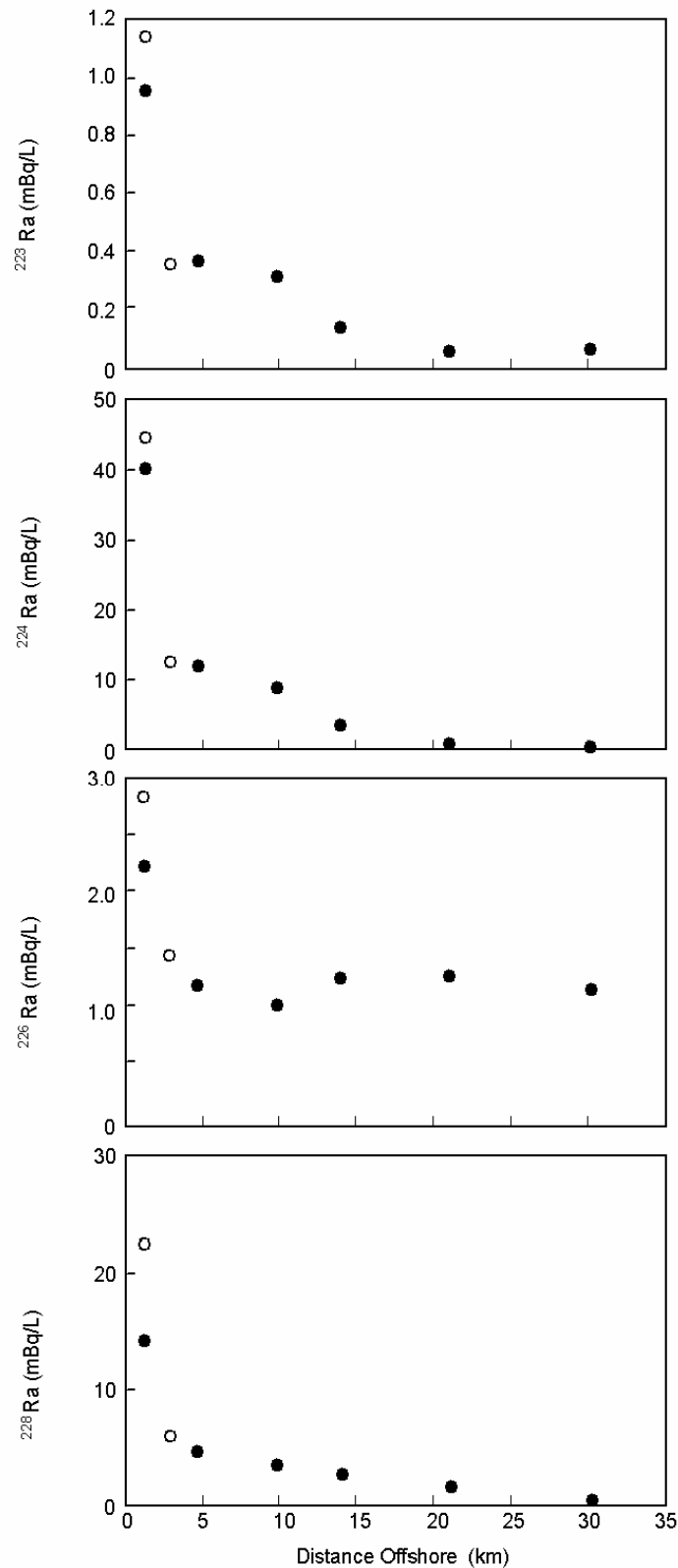


Figure 4.1. Relationship between radium isotope activity of seawater and distance offshore. Closed circles denote samples taken along a north-south transect offshore from West Barratta Creek mouth. Open circles denote samples east and western of this transect (see Figure 2.5).

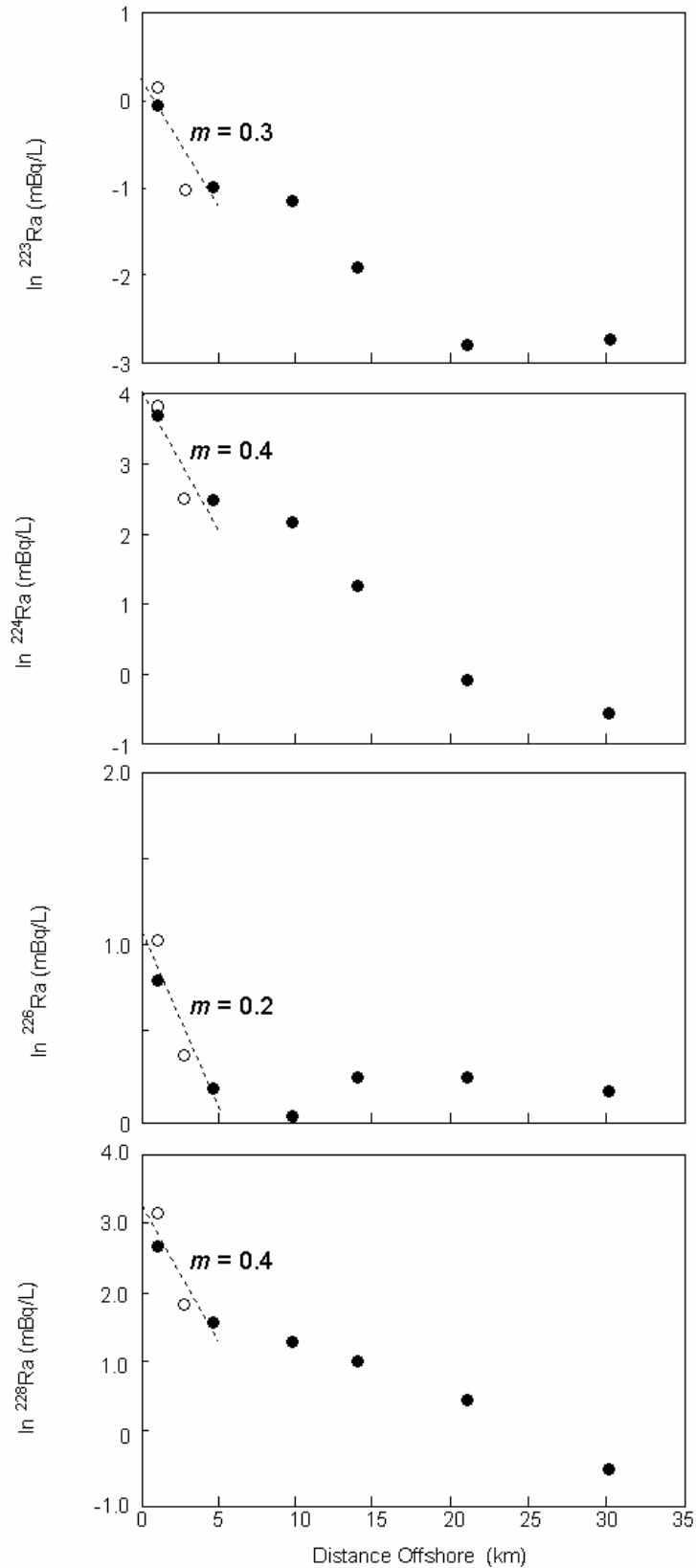


Figure 4.2. Logarithmic plot of radium isotope activity of seawater versus distance offshore, also showing rates of decrease in activity over the 0 – 5 km nearshore zone (units are log-cycles per kilometre).

Having determined mixing rates from the short-lived radium isotopes, we can estimate fluxes of the long-lived isotopes to the offshore zone from the product of the mixing rate, the water depth and the activity gradient of either ^{226}Ra or ^{228}Ra . For ^{226}Ra , the activity gradient within the 0 – 5 km zone is approximately 0.26 mBq/L/km (Figure 4.1). Multiplying this by the mixing rate of $K_{\text{H}} = 0.68 - 1.20 \times 10^6 \text{ m}^2/\text{day}$ and a mean water depth of $d = 2.5 \text{ m}$, gives a ^{226}Ra flux of $4.4 \times 10^5 - 7.8 \times 10^5 \text{ Bq/km/day}$. For ^{228}Ra , the activity gradient is approximately 2.5 mBq/L/km (Figure 4.1), and so the ^{228}Ra flux becomes $4.25 \times 10^6 - 7.50 \times 10^6 \text{ Bq/km/day}$.

The marine discharge rate of the Haughton River and Barratta Creek can be determined from the surface water modelling results for April-May (Sections 3.5 and 3.6). Radium activities in the marine discharge are estimated from the measured activities in the most downstream samples (Table A3.5). The ^{226}Ra flux from the Haughton River is $76\,300 \text{ m}^3/\text{day} \times 11 \text{ mBq/L} = 8.3 \times 10^5 \text{ Bq/day}$. The flux from Barratta Creek is $64\,800 \text{ m}^3/\text{day} \times 6 \text{ mBq/L} = 3.9 \times 10^5 \text{ Bq/day}$. Averages over the 35 km coastal zone, this represents a combined ^{226}Ra flux from surface water of $3.4 \times 10^4 \text{ Bq/km/day}$, or approximately 5 – 10% of the total ^{226}Ra flux. The ^{228}Ra fluxes from Haughton River and Barratta Creek are $76\,300 \text{ m}^3/\text{day} \times 78 \text{ mBq/L} = 5.9 \times 10^6 \text{ Bq/day}$ and $64\,800 \text{ m}^3/\text{day} \times 25 \text{ mBq/L} = 1.6 \times 10^6 \text{ Bq/day}$, respectively. Averages over the 35 km coastal zone, this represents a combined ^{228}Ra flux from surface water of $2.2 \times 10^5 \text{ Bq/km/day}$, or approximately 3 – 5% of the total ^{228}Ra flux.

If the difference between the calculated total offshore radium fluxes and the flux attributable to surface water discharge is entirely due to groundwater discharge, then the groundwater discharge rate can be calculated from the radium flux divided by the radium activity of the discharge. However, radium activities of groundwater discharge are difficult to determine due to non-conservative behaviour of dissolved radium isotopes. Hancock and Murray (1996) showed that activities of all four radium isotopes in the Bega River estuary, New South Wales, increased as the salinity increased in the tidal portion of the estuary. In saline water, the competition effects of soluble cations for iron exchange sites on sediment particles results in desorption of surface-bound radium. The same process presumably also operates as low salinity groundwaters mix with saline groundwaters in the coastal zone. Figure 4.3 shows an approximately linear relationship between radium activity and electrical conductivity for both surface water and groundwater samples. The mean ^{226}Ra and ^{228}Ra activities of groundwater samples are 10.1 and 46.2 mBq/L, respectively. If we use these values as the respective radium activities of groundwater discharge, then the estimated groundwater discharge rates become $1.4 - 2.6 \times 10^6 \text{ m}^3/\text{day}$ using ^{226}Ra , and $3.0 - 5.5 \times 10^6 \text{ m}^3/\text{day}$ using ^{228}Ra . If the maximum ^{226}Ra and ^{228}Ra activities are used (24.5 and 125.5 mBq/L respectively), then the estimated groundwater discharge rates become $6.2 \times 10^5 - 1.1 \times 10^6 \text{ m}^3/\text{day}$ using ^{226}Ra and $1.2 - 2.1 \times 10^6 \text{ m}^3/\text{day}$ using ^{228}Ra , respectively.

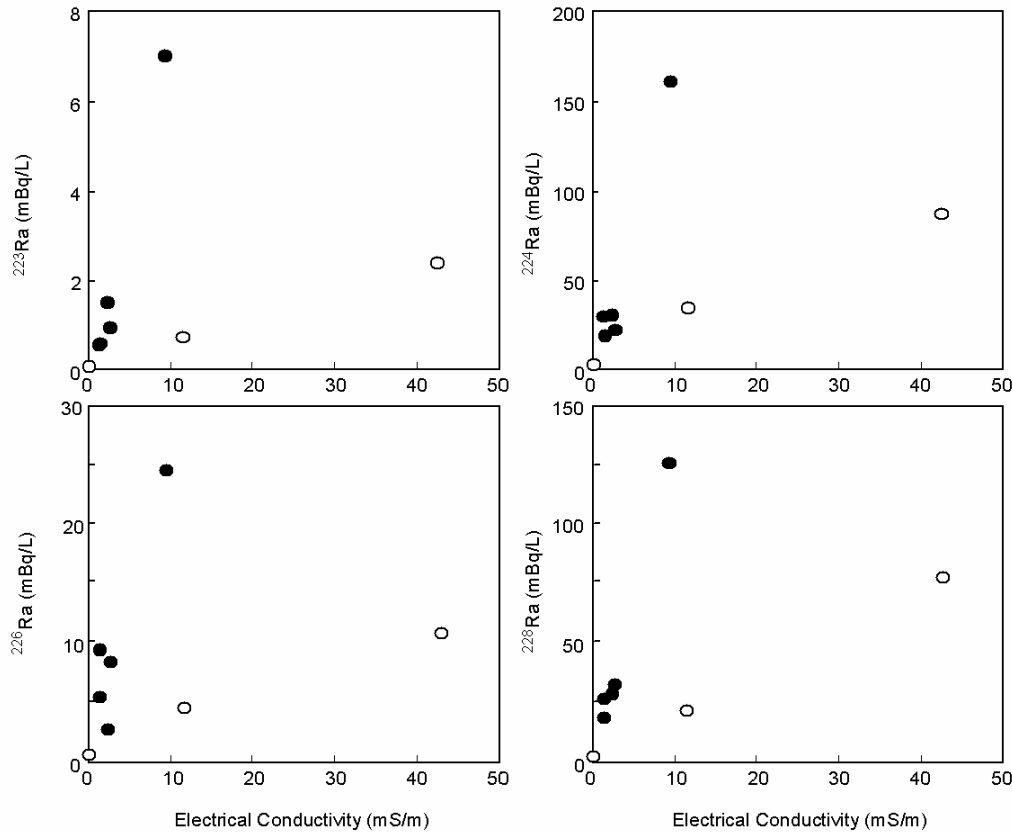


Figure 4.3. Relationship between radium isotope activity and electrical conductivity for groundwater (solid circles) and surface water (open circles) samples.

The groundwater discharge rate determined from the above analysis represents the maximum possible rate, because it does not account for radium contributed to the ocean from diffusion from ocean sediments or recycled seawater exchange. Although no direct estimates of radium fluxes from sediments have been made in the present study, we can estimate the possible magnitude of these fluxes from Equation 4.15. If the seafloor sediments are mineralogically similar to the sediments within the Lower Burdekin floodplain, then the measured groundwater activities of the radium isotopes represent equilibrium activities of water in equilibrium with seafloor sediments (γ/λ). Figure 4.4 shows the relationship between radium activity in seawater and recycled seawater exchange rate based on a water depth of 2 m. Although the rate of recycled seawater exchange has not been estimated, Ullman et al. (2003) estimated an exchange rate of 2.4 – 3.1 m³ per metre of beach width per tidal cycle, or 4.8 – 6.1 m³/m/day, for a 30 m beachface off the Delaware coast, USA. This is equivalent to a water flux of approximately $Q_s = 0.18$ m³/m²/day. Ridd (1996) estimated the seawater exchange rate through crab burrows in intertidal mangrove swamps near Gordon Creek, North Queensland to be between 10⁻³ and 10⁻² m³/m³ per tidal cycle, although the total exchange would be much greater. If the recycled seawater exchange rate measured by Ullman et al. (2003) occurred in Bowling Green Bay, then ^{226}Ra and ^{228}Ra activities of 0.2 and 1.0 mBq/L could occur within the water column solely due to this process. Measured activities within 2 km of the shore were between 1.4 and 2.9 mBq/L for ^{226}Ra and between 6 and 23 mBq/L for ^{228}Ra , and so are significantly greater than these estimated activities. These measured activities would require a pumping rate of approximately $Q_s = 2.0$ m³/m²/day, which appears inconsistent with the relatively low radon activity in ocean waters (see Section 4.4).

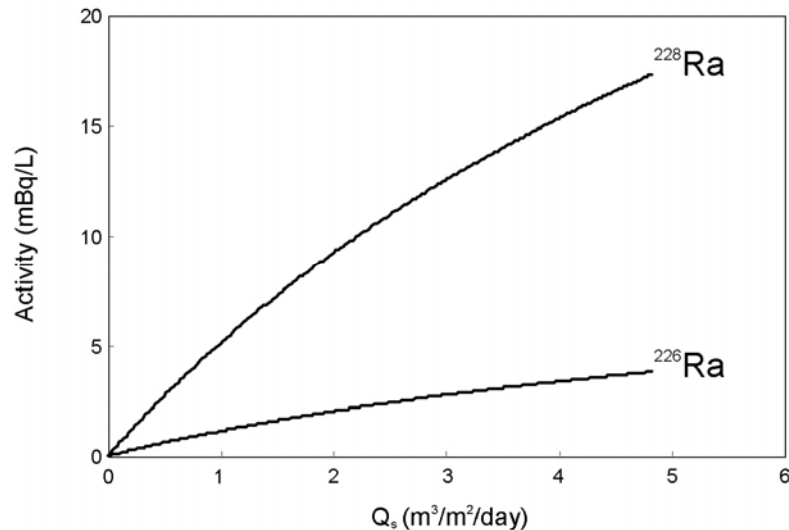


Figure 4.4. Relationship between radium activity in seawater and recycled seawater exchange rate based on a water depth of 2 m (Equation 4.15).

4.4. Radon

Figures 4.5 and 4.6 depict offshore radon activities measured by gas stripping in February 2004 and April 2004, respectively. In February, the mean radon activity was measured to be 8 mBq/L, while in April it was 15 mBq/L. The mean radon activity measured by scintillation counting in April 2004 was 21 mBq/L. The mean water depth during the April survey was 3.7 m. At both sampling times, highest radon activities were measured near the mouth of the Houghton River. In April 2004, increased radon activities were also measured near the mouth of East Barratta Creek, where a small dilution in electrical conductivity was also observed.

Using the mixing rates determined from the short-lived radium isotopes, we can calculate the radon flux at the coast that would be required to produce the measured radon activity of 21 mBq/L at a distance of 1850 m offshore. (We use the activity measured using scintillation counting for the modelling for consistency with the onshore measurements.) If the radon activity in seawater is due to groundwater discharge rather than production beneath the seafloor ($Q_s = 0$), then the radon flux can be divided by the mean radon activity of the discharge to determine the groundwater discharge rate. We use $K_h = 10^6$ m²/day, $Q_H = 76\,300$ m³/day, $Q_B = 64\,800$ m³/day, $A_H = 38$ mBq/L, $A_B = 60$ mBq/L, $A_G = 13\,000$ mBq/L, $w = 35\,000$ m, $d = 2$ m and $\lambda = 0.18$ day⁻¹. Equations 4.10, 4.12 and 4.13 then constitute three equations that must be solved for the remaining four unknowns: k/z , v , A_0 and Q_G . If we assume a value of k/z , we can thus determine Q_G . Figure 4.7 shows the predicted relationship between radon activity and distance offshore for a gas exchange coefficient of $k/z = 1$ day⁻¹, for which the groundwater discharge rate is estimated to be 900 000 m³/day. For greater values of the gas exchange coefficient, higher groundwater discharge rates will be required to fit the measured data. Figure 4.8 depicts the relationship between k/z and Q_G . Even for very low values of k/z (and hence very low values of Q_G), the model suggests that radon flux from Houghton River and Barratta Creek combined constitutes less than 1% of the total offshore radon flux.

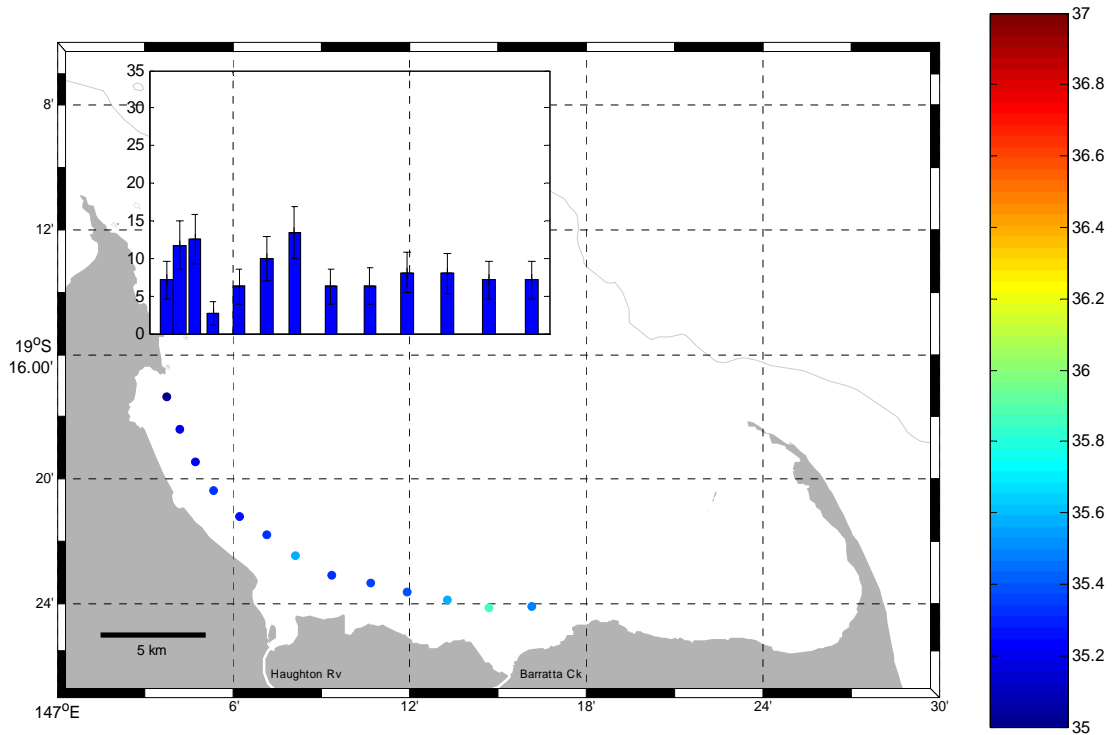


Figure 4.5. Seawater salinity (psu; coloured scale) and radon activity (mBq/L; inset bar graph) measured in Bowling Green Bay in February 2004.

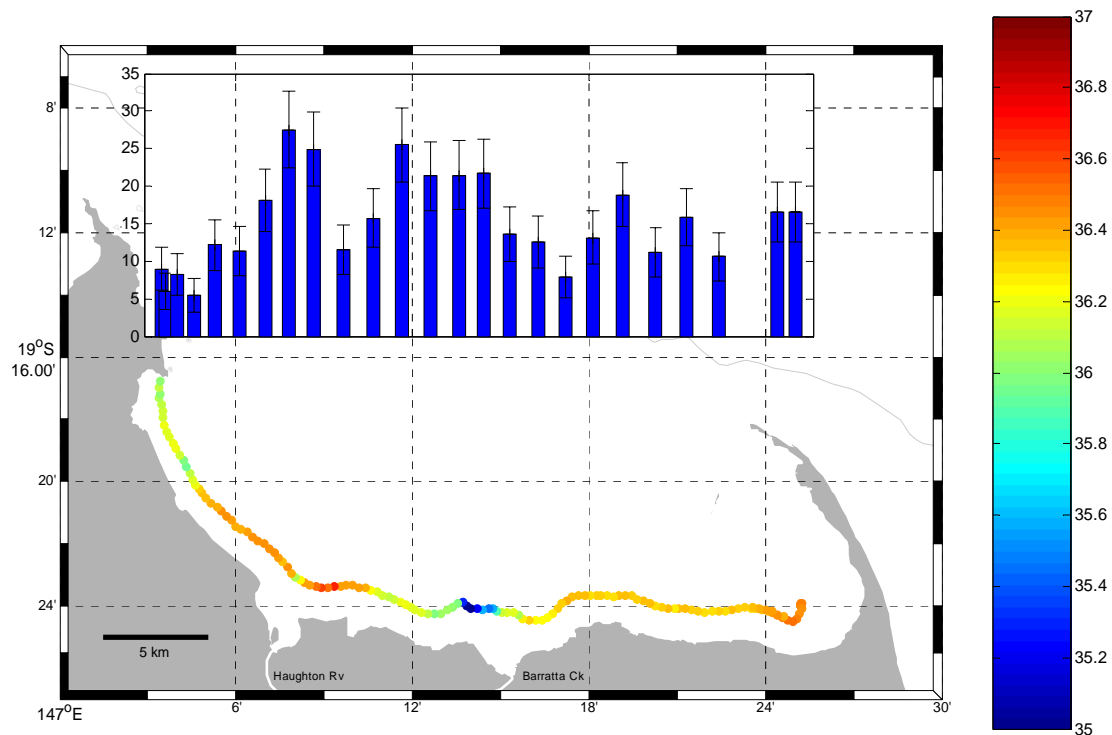


Figure 4.6. Seawater salinity (psu; coloured scale) and radon activity (mBq/L; inset bar graph) measured in Bowling Green Bay in April 2004.

There are few estimates of gas exchange rates in the literature to compare with these values. The value of k is dependent on the mean wind speed, and open ocean values ranges between 1 - 5 m/day for wind speeds between 5 and 12 m/s (Wanninkhof, 1992). Hartman and Hammond (1984) measured a mean exchange velocity for San Francisco Bay of 2 m/day, and Clark et al. (1992) measured an exchange velocity of 1 m/day for the Hudson River estuary. In both cases, the water depth is much greater than in Bowling Green Bay. The water depth in Bowling Green Bay averages 3.7 m where radon samples were collected, but is much shallower closer to shore, and $\sim 1 \text{ day}^{-1}$ at the sampling location.

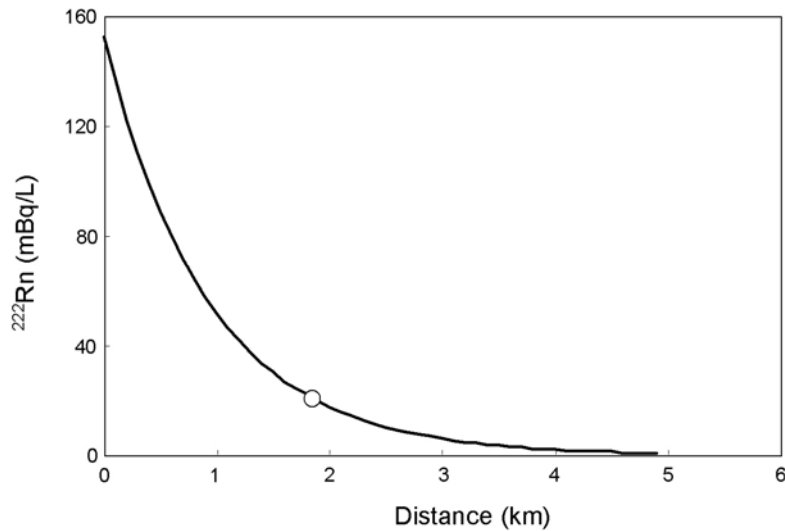


Figure 4.7. Modelled radon activity versus distance offshore, for a gas exchange coefficient of $k/z = 1 \text{ day}^{-1}$ and groundwater discharge rate of $Q_G = 900\,000 \text{ m}^3/\text{day}$. The circle denotes the mean activity measured along a transect 1850 m from the shoreline.

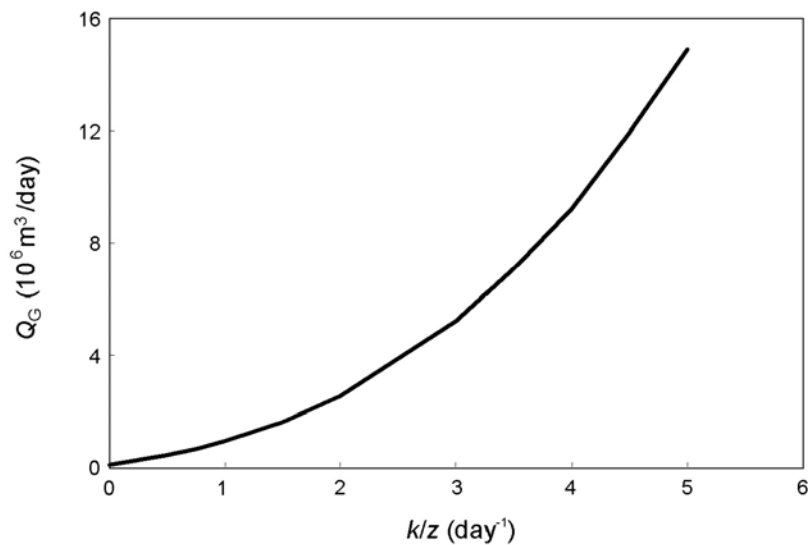


Figure 4.8. Relationship between gas exchange coefficient and estimated groundwater discharge to the ocean.

The above analysis will overestimate the groundwater discharge rate, because it does not account for radon contributed to the ocean from diffusion from ocean sediments or recycled seawater exchange. Although no direct estimates of radon fluxes from sediments have been made in the present study, radon fluxes reported within the literature range from 4-16 mBq/m²/min for Cape Lookout Bight, North Carolina (Martens et al., 1980) to 30-45 mBq/m²/min for Par Pond, South Carolina (Corbett et al., 1998). Based on a water depth of 2 m, this corresponds to a radon flux of 3-22 mBq/L/day. In the absence of any groundwater discharge, this would result in a steady-state activity of 16-120 mBq/L. We can also estimate the radon activity that would occur due to recycled seawater exchange alone from Equation 4.15. Using $\gamma/\lambda = 13\ 000$ mBq/L, $z = 2$ m, $k/z = 1$ day⁻¹ and $Q_s = 0.18$ m³/m²/day (Ullman et al., 2003) gives a radon activity in the water column due to recycled seawater exchange of 135 mBq/L. Thus only a very small seawater exchange rate would be required to produce the measured radon activity of 21 mBq/L at a water depth of $z = 2$ m. Figure 4.9 shows the required recycled seawater exchange rate as a function of the gas exchange coefficient k/z .

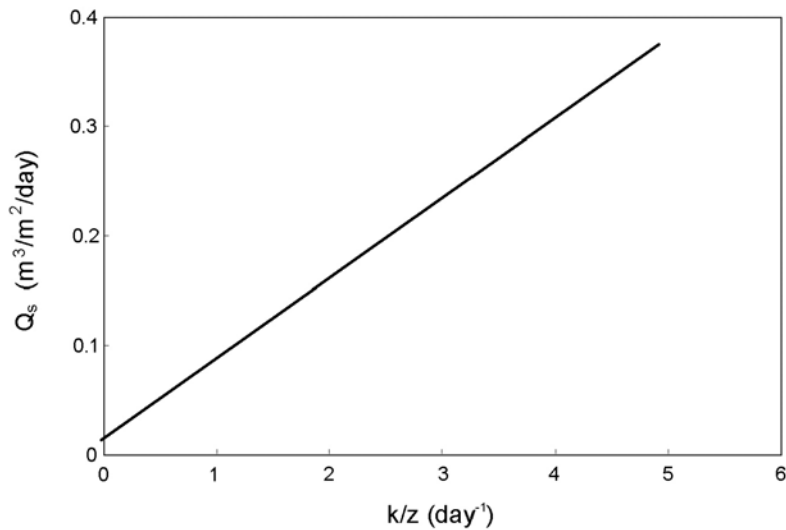


Figure 4.9. Relationship between recycled seawater exchange rate and gas exchange coefficient, required to produce the measured radon activity of 21 mBq/L at a water depth of $z = 2$ m.

4.5. Modelling

We can constrain the groundwater discharge rate by attempting to fit measured offshore activities of ²²³Ra, ²²⁴Ra, ²²⁶Ra, ²²⁸Ra and ²²²Rn with the numerical model given by Equations 4.18, and parameter values given by Equations 4.6 - 4.7, 4.12 - 4.13 and 4.19 - 4.21. The parameters required by this model are K_h , Q_H , Q_B , Q_G , Q_s/z , t_R , k/z , w and d , as well as c_H , c_B , c_G and γ/λ for each of the isotopes. We have used $K_h = 10^6$ m²/day, $Q_H = 76\ 300$ m³/day, $Q_B = 64\ 800$ m³/day, $t_R = 0.5$ days, $w = 35\ 000$ m and $d = 2$ m (Table 4.1). Values for c_H and c_B for each of the isotopes are listed in Table 4.2. They are based on the measured activities of radium and radon in surface waters. We have also used $c_G = \gamma/\lambda = 7.0, 161, 24.5, 126$ and 13000 mBq/L for ²²³Ra, ²²⁴Ra, ²²⁶Ra, ²²⁸Ra and ²²²Rn, respectively. These are the measured values of the radium isotopes in the most saline groundwater sampled and the mean measured value of ²²²Rn in all groundwater samples. The higher values for radium isotopes were used to account for desorption from sediments as salinity increases. Values of

c_L were chosen to match the observed offshore activities. This leaves Q_G , Q_s/z and k/z as the unknown parameters that must be determined by model calibration.

If we assume a maximum realistic value for $k/z = 20 \text{ day}^{-1}$, then the measured ^{222}Rn activity constrains maximum possible values for Q_G and Q_s/z . Observed ^{226}Ra and ^{228}Ra activities are relatively insensitive to Q_s/z , and so constrain Q_G . ^{223}Ra and ^{224}Ra then constrain Q_s/z . Figure 4.10 depicts two simulations that represent the minimum (broken line) and maximum (solid line) values of the groundwater discharge rate, Q_G , that are consistent with measured radium and radon activities. For $Q_G = 4.0 \times 10^5 \text{ m}^3/\text{day}$ (146 000 ML/yr), we have also used $Q_s/z = 0.4 \text{ day}^{-1}$ and $k/z = 20 \text{ day}^{-1}$ (broken line). This provides a reasonable fit to the nearshore ^{223}Ra and ^{226}Ra data, although underpredicts the nearshore ^{224}Ra and ^{228}Ra data. For $Q_G = 1 \times 10^6 \text{ m}^3/\text{day}$ (365 000 ML/yr), $Q_s/z = 0.2 \text{ day}^{-1}$ and $k/z = 10 \text{ day}^{-1}$ (solid line) we get better fits to the nearshore ^{224}Ra and ^{228}Ra data, but overpredict nearshore ^{223}Ra and ^{226}Ra data. None of the simulations accurately predict the rate of decrease in activity of the tracers with distance offshore. We believe that this is partly due to the assumption of constant depth required by our model. (This assumption allows the equations to be readily solved.) As the water depth increases with distance offshore, then this would reduce the importance of tracer flux from the sediments (Q_s/z would decrease offshore). The eddy diffusion rate (K_h) may also increase offshore, as the sheltering effect of the Bay is reduced.

Table 4.1. Input parameters used for modelling of offshore radon and radium activities. Input activities for surface and groundwater discharge are given in Table 4.2.

Parameter	Low Discharge Simulation	High Discharge Simulation
Q_G (m^3/d)	4×10^5	1×10^6
Q_H (m^3/d)	76 300	76 300
Q_B (m^3/d)	64 800	64 800
K_h (m^2/d)	10^6	10^6
Q_s/z (day^{-1})	0.4	0.2
k/z (day^{-1})	20	10
t_r (d)	0.5	0.5
w (m)	35 000	35 000
d (m)	2	2

Table 4.2. Radon and radium activities used for modelling offshore activities.

Parameter	^{223}Ra	^{224}Ra	^{226}Ra	^{228}Ra	^{222}Rn
c_H (mBq/L)	2.36	86.2	10.86	77.6	38.0
c_B (mBq/L)	1.0	50.0	6.0	25.0	60.0
c_G (mBq/L)	7.0	161	24.5	126	13000
γ/λ (mBq/L)	7.0	161	24.5	126	13000
c_L (mBq/L)	0.06	1.0	1.2	2	21

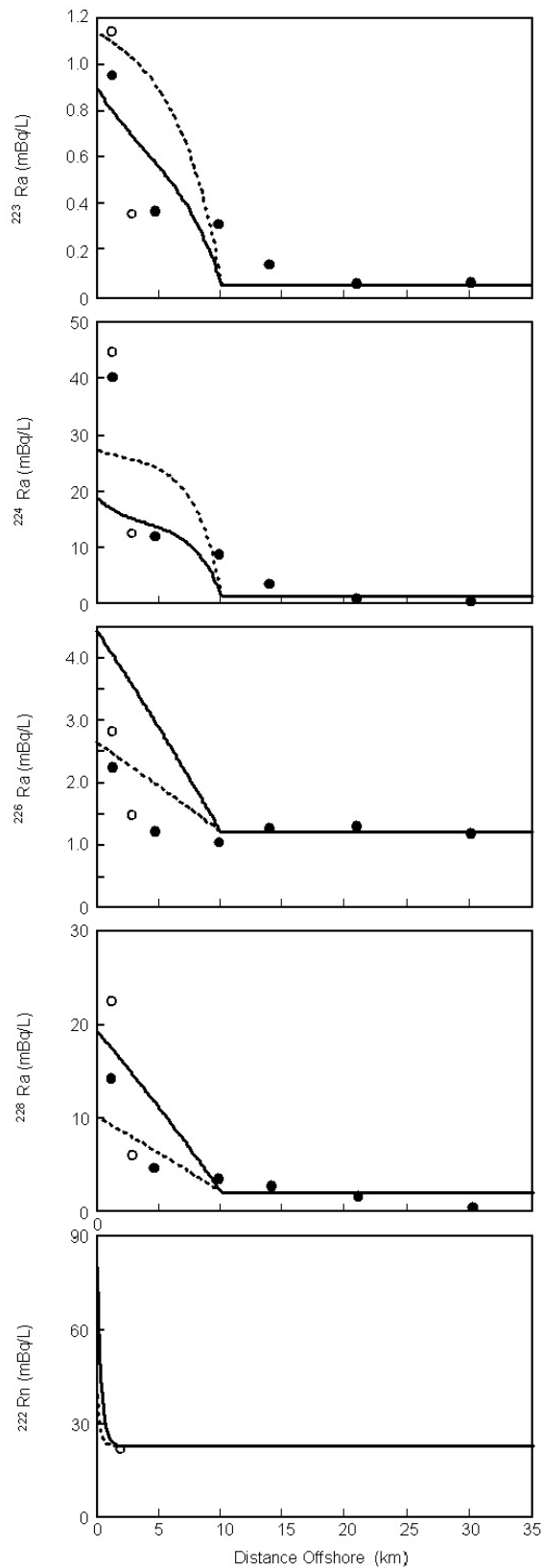


Figure 4.10. Comparison between numerical simulations of offshore tracer activities and measured values. The solid line is for $Q_G = 1 \times 10^6 \text{ m}^3/\text{day}$, $Q_s/z = 0.2 \text{ day}^{-1}$ and $k/z = 10 \text{ day}^{-1}$. The broken line is for $Q_G = 4.0 \times 10^5 \text{ m}^3/\text{day}$, $Q_s/z = 0.4 \text{ day}^{-1}$ and $k/z = 20 \text{ day}^{-1}$. Other model parameters are given in the Tables 4.1 and 4.2.

As stated above, we used the maximum measured activities of the radium isotopes in groundwater to represent both c_G and γ/λ . Because of the tendency for the activity to increase within increasing salinity, this approach seems reasonable. The use of mean measured activities does not improve the fit to the data. Use of much higher values would allow the data to be simulated using lower Q_G . If we use double the maximum measured radium activities in groundwater for c_G and γ/λ , then the data can be simulated by halving the values for Q_G , Q_s/z and k/z ($Q_G = 2.0 \times 10^5$ m³/day, $Q_s/z = 0.2$ day⁻¹ and $k/z = 10$ day⁻¹). Similarly, if we increase the radium flux in surface water by replacing Q_H and Q_B with the mean annual flow rates for Haughton River and Barratta Creek respectively (without changing c_H and c_B), then again the observed offshore activities can be reproduced using a lower value for groundwater discharge ($Q_G = 1.5 \times 10^5$ m³/day, $Q_s/z = 0.4$ day⁻¹ and $k/z = 20$ day⁻¹). Additional measurements of radium isotope activities in surface water and in groundwater would help constrain the model.

5. DISCUSSION AND CONCLUSIONS

5.1. Discharge to Surface Waters

Groundwater discharge from the floodplain aquifers of the lower Burdekin has been estimated using radon and radium isotopes in conjunction with numerical modelling. For the Burdekin River, Haughton River, Barratta Creek and Plantation Creek, we have used a one-dimensional model of radon activities within the river. The model includes radon input due to groundwater inflow, and radon loss due to radioactive decay and gas exchange to the atmosphere. The input parameters to which the model results are most sensitive are the radon activity in groundwater inflow, the gas transfer velocity across the water surface and the river width. The radon activity of groundwater inflow was determined from measurements on groundwater samples obtained from 38 bores throughout the floodplain region. Measured activities ranged between 2735 and 33750, with a mean activity of approximately 13 700 mBq/L. On the regional scale, there was no apparent pattern to the observed variations in radon activity of groundwater, and so a constant value of 13 000 mBq/L was used for the model. Although the use of this constant value may have resulted in errors in the local estimates of groundwater discharge, over larger scales the approach is justified.

A constant value for the gas exchange velocity of 1 m/day was used for the Burdekin River, Haughton River and Barratta Creek, and a value of 8 m/day was used for Plantation Creek. (The high value of k , is consistent with the relatively narrow, shallow channel and hence more turbulent flow in Plantation Creek than in the major rivers.) The choice of value was based on published studies (Raymond and Cole, 2001), but the value was also adjusted during model calibration. If ion concentrations can be used to determine groundwater inflow, then it is sometimes possible to constrain the gas exchange velocity from comparison of ion and dissolved gas concentrations (Cook et al., 2003), although this was not possible in our case. It is possible to constrain k_w , however, in river reaches where groundwater inflows are low. For the downstream reaches of the Burdekin River, k_w was thus determined to be more than 135 m²/day. Similarly, for the Barratta Creek immediately upstream of the highway, the observed radon activities constrained $k_w > 7$ m²/day in December 2003 and $k_w > 5$ m²/day in May 2004. Based on our measured values of river width, the gas exchange velocity for the larger rivers was thus constrained to be $k \geq 1$ m/day. If it were known from other means (e.g., from hydraulics) that the river is losing along a particular reach, then the value of k can be tightly constrained. An attempt was made to directly determine the gas exchange velocity using a dissolved gas artificial tracer, although the experiment was not successful due to technical difficulties with the injection system. More accurate determination of this parameter would certainly improve the accuracy of the estimated groundwater inflows. River width was estimated at a number of sites. However, the sensitivity to this parameter is high, and so additional estimates could improve the accuracy of the model.

Our model does not allow for temporal variations in river width or depth in response to variations in flow rate, nor does it account for extractions from the river by private pumps, or at the Sunwater pump stations. Provided that these extractions do not reduce the total river flow rate significantly, then the omission is not important. However, the extractions may be significant at times of low flow, and so their incorporation into the model might be justified.

We have modelled groundwater inflow to the river as discrete zones of uniform inflow rate, and abrupt boundaries between these zones. Of course, groundwater inflow rates probably vary much more smoothly. However, the model is sensitive to the total groundwater inflows. The scale length for changes in radon activity will vary with model parameters (particularly river width), but is mostly in the order of hundreds of metres to a few kilometres. This is the theoretical spatial resolution of the model. However, the spatial resolution of the model predictions is also related to the spatial intensity of the sampling that is used for model calibration. The spatial resolution of the estimated groundwater inflows will be the greater of the spatial intensity of the sampling and the scale length.

Distances along the rivers and creeks have been estimated from the 1:250 000 topographic map. The coarse scale of this map will mean that estimated distances will be less than true river distances, particularly for the Burdekin River which meanders within its floodplain. However, identical simulations can be produced by increasing the river distances and proportionally reducing river widths and reducing the groundwater inflow rate per unit length of river. (This is apparent from examination of Equation 3.3.) Because the groundwater inflow rate per unit length of river is reduced in proportion to the increase in river length, the total estimated groundwater inflow rate is unchanged.

While the model assumes steady state conditions, significant rain events occurred at each of the three sampling times, and changes in river flow may have affected the results. For example, for a flow rate of 0.5 m³/day of the Haughton River, it is estimated that the mean residence time of water between Val Bird Weir and Giru Weir is approximately 10 – 20 days. The travel time between Clare Weir and Site 52 on the Burdekin River varies from 4 – 5 days during the dry season to much less during the wet season. It is possible, therefore, that activities within the Haughton River might not reflect the flow regime at the time of sampling.

Because the model assumes steady-state flow, it is difficult to use it to simulate radon activities in tidal parts of the rivers and creeks. We have attempted to correct the measured radon activities within the tidal reaches based on measured electrical conductivities, and an assumed radon activity and electrical conductivity of the seawater end-member. This approach has allowed us to obtain estimates of groundwater discharge for tidal reaches, although the confidence of the inferred groundwater inflows is lower in these regions. Based on the modelling results, we estimate that more than 90% of groundwater inflows to the Barratta Creek occur within the tidal section of the creek. For the Haughton River, the proportion is perhaps between 30% and 50%. We were not able to determine this proportion for the Burdekin River, because of the limited sampling within the tidal reach.

Estimation of mean annual groundwater discharge from measurements made at only a few discrete times is also difficult. For the Burdekin River and Barratta Creek, detailed sampling only occurred in December 2004 and April-May 2004. For the Haughton River detailed sampling occurred only in April-May 2004. Over the 40 km reach immediately downstream of Clare Weir, the groundwater inflow to the Burdekin River is estimated to be 127 ML/day, based on samples collected on 2 May 2004. However, measurement of radon activities between Sites 6 and 14 on the Burdekin River did permit estimates of groundwater inflows to be made at five times throughout the year (Table 5.1). Between April 26 and May 2, estimated inflow rates ranged between 2.0 and 4.7 m³/day/m, even the groundwater and surface water levels would not have varied greatly over this period. The difference between these values may reflect the error of the methodology, as much as actual changes in groundwater inflows. In December, when groundwater inflows are likely to be lowest,

the inflow was estimated at 2.1 m³/day/m. Thus, while the groundwater inflow estimated for April-May was higher than for December, the difference was probably within the error of the methodology. However, comparison of surface water and groundwater hydrographs suggests that greatest groundwater inflow may occur in April – May, when groundwater levels remain high from the previous wet season, and surface water levels have fallen. Thus mean annual groundwater inflows for the 40 km reach of Burdekin may therefore be around 100 ML/day.

On the Haughton River, the estimated groundwater inflow in May 2004 for the 26 km reach between the Haughton Main Channel outlet and Giru Weir was 12.3 – 32.3 ML/day, with the uncertainty being due to the infrequency of the sampling in the upper reaches. Immediately below Giru Weir, a groundwater inflow of 5.0 ML/day occurs, and this is attributed to the raised groundwater levels surrounding the Weir. A total of 13.5 ML/day inflow occurs between Giru Weir and the mouth. On Barratta Creek, groundwater inflow between Clare Road and a site just below the tidal limit was 1.5 ML/day in December 2003 and 6.4 ML/day in May 2004. A further inflow of 24 ML/day in May 2004 occurred in the tidal section of the creek. Barratta Creek showed much greater temporal variation in groundwater inflows than either Haughton River or Burdekin River. It is worth noting that the variability in flow rate of Barratta Creek is also much greater than the Burdekin River or Haughton River (Figure 3.1), because flow is not supplemented during the dry season.

Sensitivity analysis suggested that ±50% errors in estimated groundwater inflows would arise from approximately 50% errors in river width, gas exchange velocity and radon activity of groundwater inflow, although in areas of highest inflow sensitivity to river width and gas exchange is reduced. It is difficult to accurately estimate the uncertainty of the estimated groundwater inflows, because the uncertainties of all the model parameters are unknown. The radon activity of groundwater inflow (c_i) is probably known to better than ±50%. Because the minimum value of kw is constrained, its uncertainty may be –30% - + 200%. Based on these values, we estimate that the predictions of groundwater inflow are probably accurate to –50% - + 250% in the upstream reaches. Within the tidal reaches, to uncertainties would be somewhat higher. Improved accuracy of various model parameters may increase the accuracy of groundwater inflows in the upstream reaches to within ±50%, but it would be difficult to improve the estimates further than this.

Table 5.1. Groundwater inflow rates (ML/day) along different reaches of the major rivers and creeks of the Burdekin floodplain at different sampling times.

	Burdekin River		Haughton River	Barratta Creek		Plantation Creek	
<i>Sites</i>	5 – 53	6-14	70 - 51	20-25	25-24	14-28	14-15
<i>Distance (km)</i>	34.6	12.1	26.8	33.0	17.6	26.5	10.4
9-11 Dec 2003		25		1.5		6.3	0
3 Feb 2003		29					4.4
26 April 2004		41					
27 April 2004		24					
2 May 2004	127	57					
4-6 May 2004			36	6.4	24		

5.2. Submarine Groundwater Discharge

Groundwater discharge to the ocean has been estimated from radon and radium activities measured within Bowling Green Bay. The data has been interpreted using a one-dimensional model that simulates advection and mixing within the ocean, as well as radioactive decay, gas exchange and production within seafloor sediments. Radon and radium produced within the seafloor sediments is released into the water column by advection caused by wave action and tidal fluctuations. The input parameters for the model include the eddy mixing coefficient, the gas exchange velocity (for radon only), the mean water flux that moves in and out of the sediments each tidal cycle in response to wave action and tidal pumping (the recycled seawater exchange rate), the equilibrium activity within the seafloor sediments, the submarine groundwater discharge rate, and the mean activities of submarine groundwater discharge and of discharges from Houghton River and Barratta Creek. The eddy mixing coefficient is estimated from the short-lived radium isotopes. The gas exchange velocity has not been directly estimated, and this constitutes a significant source of error for estimation of submarine groundwater discharge from the radon activity of seawater. The radium activities of Houghton River and Barratta Creek have not been well-constrained, although the radium flux contributed by surface water appears to be relatively small, and so inaccuracies in these parameters may not be of major concern. Although the equilibrium activities within seafloor sediments have not been estimated, we have assumed that the mean activities measured in groundwater samples reflect the equilibrium activity within the seafloor sediments. Perhaps the largest source of error is the recycled seawater exchange rate, and this has not been directly estimated.

Terrestrial inputs to the coastal zone (surface water and groundwater discharge) are likely to vary seasonally. The half-lives of ^{226}Ra and ^{228}Ra are sufficiently long so that these tracer activities in the marine environment should reflect the mean annual inputs. However, the half-lives of ^{223}Ra and ^{224}Ra , which constrain the eddy mixing rate, K_h , and the recycled seawater exchange rate, Q_s , are less than 12 days. Measurements of these tracers would need to be made at other times of year to determine whether there are significant seasonal variations in these parameters. If Q_s/z were much greater at other times of year, then lower values of Q_G would result, although we do not consider this to be a major source of error. Similarly, lower values of Q_G would provide a reasonable fit to the observed data if Q_{BCB} and Q_{HCH} were much greater during the wet season.

Notwithstanding these issues, simulation of all four radium isotopes and ^{222}Rn has allowed some constraints to be placed on the possible values for the groundwater discharge rate Q_G and the pumping rate Q_s/z . In particular, the groundwater discharge rate Q_G appears to be bounded between approximately 2.0×10^5 and 1.0×10^6 m^3/day (75 000 – 370 000 ML/yr). The pumping rate is in the order of $Q_s/z = 0.2 - 0.4$ day^{-1} . Larger values of either Q_G or Q_s/z result in radon activities that are much greater than the measured values. Higher values of Q_G and Q_s/z would only be possible if the gas exchange coefficient k/z was greater than 20 day^{-1} , which does not seem reasonable based on literature data (Wanninkhof, 1992). Lower values of Q_G would be produced only if the radium activities of groundwater inflow are much greater than the measured radium activities in groundwater.

5.3. Conclusions

McMahon et al. (2002) estimated total recharge for the Burdekin River delta (area 850 km²) to be between 430 000 and 850 000 ML/yr. Groundwater pumping is estimated to be between 440 000 and 830 000 ML/yr. Based on radon activities within surface waters, the total estimated groundwater discharge to surface waters is 30 000 – 150 000 ML/yr, although this figure applies to a larger area than the recharge and groundwater pumping estimates. (This figure also assumes also that the majority of the discharge to surface waters occurs to the Burdekin River, Haughton River, Barratta Creek and Plantation Creek.) The groundwater discharge directly into Bowling Green Bay is estimated to be 50 – 400 000 ML/yr. (Groundwater discharge would also occur to the coast between Peters Island and Cape Bowling Green, although this has not been quantified.)

6. REFERENCES

- Burnett W C and Dulaiova H (2003) Estimating the dynamics of groundwater input into the coastal zone via continuous radon-222 measurements. *Journal of Environmental Radioactivity*, 69:21-35.
- Cable J E, Burnett W C, Chanton J P and Weatherly G L (1996) Estimating groundwater discharge into the northeastern Gulf of Mexico using radon-222. *Earth and Planetary Science Letters*, 144:591-604.
- Chapra S C and Wilcock R J (2000) Transient storage and gas transfer in lowlands stream. *Journal of Environmental Engineering*, 126(8):708-712.
- Chung Y C, Craig H, Ku T L, Goddard J. and Broecker W. S. (1974) Radium-226 measurements from three GEOSECS intercalibration. *Earth and Planetary Science Letters*, 23(1):116-124.
- Clark J F, Simpson H J, Smethie W M and Toles C (1992) Gas exchange in a contaminated estuary inferred from chlorofluorocarbons. *Geophysical Research Letters*, 19(11):1133-1136.
- Cook P G, Favreau G, Dighton J C and Tickell S (2003) Determining natural groundwater influx to a tropical river using radon, chlorofluorocarbons and ionic environmental tracers. *Journal of Hydrology*, 277:74-88.
- Corbett D R, Burnett W C, Cable P H and Clark S B (1998) A multiple approach to the determination of radon fluxes from sediments. *Journal of Radioanalytical and Nuclear Chemistry*, 236(1-2):247-252.
- Ellins K K, Roman-Mas A and Lee R (1990) Using ^{222}Rn to examine groundwater/surface discharge interaction in the Rio Grande De Manati, Puerto Rico. *Journal of Hydrology*, 115:319-341.
- Genereux D P, Hemond H F and Mulholland P J (1993) Use of radon-222 and calcium as tracers in three-end-member mixing model for streamflow generation on the west fork of Walker Branch Watershed. *Journal of Hydrology*, 142:167-211.
- Hancock G J and Murray A S (1996) Source and distribution of dissolved radium in the Bega River estuary, Southeastern Australia. *Earth and Planetary Science Letters*, 138:145-155.
- Hartman B and Hammond D E (1984) Gas exchange rates across the sediment-water and air-water interfaces in South San Francisco Bay. *Journal of Geophysical Research*, 89:3593-3603.
- Herczeg AL, Dighton JC, Easterbrook ML and Salomons E (1994) Radon-222 and Ra-226 measurements in Australian groundwaters using liquid scintillation counting. Proc. Workshop on Radon and Radon Progeny measurements in Environmental Samples, Feb. 1994, Canberra, pp.53-57.
- Hibbs D E, Parkhill K L and Gulliver J S (1998) Sulfur hexafluoride gas tracer studies in streams. *Journal of Environmental Engineering*, 124(8):752-760.

- Lee R W and Hollyday E F (1993) Use of radon measurements in Carters Creek, Maury County, Tennessee, to determine location and magnitude of ground-water seepage. In Gundersen L C S and Wanty R B (eds) *Field Studies of Radon in Rocks, Soils, and Water*. C.K. Smoley, pp. 237-242.
- Li L, Barry D A, Stagnitti F and Parlange J Y (1999) Submarine groundwater discharge and associated chemical input to a coastal sea. *Water Resources Research*, 35(11):3253-3259.
- McMahon G A, Arunakumaren N J and Bajracharya K (2002) Estimation of the groundwater budget of the Burdekin River Delta aquifer, North Queensland. Balancing the Groundwater Budget, 12 – 17 May 2002, Darwin.
- Martens C S, Kipphut G W and Klump J V (1980) Sediment-water chemical exchange in the coastal zone traced by in situ radon-222 flux measurements. *Science*, 208:285-288.
- Moore W S (1976) Sampling radium-228 in the deep ocean. *Deep-Sea Research*, 23:647-651.
- Moore W S (1984) Radium isotope measurements using germanium detectors. *Nucl. Inst. Methods* 223:407-411.
- Moore W S (1996) Large groundwater inputs to coastal waters revealed by ^{226}Ra enrichments. *Nature*, 380:612-614.
- Moore W. S. (2003) Sources and fluxes of submarine groundwater discharge delineated by radium isotopes. *Biogeochemistry*, 66:75-93.
- Moore W S and Arnold R (1996) Measurement of ^{223}Ra and ^{224}Ra in coastal waters using a delayed coincidence counter. *Journal of Geophysical Research*, 101:1321-1329.
- Raymond P A and Cole J J (2001) Gas exchange in rivers and estuaries: Choosing a gas transfer velocity. *Estuaries*, 24(2):312-317.
- Ridd P V (1996) Flow through animal burrows in mangrove creeks. *Estuarine, Coastal and Shelf Science*, 43:617-625.
- Stieglitz T. and Ridd P (2000) Submarine groundwater discharge from paleochannels? "Wonky holes " on the inner shelf of the Great Barrier Reef, Australia. In: Hydro 2000 (26th National and 3rd International Hydrology and Water Resources Symposium of Institution of Engineers, Australia), Perth. Institution of Engineers, Australia, p.1-6.
- Wanninkhof R (1992) Relationship between wind speed and gas exchange over the ocean. *Journal of Geophysical Research*, 97(C5):7373-7382.
- Wanninkhof R, Mulholland P J and Elwood, J W. (1990) Gas exchange rates for a first-order stream determined with deliberate and natural tracers. *Water Resources Research*, 26(7):1621-1630.

7. ACKNOWLEDGEMENTS

The authors would like to thank Vivien Danis, Thabo Thayalakumaran, Tim Phillips and Tony McKenna for assistance with sampling. Ray McGowan, Gary Jensen, Phil Charlesworth and Gary Hancock provided advice throughout the project. Gary Hancock also carried out the radium analyses. Use of AIMS facilities and RV Titan for offshore sampling is greatly appreciated. The work was jointly funded by Department of Natural Resources, Mines and Energy and CSIRO Land and Water.

APPENDIX 1: Field Measurements of River Width

Table A1.1. River widths, as measured on 23-24.06.2004.

River	Site	Latitude	Longitude	Width (m)
Haughton River	Site 51	19°30.011'	147°06.674'	10
	Giru Weir – below weir	19°30.629'	147°06.697'	2
		– above weir	19°30.629'	147°06.697'
	Site 48	19°31.034'	147°06.716'	95
	42	19°31.951'	147°06.936'	135
	50	19°32.825'	147°06.859'	95
	Highway bridge			95
	Site 44 (Val Bird Weir) – below weir	19°33.769'	147°05.755'	80
		– above weir	19°33.769'	147°05.755'
		19°35.450'	147°06.019'	85
	Site 68	19°38.412'	147°06.333'	50
		19°38.897'	147°05.589'	8
	Site 69	19°41.221'	147°04.746'	10
	Site 70	19°42.430'	147°04.543'	5
Burdekin River	Site 53	19°37.782'	147°24.319'	135
	Site 14	19°38.827'	147°23.039'	135
	Site 6	19°42.208'	147°17.539'	100
	Pumping station	19°47.682'	147°14.065'	50
	Site 5 (Clare Weir) – below weir	19°51.430'	147°14.040'	100
		– above weir	19°51.430'	147°14.040'
Barratta Creek	one of several channels that comprise West Barratta Creek	19°31.723'	147°13.098'	10
	West Barratta Creek	19°33.332'	147°12.214'	76
	West Barratta Creek @ highway	19°34.080'	147°12.446'	60
	East Barratta Creek @ highway – below	19°34.295'	147°13.411'	5
		– above	19°34.295'	147°13.411'
	Site 20	19°42.414'	147°08.856'	5

APPENDIX 2: Locations of Sampling Sites

Table A2.1. Locations of surface water gauging stations.

RN number	Location	South	East
11900077	Haughton River	19°33.39	147°06.33
11900078	Haughton River	19°33.39	147°06.32
11900079	Haughton River	19°32.82	147°06.90
11900082	Haughton River	19°30.76	147°06.75
11900083	Haughton River	19°32.96	147°02.90
11900084	Haughton River - Healeys Lagoon	19°31.96	147°03.23
11900085	Haughton River - Healeys Lagoon	19°32.81	147°06.82
11910154	Haughton River – Pink Lilly Lagoon @ Highway	19°37.32	147°28.78
11910156	Sheepstation Creek	19°39.22	147°20.58
11910157	Sheepstation Creek	19°38.72	147°20.38
11910158	Sheepstation Creek	19°37.59	147°18.80
11910159	Sheepstation Creek	19°36.32	147°19.47
11910160	Sheepstation Creek	19°33.96	147°20.83
11910161	Sheepstation Creek	19°30.99	147°19.75
11910164	Plantation Creek		
11910165	Plantation Creek	19°37.02	147°21.68
11910166	Plantation Creek – Hutchings Lagoon	19°36.12	147°21.88
11910170	Plantation Creek	19°34.61	147°26.42
11910171	Plantation Creek	19°33.09	147°27.70
11910172	Lilliesmere Lagoon	19°31.83	147°24.92
11910173	Hughes Lagoon (near Jarvisfield)	19°35.61	147°27.55
11910206	East Barratta Creek	19°34.16	147°13.37
11910207	West Barratta Creek	19°34.07	147°12.45
12000151	Burdekin River - Clare Weir	19°51.36	147°14.22
12000152	Burdekin River - Clare 'A' pump station	19°47.61	147°14.27
12000153	Burdekin River - Mona Park	19°42.34	147°16.68
12000154	Burdekin River - D/S of NBWB Rocks pump station	19°42.24	147°18.43
12000155	Burdekin River - SBWB McDowell's pump station	19°41.01	147°21.15
12000156	Burdekin River - adjacent to Osborne School	19°40.29	147°22.13
12000157	Burdekin River Bridge	19°38.26	147°23.68
12000166	Burdekin River - Groper Creek Tide Gauge	19°41.19	147°31.88

Table A2.2. Locations of surface water sampling sites.

Site	Location	South	East
1	Burdekin River – Mouth	19°39.700'	147°35.014'
2	Burdekin River - Upstream of Rita Is boat ramp	19°39.362'	147°30.696'
3	Burdekin River - Rita Island boat ramp	19°39.957'	147°31.737'
4	Ana Branch bridge @ Rita Island	19°37.453'	147°28.970'
5	Clare Weir	19°51.430'	147°14.040'
6	The Rocks' pumping station	19°42.208'	147°17.539'
7	Groper Creek – Mouth	19°42.223'	147°35.060'
8	Groper Creek / Heath Creek	19°42.167'	147°33.704'
9	Groper Creek - Boat ramp	19°41.644'	147°32.125'
10	Groper Creek / MacDonald Creek	19°40.873'	147°31.636'
11	Plantation Creek - golf course	19°35.071'	147°25.596'
12	Plantation Creek - ski club	19°35.334'	147°22.830'
13	Plantation Creek @ Giddy creek road	19°37.034'	147°21.617'
14	Burdekin River - Pump Station No. 3	19°38.827'	147°23.039'
15	Plantation Creek - Highway culvert	19°35.220'	147°23.867'
16	Collinsons Lagoon	19°33.517'	147°17.361'
17	East Baratta Creek @ Highway	19°34.295'	147°13.411'
18	West Baratta Creek @ DNR gauging station	19°34.080'	147°12.446'
19	Barattas Creek @ Allen road	19°37.130'	147°12.189'
20	Barattas Creek @ Clare road	19°42.414'	147°08.856'
21	Haughton River ~5km upstream of Giru boat ramp	19°29.270'	147°06.829'
22	Haughton River - Mouth	19°24.880'	147°07.968'
23	Haughton River @ Boat ramp	19°28.122'	147°05.850'
24	Barattas Creek - the mouth @ Hucks Landing	19°26.254'	147°14.940'
25	Barattas Creek ~ 19km upstream of boat ramp	19°30.127'	147°14.751'
26	Barattas Creek	19°28.704'	147°13.965'
27	Barattas Creek	19°27.288'	147°15.452'
28	Plantation Creek boat ramp	19°32.168'	147°30.793'
29	Rita Creek boat ramp @ Phillips landing	19°35.232'	147°33.013'
30	Sheep Station Creek @ SSC road (Ahern bridge)	19°39.249'	147°20.477'
31	Sheep Station Creek @ Pyards culvert	19°37.104'	147°18.900'
32	Sheep Station Creek @ SSC road (past Kellys lagoon)	19°35.544'	147°20.095'
33	Kellys Lagoon	19°36.088'	147°19.971'
34	Castinelli's Lagoon	19°35.941'	147°20.497'
35	Dicks Bank - Downstream culvert @ highway	19°33.848'	147°20.700'
36	Burke's Bank - Downstream culvert @ rail crossing	19°32.473'	147°20.348'
37	Gorizia's Lagoon	19°30.926'	147°19.650'
38	Jack's Lagoon	19°29.992'	147°19.407'
39	Sheep Station Creek	19°28.728'	147°18.396'
40	RB1 channel drainage system @ sayers road	19°35.542'	147°16.845'
41	Lillimere Lagoon - downstream of Kalamia mill	19°31.086'	147°25.220'
42	Haughton River	19°31.951'	147°06.936'
43	Haughton River	19°32.370'	147°06.909'
44	Haughton River - Val Bird Weir	19°33.769'	147°05.755'
45	Haughton River - John Ichurra's pump station	19°35.450'	147°05.780'
46	West Baratta Creek @ road culvert	19°30.500'	147°13.136'
47	Baratta Creek mouth @ Jerona	19°26.922'	147°14.455'
48	Haughton @ pump station behind mill	19°31.034'	147°06.716'
49	Plantation Creek @ bridge	19°38.301'	147°22.869'
50	Haughton @ cane railway bridge north of highway	19°32.825'	147°06.859'
51	Haughton downstream of Giru	19°30.011'	147°06.674'
52	Burdekin upstream of Anabranh	19°37.635'	147°27.068'
53	Burdekin downstream of bridge	19°37.782'	147°24.319'
54	Burdekin upstream of pump station no. 3	19°41.021'	147°21.199'

55	Burdekin downstream of Clare	19°44.344'	147°16.369'
56	Burdekin downstream of Clare Weir	19°48.666'	147°14.091'
57	Haughton River	19°30.429'	147°06.697'
58	Haughton River	19°29.859'	147°06.924'
59	Haughton River	19°28.787'	147°06.364'
60	Haughton River	19°28.063'	147°06.645'
61	Haughton River	19°27.540'	147°06.421'
62	Haughton River	19°27.927'	147°07.092'
63	Haughton River	19°27.108'	147°07.570'
64	Haughton River	19°26.178'	147°07.076'
65	Haughton River	19°25.241'	147°07.138'
66	Barrata Creek @ Pump Station	19°33.009'	147°12.279'
67	Barrata Creek @ Baudino Road	19°39.578'	147°09.157'
68	Haughton River @ Majors Road	19°38.412'	147°06.333'
69	Haughton River @ Bill Britt Road	19°41.221'	147°04.746'
70	Haughton River @ Blacks Road DPI channel	19°42.430'	147°04.543'
71	Sunwater gauging station	19°49.797'	147°18.045'
72	Pumping station	19°48.815'	147°15.534'
73	Gauging station	19°47.192'	147°15.618'
74	Fowlers lagoon culvert	19°43.701'	147°20.768'
75	Harper Road / Oats Road channel crossing	19°45.010'	147°25.866'
76	Alma Creek channel	19°44.688'	147°28.713'
77	Saltwater creek @ Highway crossing	19°46.392'	147°30.941'
78	Inkerman Lagoon waterboard channel	19°45.161'	147°28.943'
79	Iyah Creek	19°42.606'	147°27.018'
80	Papale's Farm drainage channel	19°42.158'	147°22.091'
81	Sibon Road channel crossing @ silo	19°42.783'	147°25.125'
83	Barratta Creek	19°30.251'	147°14.656'
84	Barratta Creek	19°30.073'	147°14.315'
85	Barratta Creek	19°29.901'	147°13.812'
86	Barratta Creek	19°29.670'	147°13.394'
87	Barratta Creek	19°29.272'	147°13.757'
88	Barratta Creek	19°29.311'	147°14.286'
89	Barratta Creek	19°29.244'	147°14.528'
90	Barratta Creek	19°28.895'	147°14.207'
91	Barratta Creek	19°28.479'	147°14.001'
92	Barratta Creek	19°28.640'	147°14.488'
93	Barratta Creek	19°28.277'	147°14.842'
94	Barratta Creek	19°27.660'	147°15.223'
95	Barratta Creek	19°27.192'	147°15.095'
96	Barratta Creek	19°30.127'	147°14.751'

Table A2.3. Locations of groundwater sampling bores.

Bore	South	East
11900178	19°32.00'	147°08.45'
11900184	19°32.20'	147°10.20'
11900199B	19°32.20'	147°10.20'
11900212	19°38.15'	147°06.98'
11900218	19°35.58'	147°08.07'
11910036	19°30.41'	147°20.82'
11910037	19°29.88'	147°22.35'
11910048	19°32.34'	147°25.77'
11910049	19°34.57'	147°24.90'
11910066	19°34.70'	147°22.10'
11910073	19°35.69'	147°24.67'
11910082	19°37.34'	147°18.07'
11910095	19°37.37'	147°22.20'
11910117	19°35.76'	147°19.78'
11910119	19°33.22'	147°20.90'
11910124	19°34.04'	147°26.73'
11910190	19°34.16'	147°12.77'
11910257A	19°35.99'	147°28.47'
11910258	19°32.11'	147°23.28'
11910263E	19°31.61'	147°27.93'
11910268A	19°32.12'	147°23.27'
11910268B	19°32.12'	147°23.27'
11910268C	19°32.12'	147°23.27'
11910268D	19°32.12'	147°23.27'
11910268E	19°32.12'	147°23.27'
11910270	19°29.87'	147°22.35'
11910744	19°35.39'	147°17.15'
11910808	19°39.17'	147°19.88'
11910810	19°37.62'	147°18.85'
11910877	19°33.42'	147°16.63'
11910878	19°33.42'	147°16.63'
11910942	19°33.79'	147°20.20'
11910975	19°36.56'	147°15.22'
11911051	19°36.47'	147°11.73'
12100166F	19°43.87'	147°31.93'
12000079	19°40.57'	147°26.03'
12000114	19°39.49'	147°25.38'
12000204D	19°40.94'	147°27.83'
12000251	19°43.50'	147°17.98'
12000871	19°40.77'	147°22.35'

Table A2.4. Offshore sampling locations.

Station	South	East	Water Depth (m)
F1	19°40.113'	147°26.928'	
F2	19°40.211'	147°24.488'	
F3	19°39.793'	147°22.134'	
F4	19°39.325'	147°19.865'	
F5	19°38.882'	147°17.766'	
F6	19°38.438'	147°15.554'	
F7	19°37.404'	147°13.483'	
F8	19°36.271'	147°11.895'	
F9	19°35.286'	147°10.335'	
F10	19°33.956'	147°08.860'	
F11	19°32.380'	147°07.839'	
F12	19°30.632'	147°06.960'	
F13	19°28.957'	147°06.251'	
A1	19°40.299'	147°41.717'	
A2	19°40.487'	147°40.716'	
A3	19°40.214'	147°37.364'	
A4	19°40.210'	147°35.550'	
A5	19°39.887'	147°33.807'	
A6	19°39.535'	147°31.901'	
A7	19°39.447'	147°30.233'	
A8	19°39.904'	147°28.694'	
A9	19°40.529'	147°27.117'	
A10	19°40.464'	147°25.535'	
A11	19°40.162'	147°24.078'	
A12	19°40.152'	147°22.648'	
A13	19°40.212'	147°21.051'	
A14	19°39.870'	147°19.395'	
A15	19°39.250'	147°17.803'	
A16	19°38.995'	147°16.092'	
A17	19°38.804'	147°14.431'	
A18	19°38.006'	147°13.014'	
A19	19°36.854'	147°11.657'	
A20	19°35.729'	147°10.206'	
A21	19°34.553'	147°08.788'	
A22	19°33.248'	147°07.648'	
A23	19°31.766'	147°06.701'	
A24	19°30.078'	147°05.985'	
A25	19°28.439'	147°05.802'	
17R	19°40.250'	147°40.055'	2.7
16R	19°40.100'	147°35.000'	2.7
13R	19°38.415'	147°30.400'	4.1
19R	19°40.107'	147°24.505'	2.0
20R	19°40.128'	147°19.933'	3.7
14R	19°38.740'	147°13.893'	1.7
18R	19°33.692'	147°07.853'	6.4
15R	19°28.755'	147°05.697'	6.6
B7	19°14.705'	147°25.480'	23.4
B6	19°23.018'	147°25.498'	16.4
B5	19°29.373'	147°25.438'	13.4

B1	19°40.952'	147°24.762'	1.4
B2	19°37.824'	147°25.282'	3.6
B3	19°33.189'	147°26.065'	6.8
H1	19°39.181'	147°12.889'	3.2
CBG1	19°40.005'	147°42.020'	2.7

APPENDIX 3: Results of Chemical Analyses

Table A3.1. Radon activities in groundwater.

Bore	Date	²²² Rn (Bq/L)
11900178	27/10/2004	11623 ± 215
11900184	27/10/2004	10876 ± 202
11900199B	27/10/2004	2735 ± 52
11900212	27/10/2004	29662 ± 547
11900218	27/10/2004	20233 ± 374
11910036	21/01/2004	6460 ± 310
11910048	20/01/2004	9970 ± 400
11910049	19/01/2004	9160 ± 400
11910066	21/01/2004	12980 ± 420
11910073	20/01/2004	19850 ± 520
11910082	22/01/2004	12100 ± 400
11910095	22/01/2004	14770 ± 420
11910117	22/01/2004	12040 ± 400
11910119	21/01/2004	12510 ± 400
11910124	28/01/2004	7940 ± 260
11910190	28/01/2004	27750 ± 660
11910257A	20/01/2004	15470 ± 460
11910258	28/01/2004	33750 ± 800
11910263E	21/01/2004	10750 ± 370
11910268A	28/01/2004	16410 ± 420
11910268B	28/01/2004	11210 ± 310
11910268C	28/01/2004	14680 ± 370
11910268D	28/01/2004	12570 ± 330
11910268E	28/01/2004	12740 ± 340
11910744	22/01/2004	12790 ± 410
11910808	22/01/2004	9510 ± 350
11910810	22/01/2004	18020 ± 460
11910877	22/01/2004	21690 ± 540
11910878	22/01/2004	10020 ± 380
11910942	21/01/2004	10380 ± 380
11910975	22/01/2004	9140 ± 430
11911051	27/10/2004	19308 ± 356
12100166F	19/01/2004	9300 ± 390
12000079	19/01/2004	10790 ± 410
12000114	19/01/2004	12680 ± 440
12000204D	20/01/2004	7410 ± 340
12000251	27/10/2004	12130 ± 225
12000871	27/10/2004	10535 ± 195

Table A3.2. Radon measurements in surface waters.

Site	Location	Date	Time	Sample No.	¹ Radon (mBq/L)	² Radon (mBq/L)
1	Burdekin River mouth	08.12.03	13.30	BS1	43 ± 9	
2	Burdekin River upstream of Rita Is. boat ramp	08.12.03	14.15	BS2	60 ± 10	
3	Burdekin River - Rita Island boat ramp	08.12.03	14.40	BS3	24 ± 9	
		26.04.04	1530			77 ± 8
		02.05.04	1015	4z52	130 ± 4	
4	Ana Branch bridge @ Rita Island	08.12.03	15.20	BS4	27 ± 9	
5	Clare Weir	09.12.03	09.15	BS5	25 ± 8	
		27.04.04	0850	4z15	51 ± 3	
6	Burdekin @ The Rocks' pumping station	09.12.03	09.50	BS6	43 ± 9	
		03.02.04	17:30	BS51	27 ± 8	
		26.04.04	1330	4z4	81 ± 4	77 ± 9
		27.04.04	0937	4z16	66 ± 4	
7	Groper Creek mouth	09.12.03	12.15	BS7	21 ± 8	
8	Groper Creek / Heath Creek	09.12.03	12.35	BS8	44 ± 11	
9	Groper Creek @ boat ramp	09.12.03	13.00	BS9	44 ± 12	
10	Groper Creek / MacDonald Creek	09.12.03	13.26	BS10	61 ± 10	
11	Plantation Creek - golf course	09.12.03	15.00	BS11	38 ± 9	
		03.05.04	1400	4z59	256 ± 5	
12	Plantation Creek - ski club	09.12.03	15.30	BS12	33 ± 11	
		4.05.04	15:50	4z69	812 ± 13	
13	Plantation Creek @ Giddy creek road	09.12.03	15:45	BS13	83 ± 12	
		03.02.04	13.30	BS46, 47	60 ± 10, 66 ± 7	82 ± 8
14	Burdekin River @ Pump station No. 3	09.12.03	16.15	BS14	114 ± 13	
		03.02.04	1730	BS50	46 ± 7	
		26.04.04	1150	4z3	174 ± 6	150 ± 12
		27.04.04	1025	4z17	119 ± 4	
15	Plantation Creek @ Highway culvert	09.12.03	16.40	BS15	42 ± 11	
		03.02.04	15.30	BS48	87 ± 9	
		03.05.04	15:00	4z61	66 ± 3	
16	Collinsons Lagoon	10.12.03	13.50	BS16	51 ± 18	
		28.04.04	0931	4z24	97 ± 4	

17	East Baratta Creek @ Highway	10.12.03	14.15	BS17	53 ± 15	
		06.02.04	0715			101 ± 9
		06.05.04	0931	4z113	37 ± 13	
18	West Baratta Creek @ DNR gauging station	10.12.03	14.30	BS18	13 ± 12	
		06.05.04	1029	4z114	85 ± 4	
19	Barattas Creek @ Allen road	10.12.03	15.10	BS19	32 ± 14	
		06.05.04	1137	4z115	113 ± 5	
20	Barattas Creek @ Clare road	10.12.03	15.35	BS20	16 ± 14	
		06.05.04	1247	4z116	74 ± 4	
21	Haughton River ~5km upstream of Giru boat	11.12.03	09.45	BS21	263 ± 20	
		05.05.04	1218	4z103	148 ± 5	
22	Haughton River – Mouth	11.12.03	10.40	BS22	13 ± 11	
23	Haughton River @ Cromarty Creek boat ramp	11.12.03	11.10	BS23	29 ± 11	
		05.02.04	1130			97 ± 15
		05.05.04	1052	4z106	63 ± 4	
24	Barattas Creek mouth @ Hucks Landing	11.12.03	12.45	BS24	12 ± 11	
		04.05.04	1234	4z85	64 ± 4	
25	Barattas Creek ~ 19km u/s of boat ramp	11.12.03	13.45	BS25	69 ± 20	
		04.05.04	0912	4z70	359 ± 7	
26	Barattas Creek	11.12.03	14.20	BS26	87 ± 16	
27	Barattas Creek	11.12.03	14.45	BS27	33 ± 13	
28	Plantation Creek boat ramp	11.12.03	16.40	BS28	96 ± 15	
		03.05.04	15:00	4z60	275 ± 9	
29	Rita Creek boat ramp @ Phillips landing	11.12.03	17.25	BS29	42 ± 13	
30	Sheep Station Creek @ SSC road (Ahern bridge)	15.12.03	09.35	BS30	20 ± 13	
		29.04.04	0927	4z39	123 ± 6	
31	Sheep Station Creek @ Pyards culvert	29.04.04	1025	4z40	166 ± 7	
32	Sheep Station Creek @ SSC road	29.04.04	1056	4z41	56 ± 5	
33	Kellys Lagoon	29.04.04	1118	4z42	47 ± 5	
34	Castinelli's Lagoon	15.12.03	11.15	BS34	0 ± 14	
		29.04.04	1150	4z43	4 ± 4	
35	Dicks Bank - Downstream culvert @ highway	15.12.03	11.35	BS35	9 ± 12	
		29.04.04	1517	4z44	26 ± 4	
36	Burke's Bank - Downstream culvert @ rail crossing	15.12.03	12.00	BS36	23 ± 13	
		29.04.04	1555	4z45		

					47 ± 5	
37	Gorizia's Lagoon	29.04.04	1622	4z46	247 ± 3	
38	Jack's Lagoon	15.12.03	13.05	BS38	10 ± 13	
		29.04.04	1650	4z47	27 ± 3	
39	Sheep Station Creek	15.12.03	14.15	BS39	7 ± 16	
40	RB1 channel drainage system @ sayers road	28.04.04	0841	4z23	134 ± 4	
41	Lillimere Lagoon – d/stream of Kalamia mill	28.04.04	1011	4z25	13 ± 2	
42	Haughton River	06.02.04	09:45			294 ± 16
		26.04.04	10:30	4z2	89 ± 5	55 ± 7
		04.05.04	11:30	4z63	79 ± 4	
44	Haughton River - Val Bird Weir - below weir	4.05.04	1430	4z67	38 ± 2	
	- above weir	4.05.04	1430	4z68	226 ± 5	
46	West Baratta Creek @ road culvert	05.02.04	14.15	BS52	53 ± 16	55 ± 7
		01.05.04	16:00	4z51	337 ± 8	
47	Barattas Creek mouth @ Jerona	05.02.04	15.35	BS53	52 ± 10	87 ± 14
48	Haughton @ pump station behind mill	04.05.04	12:00	4z64	53 ± 3	
49	Plantation Creek @ bridge	03.02.04	1620	BS49	53 ± 8	
50	Haughton @ cane railway bridge north of highway	04.05.04	11:10	4z62	67 ± 4	
			12:50	4z66	46 ± 3	
51	Haughton downstream of Giru	04.05.04	12:30	4z65	686 ± 11	
52	Burdekin upstream of Anabbranch	02.05.04	1115	4z53	206 ± 5	
53	Burdekin downstream of bridge	02.05.04	1145	4z54	495 ± 8	
54	Burdekin upstream of pump station no. 3	02.05.04	1230	4z55	452 ± 8	
55	Burdekin downstream of Clare	02.05.04	1330	4z57	298 ± 6	
56	Burdekin downstream of Clare Weir	02.05.04	1430	4z58	263 ± 6	
57	Haughton River	05.05.04	0916	4z101	343 ± 7	
58	Haughton River	05.05.04	0954	4z102	280 ± 6	
59	Haughton River	05.05.04	1028	4z104	89 ± 4	
60	Haughton River	05.05.04	1040	4z105	41 ± 3	
61	Haughton River	05.05.04	1106	4z107	48 ± 3	
62	Haughton River	05.05.04	1109	4z108	51 ± 4	
63	Haughton River	05.05.04	1132	4z109	34 ± 3	
64	Haughton River	05.05.04	1145	4z110	37 ± 3	
65	Haughton River	05.05.04	1204	4z111	38 ± 3	

66	Barratta Creek @ Pump Station	06.05.04	0832	4z112	55 ± 3
67	Barratta Creek @ Baudino Road	06.05.04	1358	4z117	65 ± 4
68	Haughton River @ Majors Road	06.05.04	1604	4z118	99 ± 5
69	Haughton River @ Bill Britt Road	06.05.04	1648	4z119	98 ± 5
70	Haughton River @ Blacks Road DPI channel	06.05.04	1739	4z120	153 ± 5
71	Sunwater gauging station	27.04.04	1225	4z18	24 ± 3
72	Pumping station	27.04.04	1300	4z19	122 ± 6
73	Gauging station	27.04.04	1337	4z20	385 ± 8
74	Fowlers lagoon culvert	27.04.04	1418	4z21	27 ± 3
75	Harper Road / Oats Road channel crossing	27.04.04	1508	4z14	46 ± 3
76	Alma Creek channel	27.04.04	1557	4z22	155 ± 5
77	Saltwater creek @ Highway crossing	28.04.04	1214	4z26	92 ± 3
78	Inkerman Lagoon waterboard channel	28.04.04	1320	4z27	26 ± 2
79	Iyah Creek	28.04.04	1351	4z28	63 ± 2
80	Papale's Farm drainage channel	28.04.04	1437	4z29	97 ± 3
81	Sibon Road channel crossing @ silo	28.04.04	1541	4z30	43 ± 2
83	Barratta Creek	04.05.04	0956	4z71	406 ± 7
84	Barratta Creek	04.05.04	1009	4z72	307 ± 7
85	Barratta Creek	04.05.04	1018	4z73	298 ± 6
86	Barratta Creek	04.05.04	1029	4z74	270 ± 6
87	Barratta Creek	04.05.04	1040	4z75	212 ± 5
88	Barratta Creek	04.05.04	1049	4z76	231 ± 7
89	Barratta Creek	04.05.04	1059	4z77	236 ± 7
90	Barratta Creek	04.05.04	1109	4z78	183 ± 6
91	Barratta Creek	04.05.04	1121	4z79	203 ± 7
92	Barratta Creek	04.05.04	1130	4z80	167 ± 6
93	Barratta Creek	04.05.04	1144	4z81	137 ± 6
94	Barratta Creek	04.05.04	1156	4z82	131 ± 6
95	Barratta Creek	04.05.04	1207	4z83	100 ± 6
96	Barratta Creek	04.05.04	1218	4z84	58 ± 11

¹ Measured by liquid scintillation

² Measured by gas stripping

Table A2.3. Radon activities in Bowling Green Bay.

Station	Date	Time	Radon (mBq/L)	Salinity (psu)
F1	9/02/2004	12:52	7 ± 3	35.5
F2	9/02/2004	13:07	7 ± 3	35.9
F3	9/02/2004	13:22	8 ± 3	35.6
F4	9/02/2004	13:37	8 ± 3	35.4
F5	9/02/2004	13:52	6 ± 2	35.4
F6	9/02/2004	14:07	6 ± 2	35.3
F7	9/02/2004	14:22	13 ± 3	35.6
F8	9/02/2004	14:37	10 ± 3	35.3
F9	9/02/2004	14:52	6 ± 2	35.3
F10	9/02/2004	15:07	3 ± 2	35.3
F11	9/02/2004	15:22	13 ± 3	35.2
F12	9/02/2004	15:37	12 ± 3	35.2
F13	9/02/2004	15:52	7 ± 2	35.0
A1	29/04/2004	11:07	17 ± 4	36.5
A2	29/04/2004	11:17	17 ± 4	36.5
A3	29/04/2004	12:09	11 ± 3	36.3
A4	29/04/2004	12:19	16 ± 4	36.3
A5	29/04/2004	12:29	11 ± 3	36.3
A6	29/04/2004	12:40	19 ± 4	36.3
A7	29/04/2004	12:50	13 ± 4	36.3
A8	29/04/2004	13:00	8 ± 3	36.3
A9	29/04/2004	13:10	13 ± 3	36.3
A10	29/04/2004	13:20	14 ± 4	36.1
A11	29/04/2004	13:30	22 ± 5	35.4
A12	29/04/2004	13:40	21 ± 5	35.5
A13	29/04/2004	13:50	21 ± 5	36.1
A14	29/04/2004	14:00	26 ± 5	36.2
A15	29/04/2004	14:10	16 ± 4	36.2
A16	29/04/2004	14:20	12 ± 3	36.5
A17	29/04/2004	14:30	25 ± 5	36.4
A18	29/04/2004	14:40	28 ± 5	36.3
A19	29/04/2004	14:50	18 ± 4	36.4
A20	29/04/2004	15:00	11 ± 3	36.4
A21	29/04/2004	15:10	12 ± 3	36.4
A22	29/04/2004	15:20	5 ± 2	36.2
A23	29/04/2004	15:30	8 ± 3	36.1
A24	29/04/2004	15:40	6 ± 2	36.2
A25	29/04/2004	15:50	9 ± 3	36.1
17R	29/04/2004	11:16	21	
16R	29/04/2004	12:18	6	
13R	29/04/2004	12:45	21	
19R	29/04/2004	13:23	36	
20R	29/04/2004	13:52	31	
14R	29/04/2004	14:28	41	
18R	29/04/2004	15:13	3	
15R	29/04/2004	15:44	10	

Table A3.4. Field parameters and major ion concentrations for surface waters.

Site	Date	Lab pH	EC (μ S/cm)	TDS (mg/L)	Hardness	Alkalinity	Na (mg/L)	K (mg/L)	Ca (mg/L)	Mg (mg/L)	SO ₄ (mg/L)	Cl (mg/L)	Bicarb (mg/L)	Carbonate (mg/L)	Nitrate (μ g N/L)
1	08.12.03	8.14	31400	20500	3120	100	6200	214	123	682	1170	12100	122	< 0.1	11
2	08.12.03	7.97	1332	685	124	70	194	13	14	22	56	345	85	< 0.1	108
3	08.12.03	7.96	4860	2240	293	75	765	33	41	47	170	1140	92	< 0.1	97
	26.04.04	7.95	17370	14040	2680	94	4440	139	186	540	1140	7530	115	< 0.1	2
	02.05.04	8.24	22100	14000	2610	91	4420	166	160	540	1000	7660	111	< 0.1	7
	03.05.04	7.02	177	92	57	65	13	3	12	7	5	13	79	< 0.1	9
	06.05.04		23300												
4	08.12.03	7.72	169	86	44	66	13	6	9	5	3	10	81	< 0.1	121
5	09.12.03	7.12	147	88	49	54	12	6	10	6	14	9	66	< 0.1	180
	27.04.04	7.77	160	82	49	57	12	5	10	6	5	10	70	< 0.1	182
6	09.12.03	7.54	165	84	52	62	13	6	11	6	4	8	76	< 0.1	202
	26.04.04	7.71	130	93	51	68	13	5	10	6	6	13	83	< 0.1	165
	27.04.04	7.58	165	83	51	56	12	5	10	6	5	12	69	< 0.1	175
7	09.12.03	8.08	54500	37100	6510	128	11100	422	449	1310	2810	21000	156	< 0.1	7
8	09.12.03	7.88	53200	36900	6340	134	11300	423	433	1290	2580	20700	163	< 0.1	6
9	09.12.03	7.96	37500	24300	4780	109	7550	164	294	982	1650	13600	133	< 0.1	14
10	09.12.03	8.00	27200	17200	2930	100	5400	195	208	584	1070	9700	122	< 0.1	35
11	09.12.03	7.57	178	87	44	71	14	6	9	5	4	6	86	< 0.1	23
	03.05.04	7.52	171	89	57	60	12	4	12	6	6	13	73	< 0.1	45
12	09.12.03	7.43	175	87	45	69	14	6	10	5	5	3	84	< 0.1	22
	04.05.04	7.70	184	97	62	64	14	5	14	7	7	13	78	< 0.1	109
13	09.12.03	7.37	173	83	49	67	14	6	10	6	3	5	81	< 0.1	152
	03.02.04	7.37	190												
14	09.12.03	7.71	173	85	47	67	14	6	10	6	3	6	82	< 0.1	157
	26.04.04	7.67	151	91	56	60	13	4	12	6	6	13	73	< 0.1	140
	27.04.04	7.74	166	86	52	59	12	5	11	6	5	12	71	< 0.1	169
15	09.12.03	7.48	176	86	45	68	13	6	10	5	6	6	83	< 0.1	56
16	10.12.03	6.73	821	436	159	133	106	6	34	18	14	179	162	< 0.1	8
	28.04.04	7.10	680	333	164	67	62	5	33	20	27	146	82	< 0.1	6
17	10.12.03	7.48	471	251	100	79	41	7	23	11	58	53	96	< 0.1	3060
	06.05.04	7.72	201	105	57	45	18	4	13	6	19	18	55	< 0.1	71

18	10.12.03	8.07	414	219	110	96	41	5	20	14	14	66	117	< 0.1	17
	06.05.04	7.63	210	107	60	52	18	5	14	7	14	21	63	< 0.1	15
19	10.12.03	7.91	426	232	111	97	43	6	23	13	37	51	119	< 0.1	803
	06.05.04	7.77	234	115	64	58	20	4	14	7	12	23	71	< 0.1	51
20	10.12.03	7.88	249	134	63	78	24	6	13	7	22	16	95	< 0.1	403
	06.05.04	7.65	202	106	65	70	17	4	14	7	8	14	85	< 0.1	46
21	11.12.03	7.38	50100	33400	6100	110	10000	366	413	1230	2580	18700	134	< 0.1	14
	05.05.04	7.41	38600	26350	5123	180	8280	276	337	1040	2380	13940	219	< 0.1	11
22	11.12.03	8.38	55000	36700	6780	108	11100	425	439	1380	2890	20400	120	6	15
23	11.12.03	7.90	64300	44300	8370	120	13500	511	526	1710	3100	24900	146	< 0.1	6
	05.05.04	7.51	47700	33390	6590	138	10630	353	416	1350	2500	18060	168	< 0.1	7
24	11.12.03	8.45	57700	39500	7240	133	11800	440	468	1470	3220	22000	151	6	4
	04.05.04	7.91	47500	32950	6410	129	10480	344	383	1330	2800	17550	157	< 0.1	7
25	11.12.03	7.43	967	519	124	123	148	12	21	18	40	207	151	< 0.1	15
	04.05.04	7.33	2380	1250	279	89	368	13	26	52	111	620	109	< 0.1	6
26	11.12.03	7.71	43800	31500	5170	166	9000	318	365	1030	4650	16000	202	< 0.1	10
27	11.12.03	8.26	62500	43800	7480	153	13500	495	517	1500	3400	24300	186	< 0.1	7
28	11.12.03	8.03	57800	39500	6950	269	12000	446	472	1400	2980	22100	328	< 0.1	5
	03.05.04	7.36	25700	16850	3370	173	5120	191	289	640	1400	9070	211	< 0.1	10
29	11.12.03	8.45	48500	32700	5650	142	10000	360	377	1140	2540	18100	162	6	6
30	15.12.03	7.11	166	83	50	59	13	5	11	5	4	9	73	< 0.1	157
	29.04.04	7.11	196	99	59	62	16	4	12	7	5	16	76	< 0.1	67
31	15.12.03	7.14	184	93	55	65	15	5	12	6	5	11	79	< 0.1	97
	29.04.04	6.78	198	100	58	60	17	5	12	7	7	18	73	< 0.1	66
32	15.12.03	7.21	188	94	53	63	15	5	12	6	4	14	77	< 0.1	25
	29.04.04	7.33	194	97	57	61	16	4	12	7	5	17	74	< 0.1	22
33	15.12.03	8.74	268	144	70	102	26	5	14	8	4	25	107	8	6
	29.04.04	7.17	203	96	49	58	17	4	10	6	8	17	71	< 0.1	7
34	15.12.03	8.37	207	111	58	78	18	4	13	6	6	16	92	2	7
	29.04.04	8.07	226	108	55	68	19	3	11	7	10	18	83	< 0.1	5
35	15.12.03	7.74	189	101	54	69	15	5	12	6	6	13	85	< 0.1	7
	29.04.04	7.36	195	99	57	62	16	4	12	7	7	16	75	< 0.1	19
36	15.12.03	7.02	192	99	55	69	16	5	12	6	5	14	84	< 0.1	14
	29.04.04	7.29	194	99	58	63	16	4	12	7	6	16	77	< 0.1	20
37	15.12.03	7.63	199	102	56	71	17	5	12	6	4	16	86	< 0.1	7
	29.04.04	7.01	195	99	55	62	16	4	11	7	7	17	76	< 0.1	3

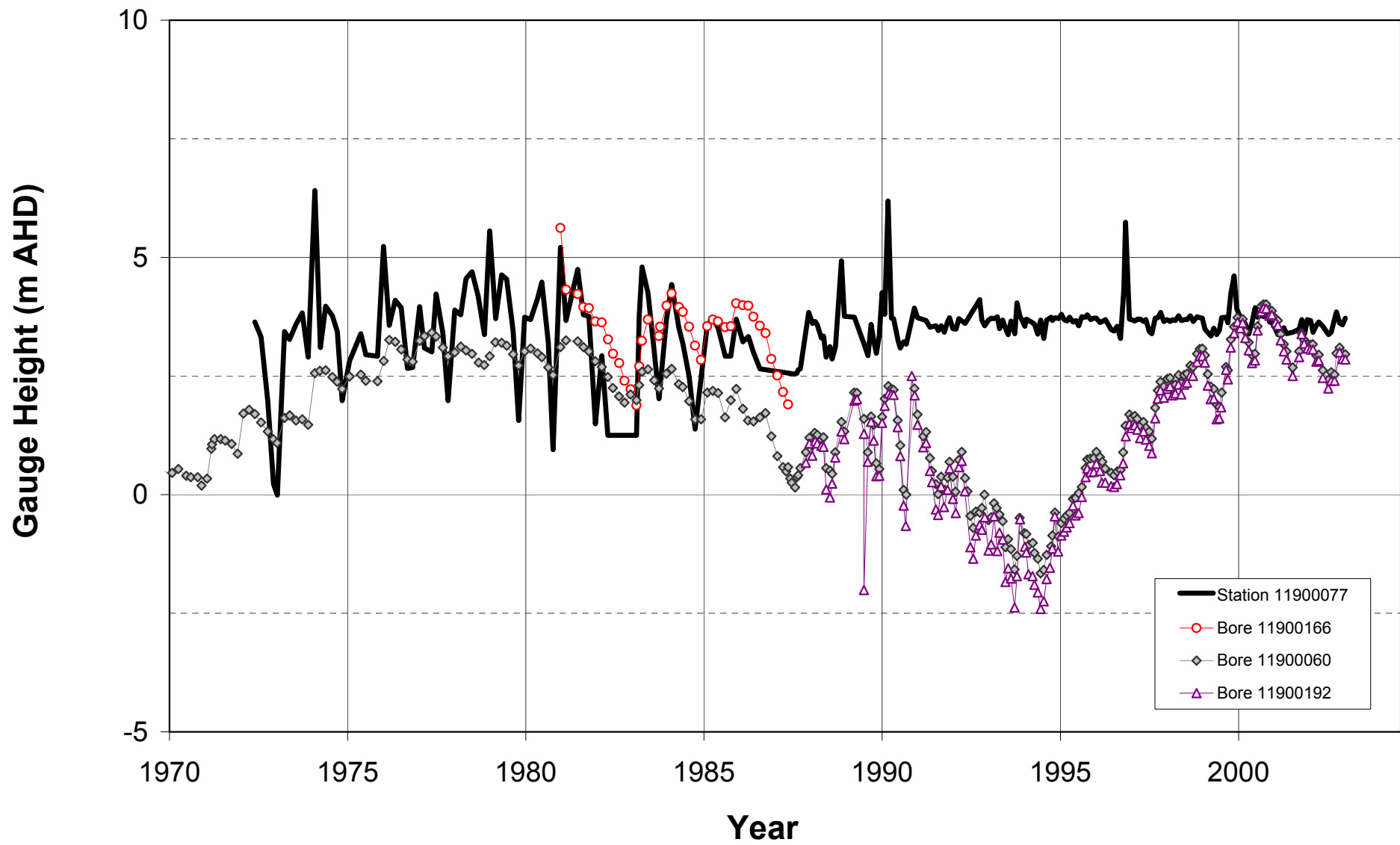
38	15.12.03	8.67	204	108	57	77	17	5	12	6	7	14	85	5	5
	29.04.04	7.41	198	98	54	63	16	3	12	6	6	17	77	< 0.1	8
39	15.12.03	7.12	343	184	91	121	33	7	19	11	10	32	148	< 0.1	8
40	15.12.03	9.80	427	243	89	123	50	4	19	10	14	61	80	34	73
	28.04.04	7.73	496	269	138	110	50	4	31	15	21	82	134	< 0.1	6
41	15.12.03	8.03	220	115	59	75	19	4	12	7	10	18	92	< 0.1	9
	28.04.04	7.46	266	136	67	73	24	5	13	8	19	23	89	< 0.1	11
42	16.12.03	7.25	197	98	56	70	16	4	13	6	7	11	86	< 0.1	13
	04.05.04	8.05	230	122	62	69	25	2	13	7	7	27	84	< 0.1	0.6
43	16.12.03	7.20	196	101	55	69	16	5	12	6	6	15	84	< 0.1	11
44	16.12.03	7.15	190	94	55	67	15	4	12	6	7	10	81	< 0.1	10
	04.05.04	8.05	192	103	59	65	16	3	13	6	8	16	79	< 0.1	4
45	16.12.03	7.49	202	103	61	71	16	4	14	6	7	13	86	< 0.1	9
46	01.05.04	7.33	11 640												
48	04.05.04	7.87	207	108	51	59	23	2	11	6	7	25	72	< 0.1	8
50	04.05.04	7.84	202	108	60	66	19	3	13	7	8	19	80	< 0.1	3
51	04.05.04	7.60	7920	4610	1130	75	1410	49	151	183	348	2430	91	< 0.1	7
52	02.05.04	8.49	172	94	57	65	13	4	12	7	6	13	71	4.0	68
53	02.05.04	8.01	174	91	56	59	13	4	12	6	6	14	72	< 0.1	100
54	03.05.04	7.82	180	94	58	61	14	4	12	7	6	15	74	< 0.1	159
55	02.05.04	7.82	226	116	72	65	18	4	15	9	6	26	79	< 0.1	132
56	03.05.04	8.40	170	90	57	58	13	5	12	6	6	14	69	1.0	112
57	05.05.04	7.85	264	133	56	57	31	2	11	7	7	41	69	< 0.1	3
58	05.05.04	7.50	25900	15500	3150	107	5080	170	206	640	121	9220	130	< 0.1	15
59	05.05.04	7.48	43400	28680	5480	136	8780	289	359	1120	2120	15940	166	< 0.1	9
60	05.05.04	7.47	46100	31920	6250	138	10000	332	399	1280	2500	17330	168	< 0.1	8
61	05.05.04	7.56	49600	34580	7190	136	10980	363	440	1480	2590	18660	166	< 0.1	9
62	05.05.04	7.61	50800	35190	6240	131	10800	373	428	1260	2820	19430	160	< 0.1	9
63	05.05.04	7.68	51600	35120	6810	130	11050	399	454	1380	2430	19330	158	< 0.1	7
64	05.05.04	7.75	52000	35300	6750	127	10650	386	463	1360	3040	19330	155	< 0.1	7
65	05.05.04	7.84	52300	34820	6640	126	10900	391	460	1330	2630	19030	154	< 0.1	9
66	06.05.04	6.75	235	118	60	51	22	4	13	7	15	27	62	< 0.1	22
67	06.05.04	7.77	166	87	54	57	13	4	13	6	6	11	70	< 0.1	3
68	06.05.04	7.78	194	102	45	51	21	2	10	5	4	30	62	< 0.1	3
69	06.05.04	7.46	213	108	68	75	17	3	16	7	6	14	92	< 0.1	3
70	06.05.04	8.41	162	90	54	61	13	4	12	6	9	11	74	< 0.1	85

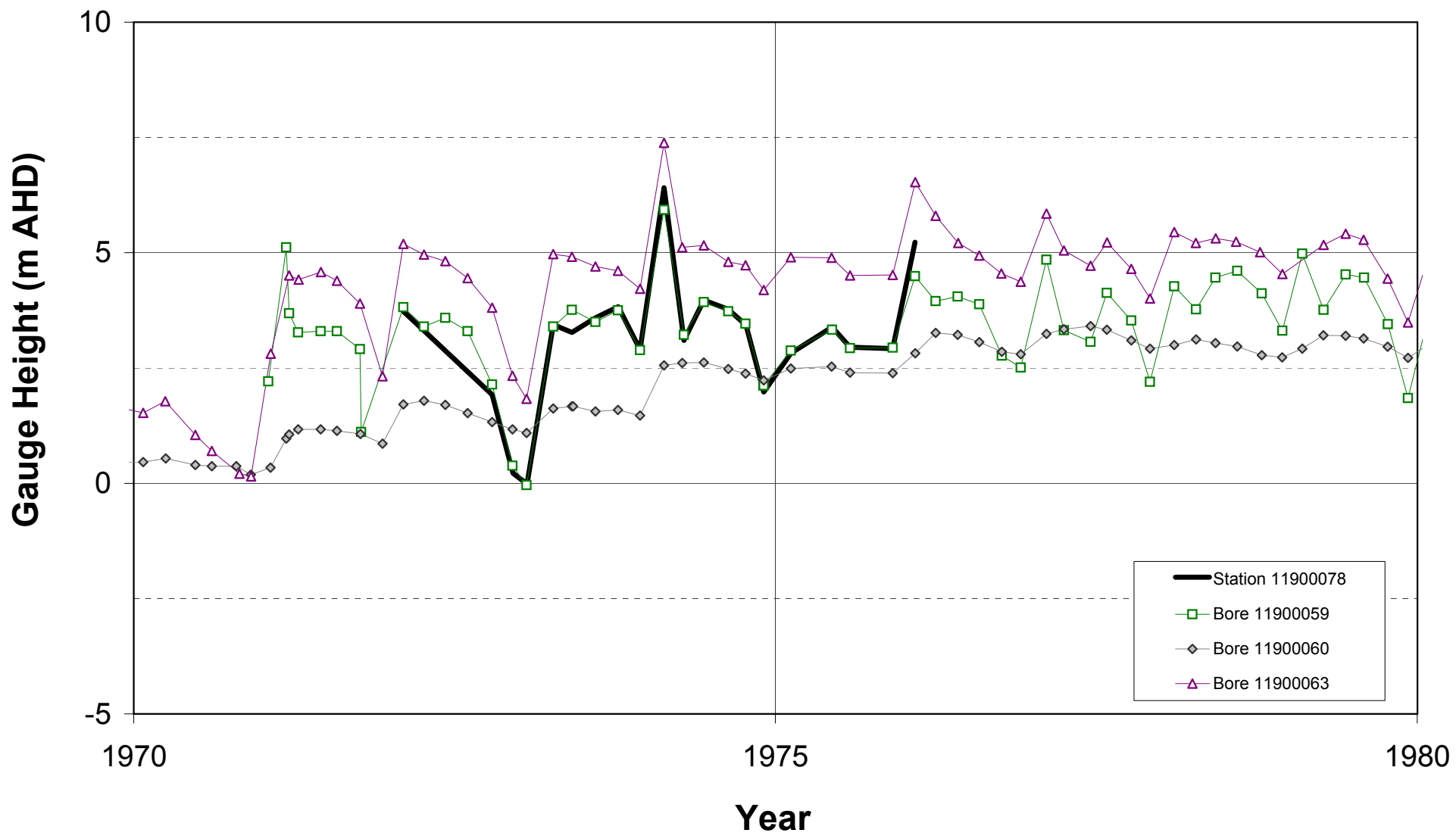
71	27.04.04	9.01	181	92	49	67	16	4	9	6	4	13	70	6	6
72	27.04.04	7.57	574	102	62	62	15	5	13	7	12	14	75	< 0.1	25
73	27.04.04	7.87	485	235	124	97	44	2	22	17	11	81	118	< 0.1	3
74	27.04.04	7.34	179	93	56	64	14	4	12	7	5	13	78	< 0.1	69
75	27.04.04	7.23	214	115	64	79	17	4	13	8	6	19	97	< 0.1	12
76	27.04.04	7.62	674	365	103	197	108	3	20	13	28	75	240	< 0.1	20
77	28.04.04	7.20	250	124	66	77	22	2	13	8	9	25	94	< 0.1	2
78	28.04.04	7.55	221	110	63	67	19	3	13	8	8	19	82	< 0.1	13
79	28.04.04	7.22	180	93	56	61	14	4	12	6	7	13	74	< 0.1	8
80	28.04.04	7.74	172	88	54	57	13	5	11	6	6	12	70	< 0.1	188
81	28.04.04	7.62	173	92	55	67	12	5	11	6	6	11	82	< 0.1	112
83	04.05.04	7.29	4190	2270	486	87	710	23	36	96	164	1190	106	< 0.1	9
84	04.05.04	7.22	5280	2890	603	89	900	30	41	122	236	1510	109	< 0.1	9
85	04.05.04	7.26	6120	2430	690	90	1090	36	44	141	256	1810	110	< 0.1	12
86	04.05.04	7.48	6940	3897	816	94	1230	51	65	159	256	2080	115	< 0.1	15
87	04.05.04	7.31	8230	4730	882	95	1480	59	54	181	404	2490	116	< 0.1	14
88	04.05.04	7.34	10410	6120	1120	98	1960	72	69	230	484	3250	120	< 0.1	15
89	04.05.04	7.38	12620	7320	1370	105	2330	84	77	286	520	3950	128	< 0.1	12
90	04.05.04	7.42	16310	9980	1980	108	3250	109	117	409	720	5320	132	< 0.1	12
91	04.05.04	7.45	20500	12600	3090	116	3730	131	404	510	860	6900	141	< 0.1	11
92	04.05.04	7.52	25100	15750	3160	110	4750	167	319	570	1230	8650	134	< 0.1	9
93	04.05.04	7.62	31900	20830	4290	130	6600	224	398	800	1540	11200	158	< 0.1	10
94	04.05.04	7.67	36300	23620	4220	130	7150	244	253	870	1900	13130	159	< 0.1	7
95	04.05.04	7.82	42500	28510	5300	130	9000	300	340	1080	2080	15640	158	< 0.1	7
96	04.05.04	7.89	46500	31910	6250	128	9930	339	372	1290	2660	17250	156	< 0.1	9

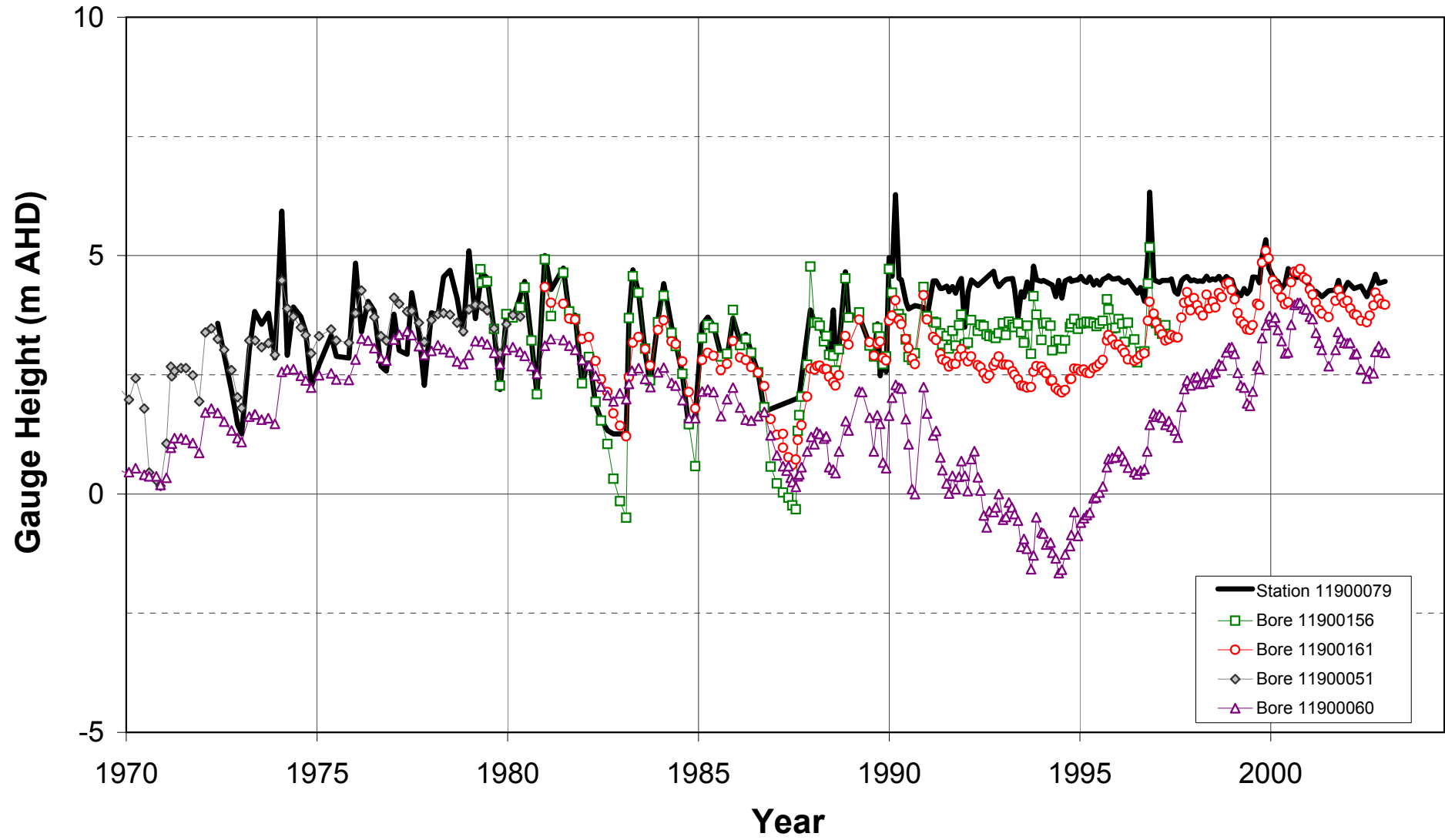
Table A3.5. Radium activities in surface water and groundwaters.

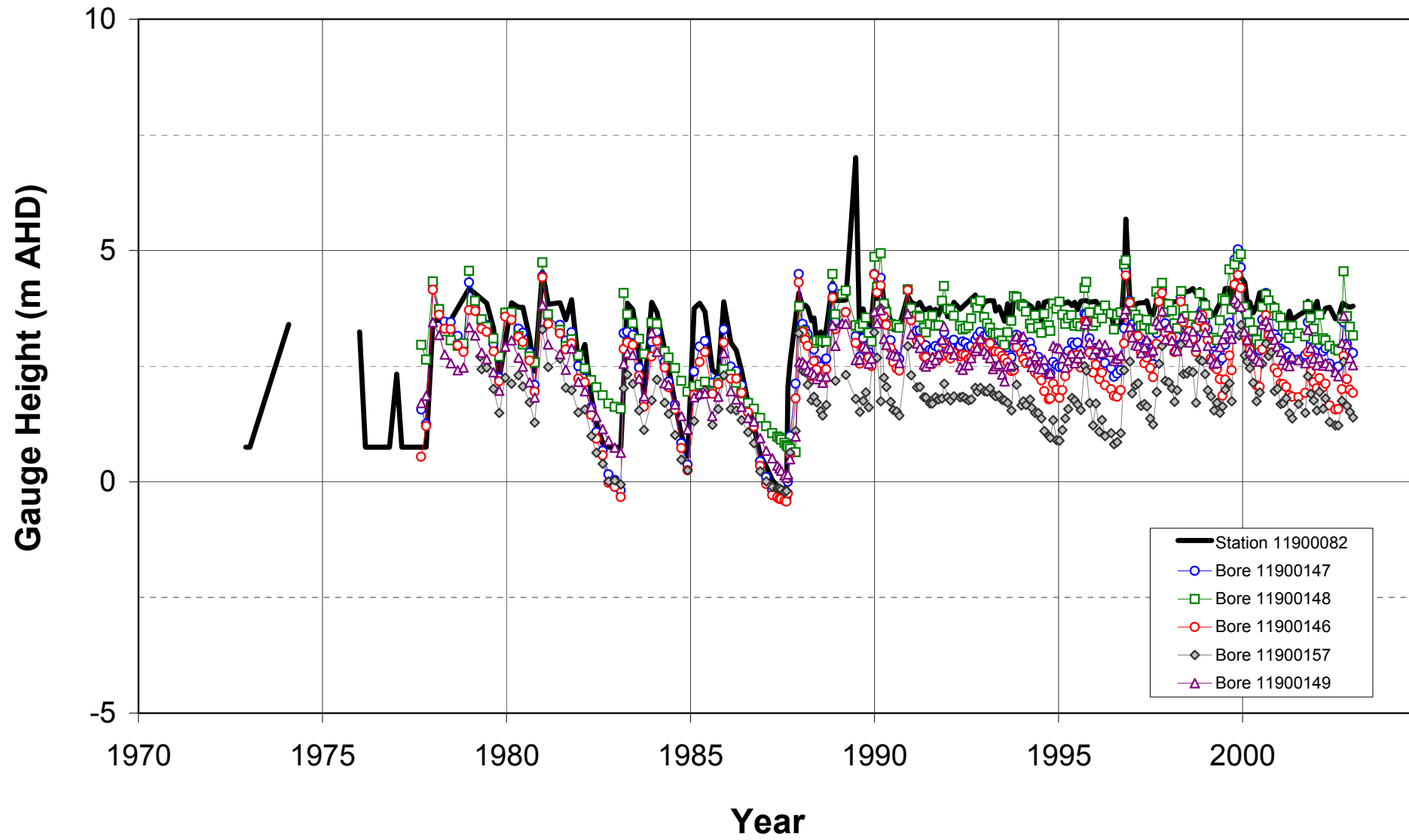
Location	Date	Time	²²³ Ra (mBq/L)	²²⁴ Ra (mBq/L)	²²⁶ Ra (mBq/L)	²²⁸ Ra (mBq/L)
<i>Offshore samples</i>						
B7	28.04.04	10:05	0.065	0.57	1.18	0.59
B6	28.04.04	10:45	0.061	0.91	1.28	1.62
B5	28.04.04	11:12	0.146	3.49	1.27	2.77
B3	28.04.04	15:04	0.317	8.73	1.03	3.64
B2	28.04.04	14:25	0.372	12.1	1.20	4.75
B1	28.04.04	14:12	0.956	40.3	2.23	14.3
H1	28.04.04	15:46	1.147	44.6	2.83	22.5
CBG1	28.04.04	10:52	0.359	12.4	1.46	6.08
<i>Surface Water samples</i>						
Site 23: Haughton @ Cromarty Creek Landing	01.05.04	14:00	2.36	86.2	10.86	77.6
Site 42: Haughton, north of Highway	01.05.04	15:00	0.031	2.25	0.63	2.19
Site 46: Barratta creek @ culvert	01.05.04	16:00	0.685	33.5	4.58	21.2
<i>Groundwater samples</i>						
11900178	27.04.04	12:30	1.449	29.48	2.76	28.5
11900184	27.04.04	13:30	0.894	21.36	8.39	32.2
11910037	28.04.04	11:00	0.516	29.20	5.48	18.3
11910263E	28.04.04	15:30	6.98	160.8	24.5	125.5
11910270	28.04.04	12:00	0.539	18.27	9.44	26.3

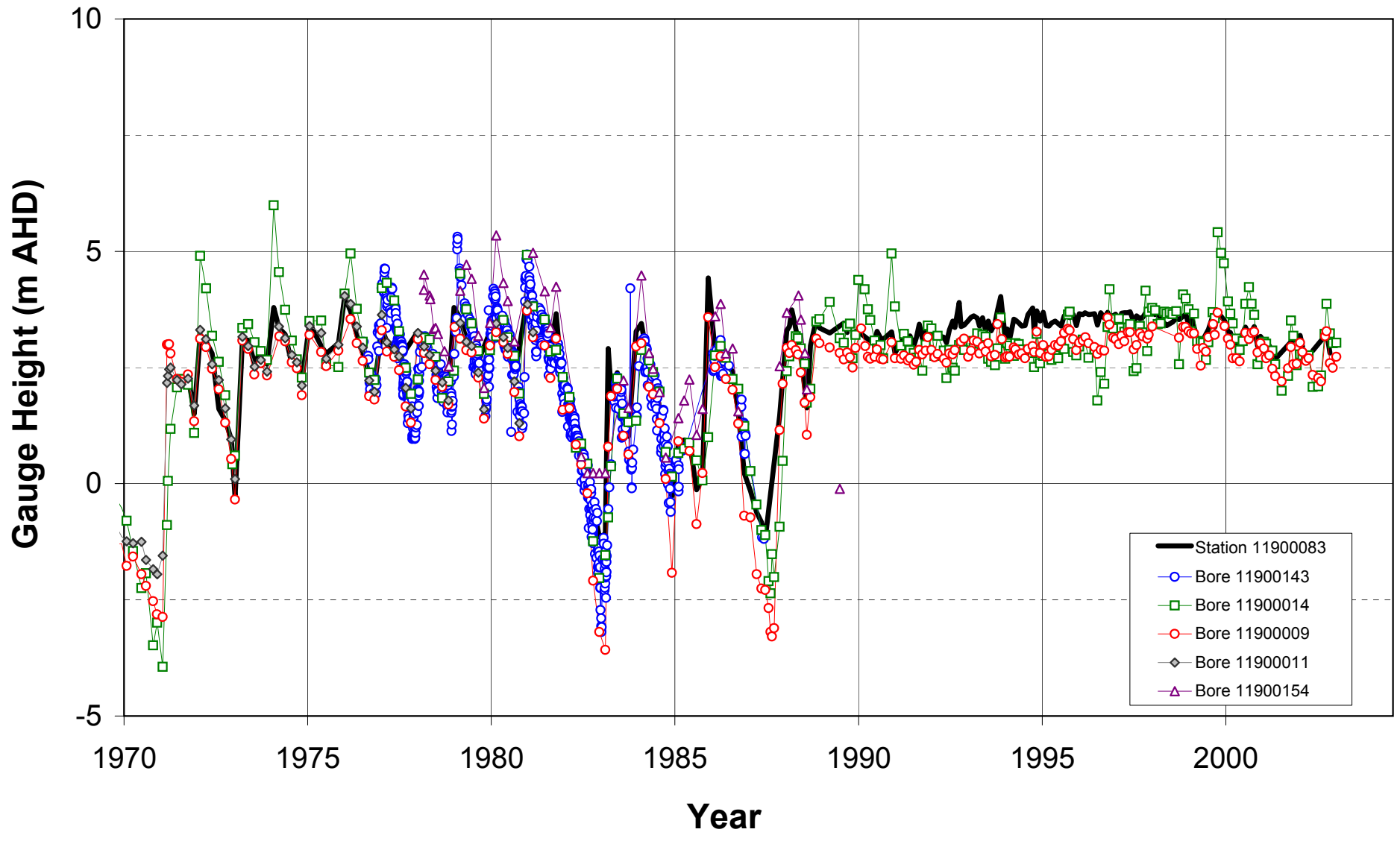
APPENDIX 4: Comparison of surface water gauge heights and groundwater elevations.

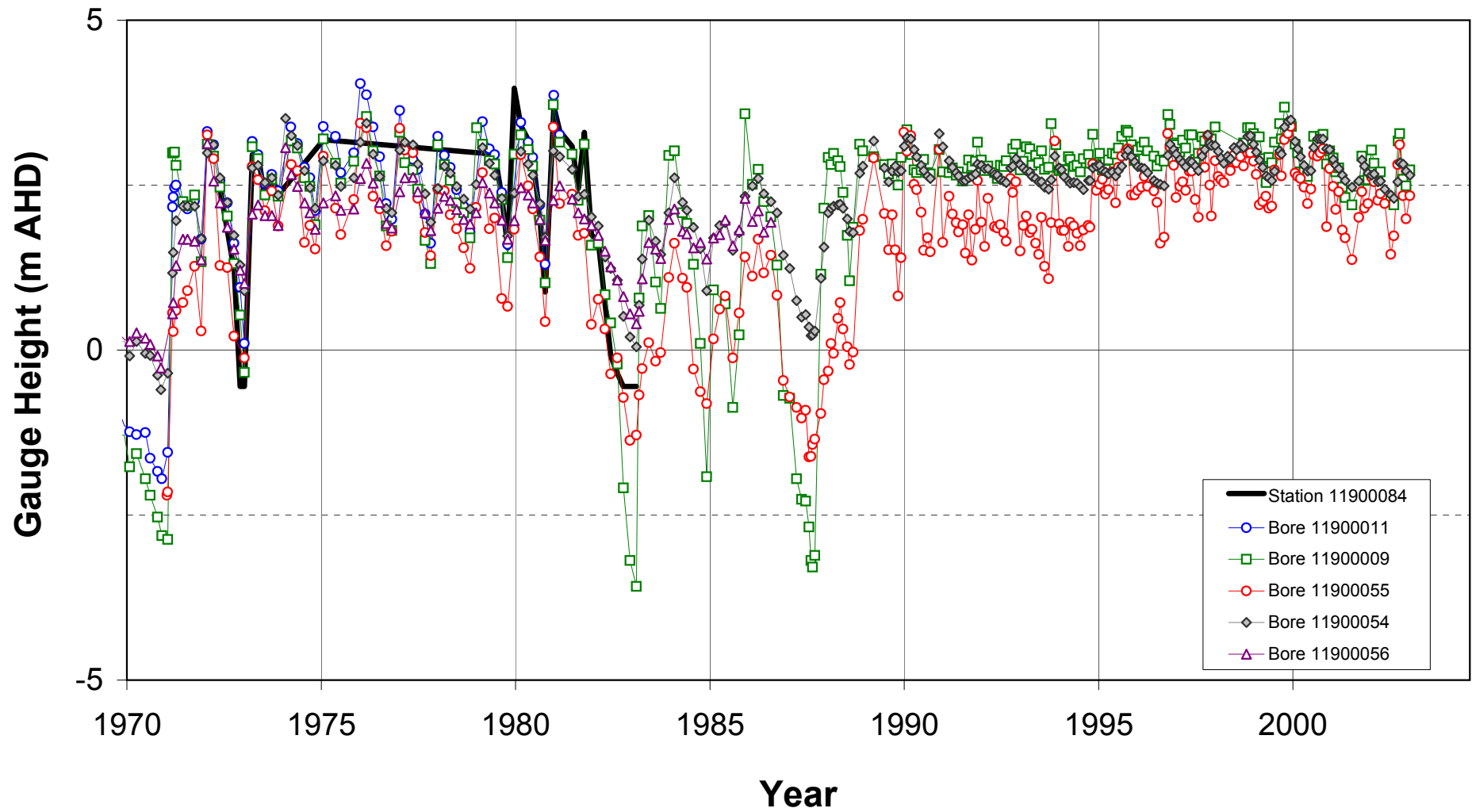


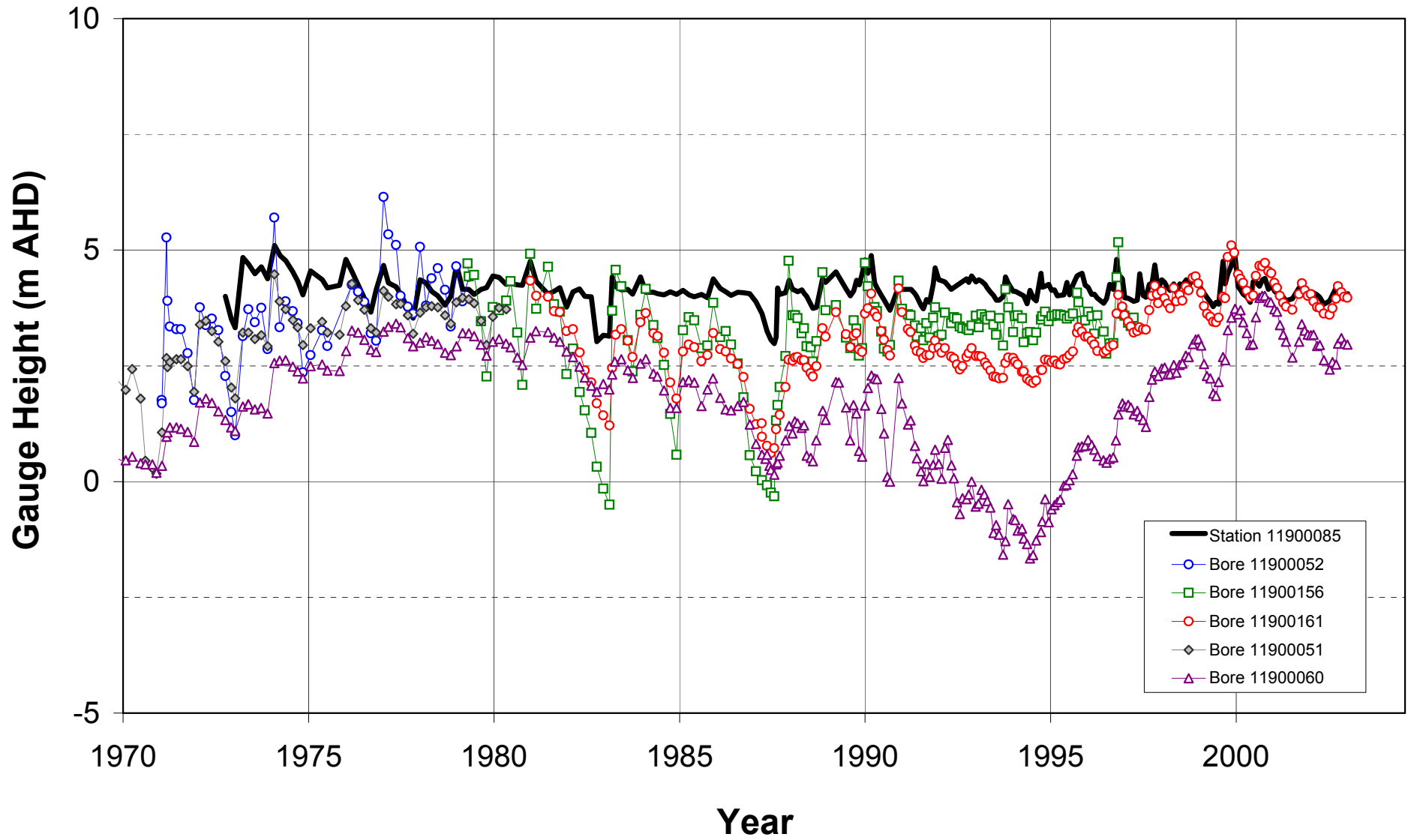


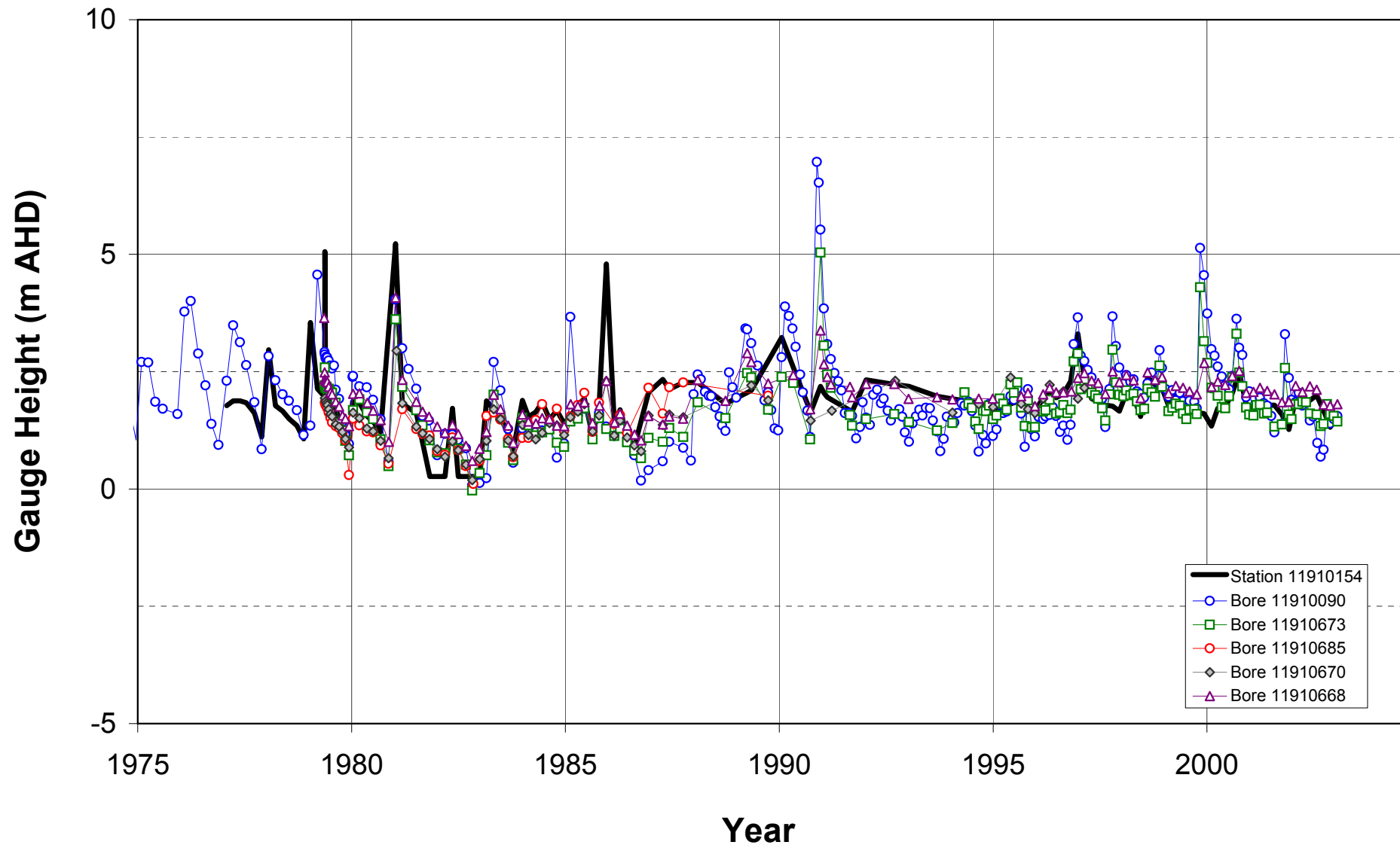


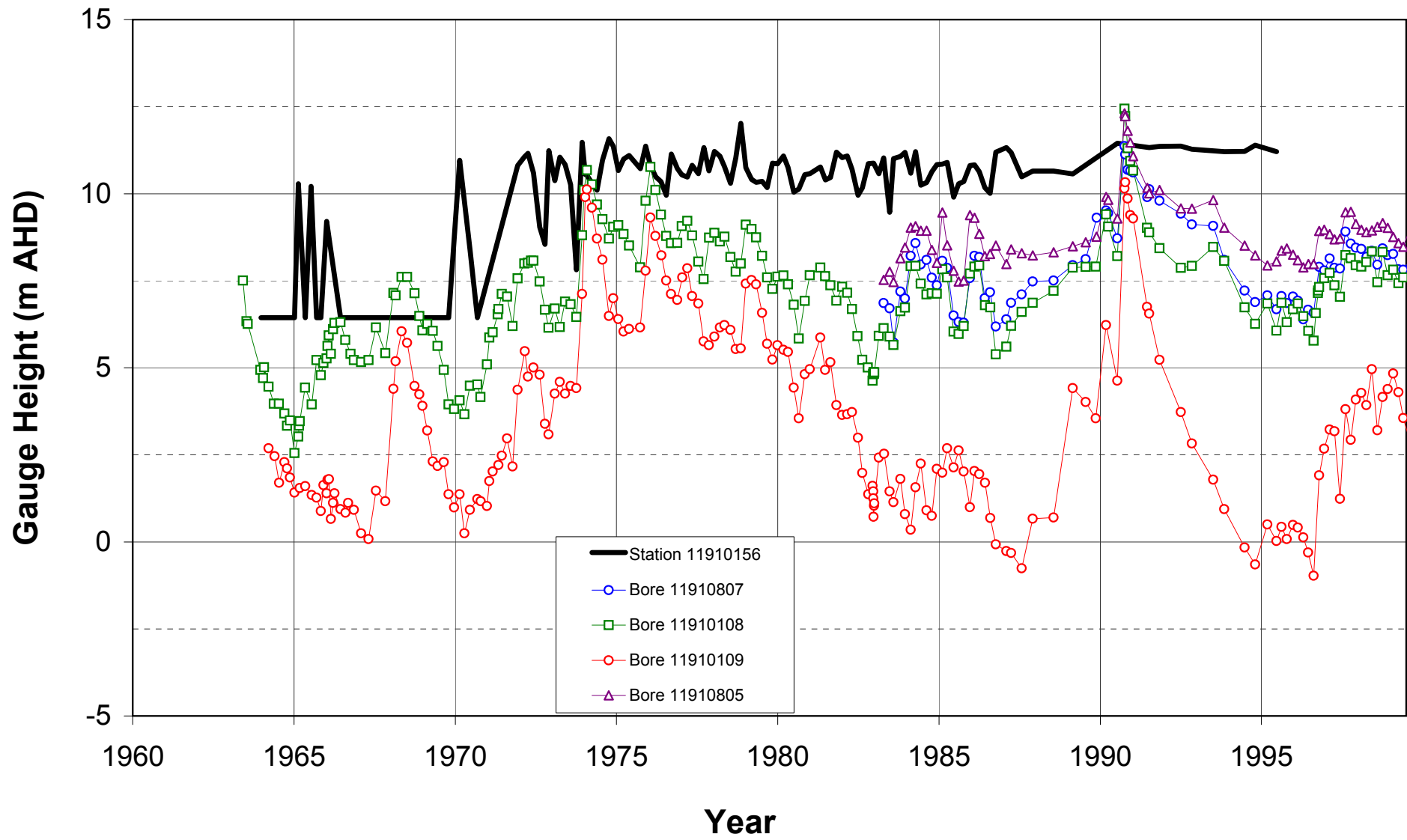


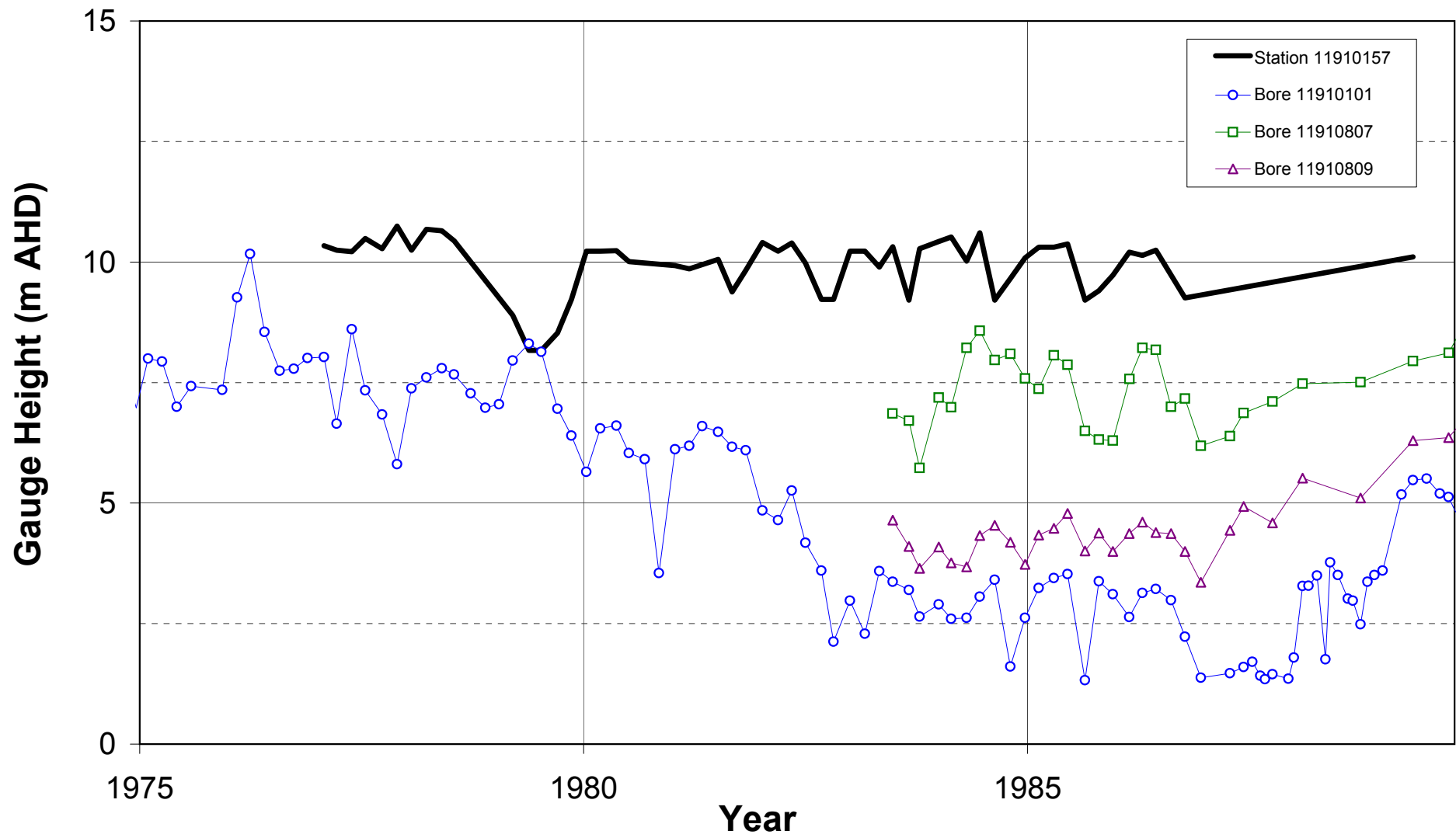


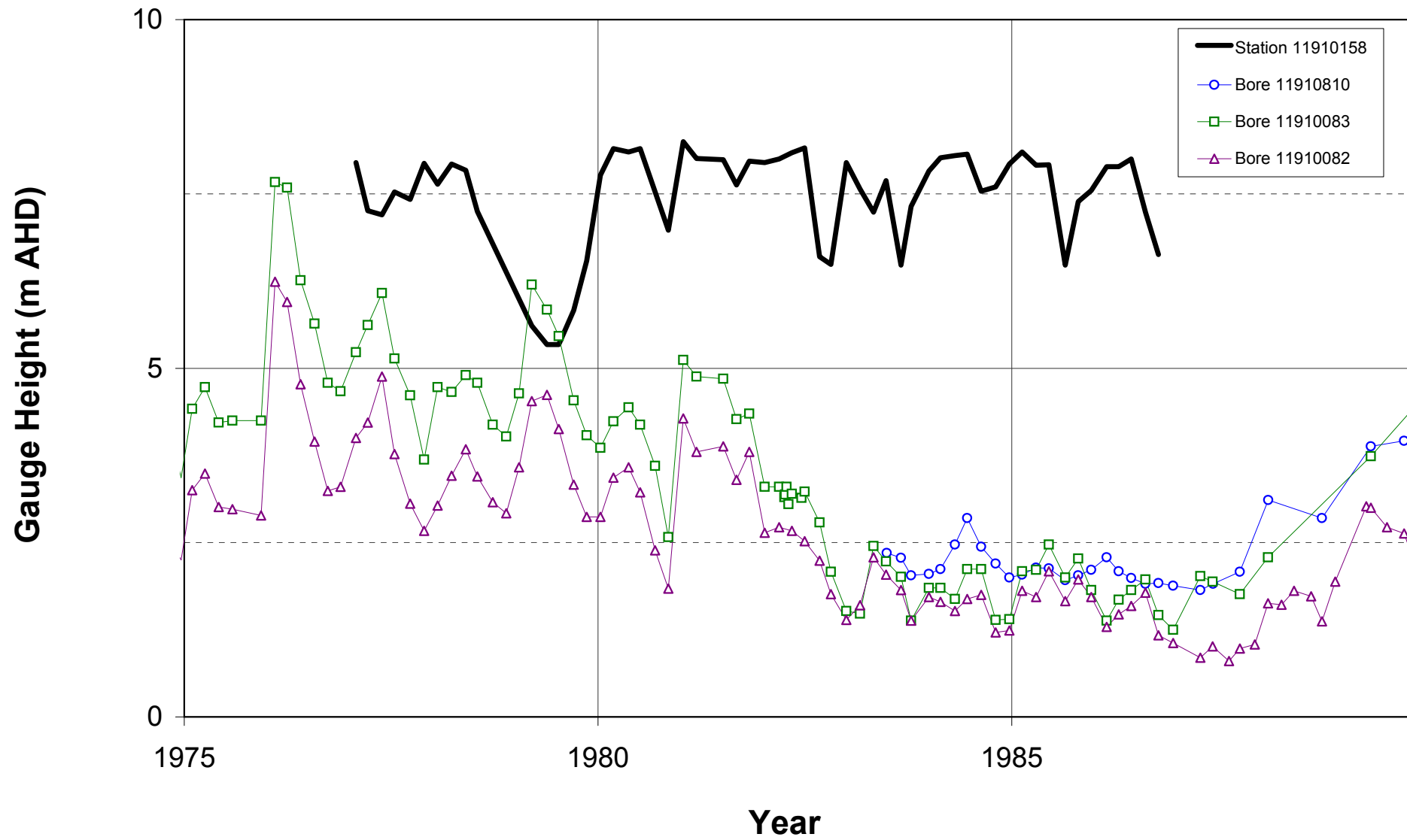


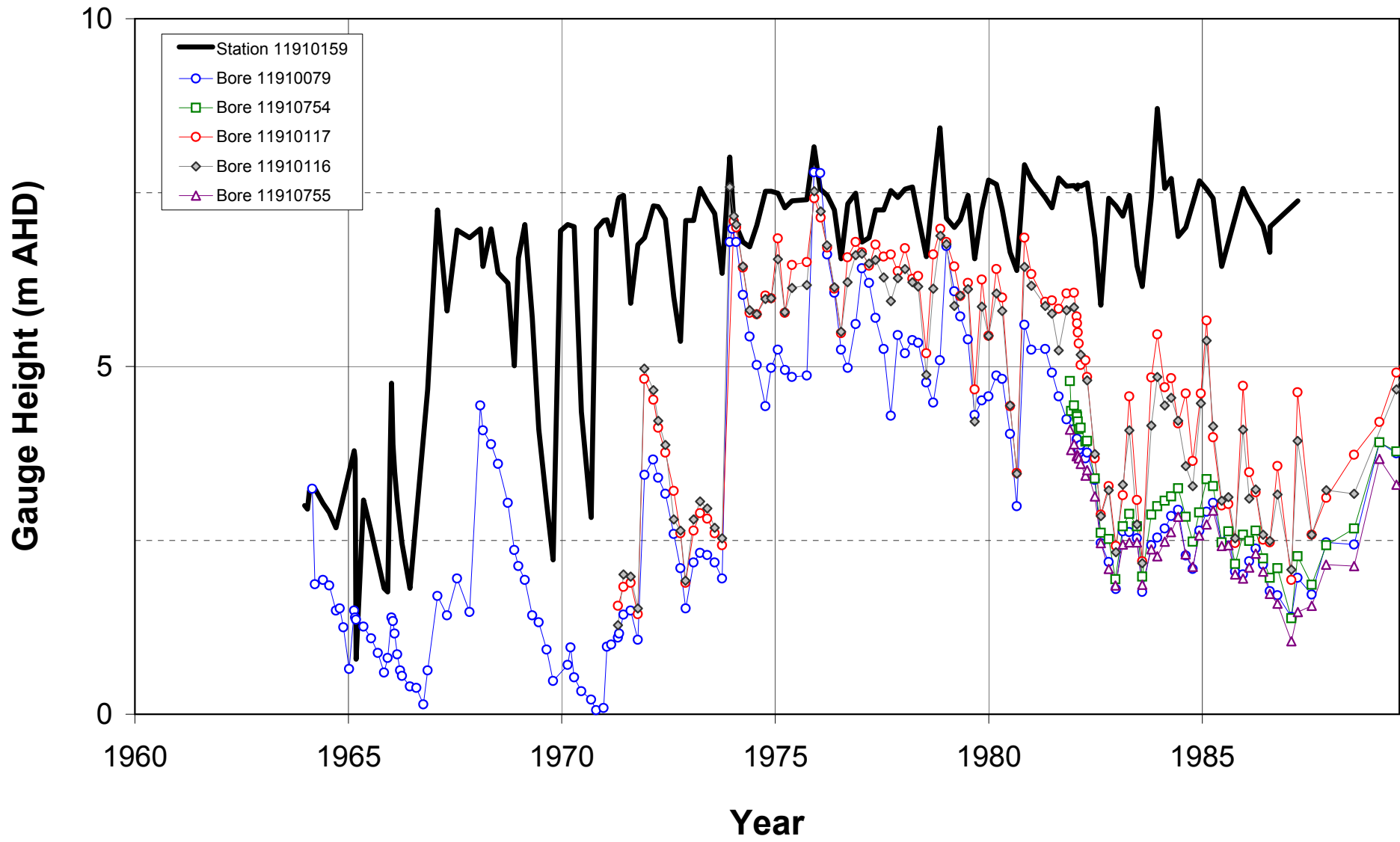


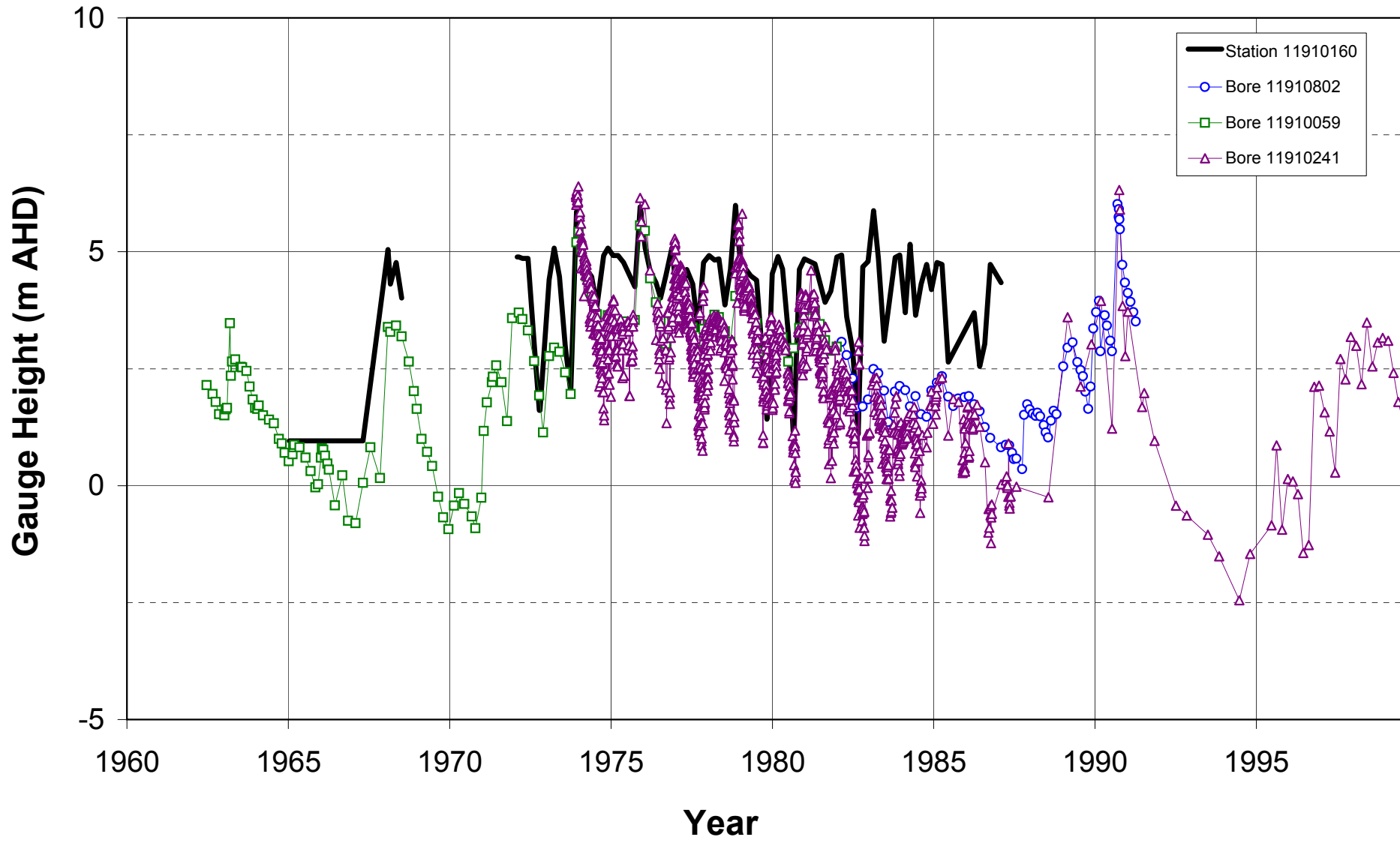


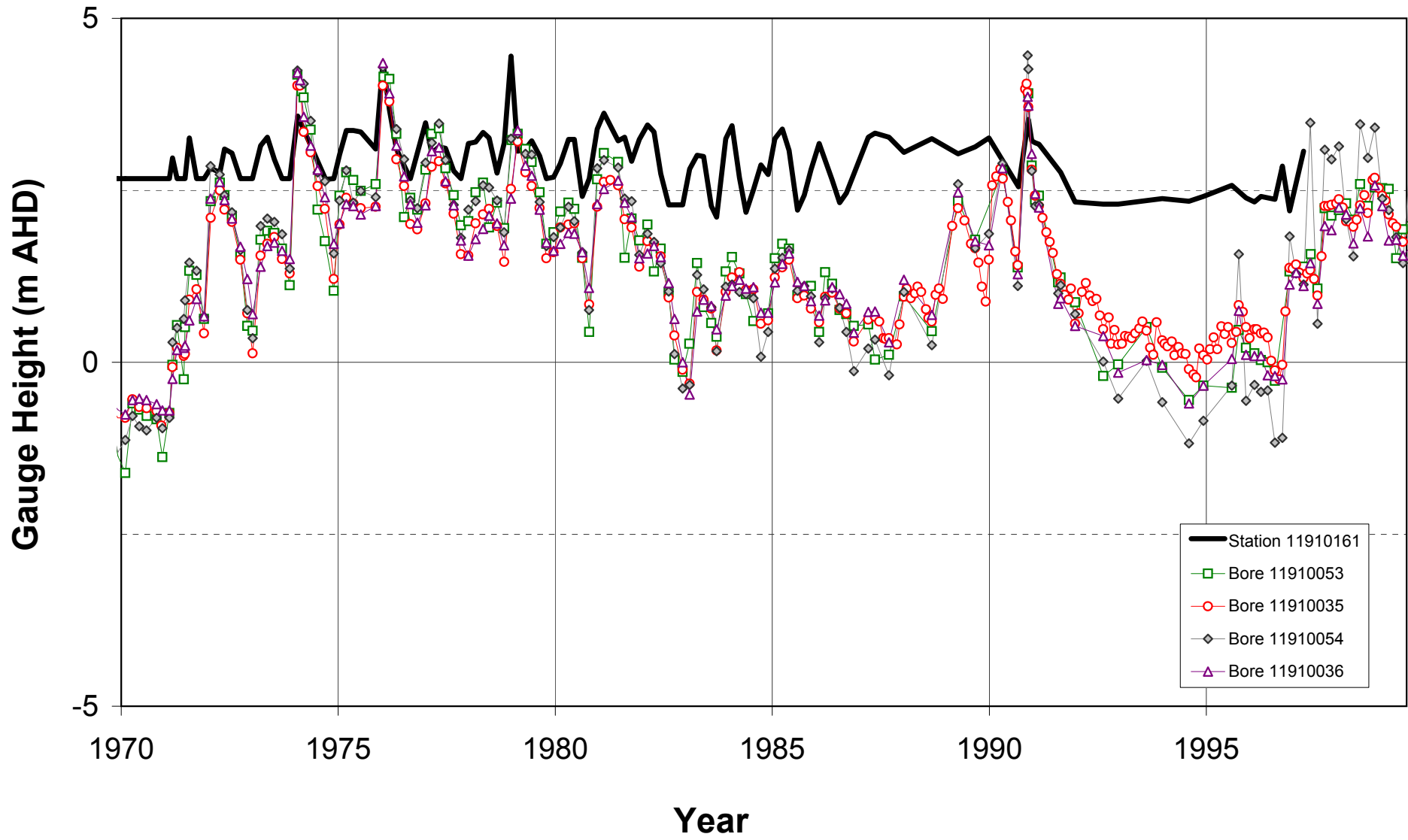


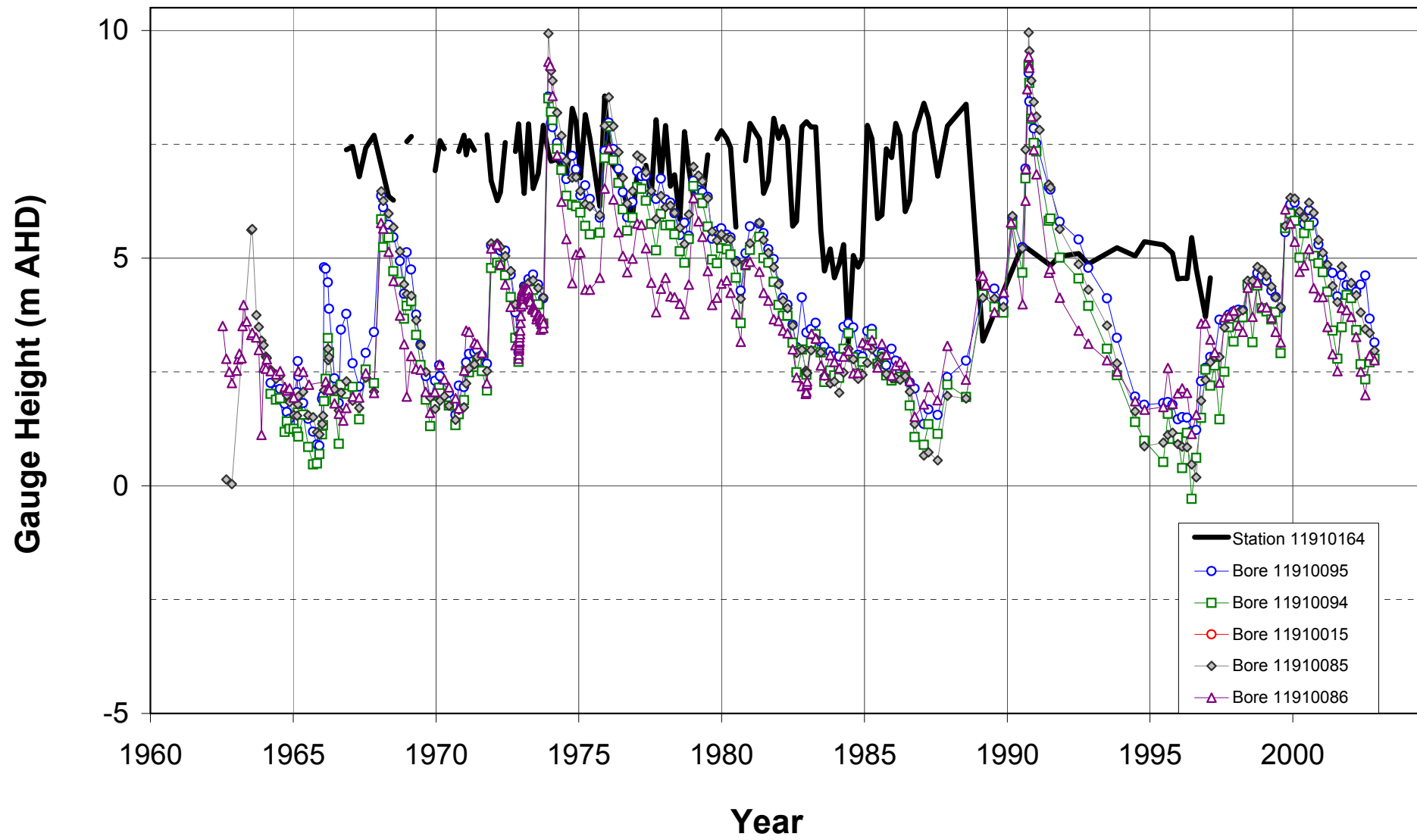


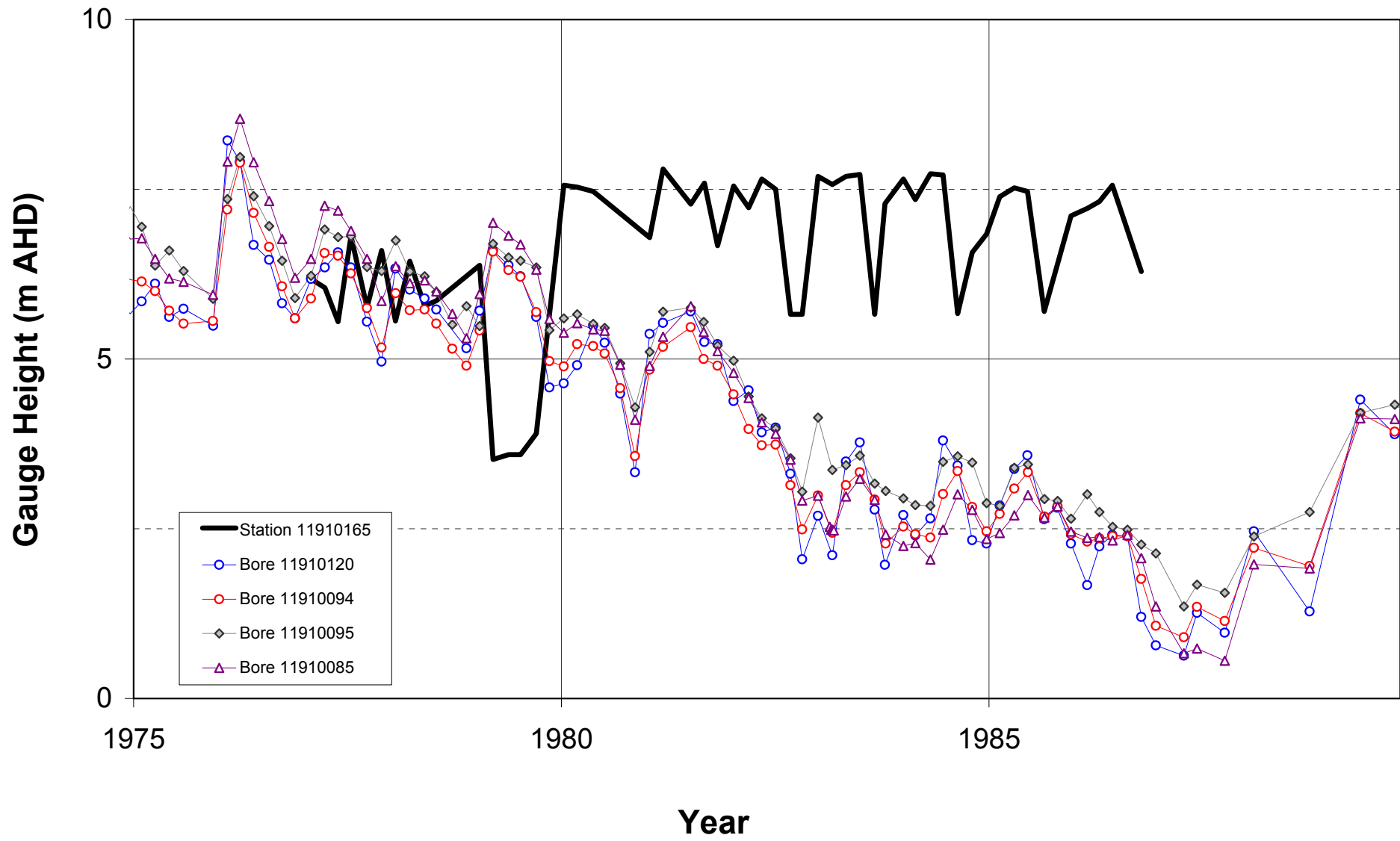












11910166

